$5

QEX

INCLUDING: COMMUNICATIONS QUARTERLY

Forum for Communications Experimenters

May/June 2000

1

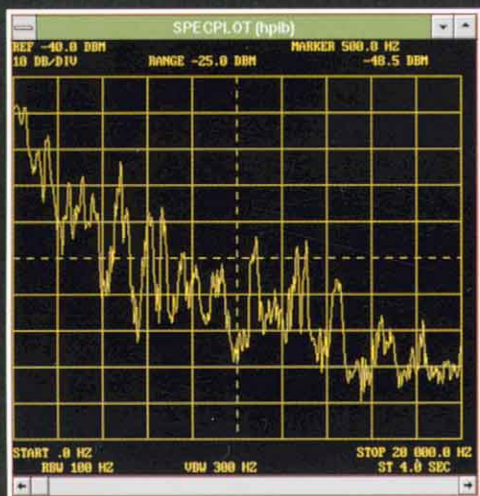

2

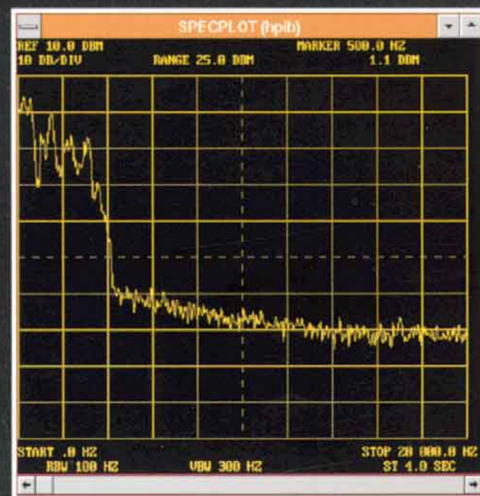

3

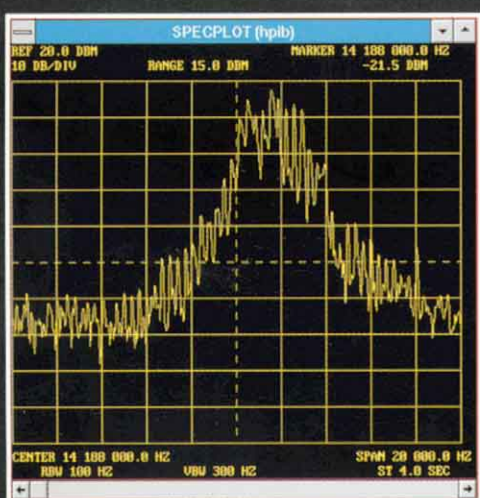

DSP meets voice:

1) Full-range speech spectrum
2) Compressed speech spectrum
3) Compressed SSB signal

Article by KF6DX inside!

QEX's 200th Issue!

ARRL The national association for AMATEUR RADIO
225 Main Street
Newington, CT USA 06111-1494

QEX

INCLUDING: COMMUNICATIONS QUARTERLY

QEX (ISSN: 0886-8093) is published bimonthly in January, March, May, July, September, and November by the American Radio Relay League, 225 Main Street, Newington CT 06111-1494. Yearly subscription rate to ARRL members is $22; nonmembers $34. Other rates are listed below. Periodicals postage paid at Hartford, CT and at additional mailing offices.

POSTMASTER: Form 3579 requested. Send address changes to: QEX, 225 Main St, Newington, CT 06111-1494

Issue No 200

David Sumner, K1ZZ
Publisher

Doug Smith, KF6DX
Editor

Robert Schetgen, KU7G
Managing Editor

Lori Weinberg
Assistant Editor

Zack Lau, W1VT
Contributing Editor

Production Department

Mark J. Wilson, K1RO
Publications Manager

Michelle Bloom, WB1ENT
Production Supervisor

Sue Fagan
Graphic Design Supervisor

David Pingree, N1NAS
Technical Illustrator

Joe Shea
Production Assistant

Advertising Information Contact:

John Bee, N1GNV, *Advertising Manager*
860-594-0207 direct
860-594-0200 ARRL
860-594-0259 fax

Circulation Department

Debra Jahnke, *Manager*
Kathy Capodicasa, N1GZO, *Deputy Manager*
Cathy Stepina, *QEX Circulation*

Offices

225 Main St, Newington, CT 06111-1494 USA
Telephone: 860-594-0200
Telex: 650215-5052 MCI
Fax: 860-594-0259 (24 hour direct line)
e-mail: **qex@arrl.org**

Subscription rate for 6 issues:

In the US: ARRL Member $22, nonmember $34;

US, Canada and Mexico by First Class Mail: ARRL member $35, nonmember $47;

Elsewhere by Surface Mail (4-8 week delivery): ARRL member $27, nonmember $39;

Elsewhere by Airmail: ARRL member $55, nonmember $67.

Members are asked to include their membership control number or a label from their *QST* wrapper when applying.

In order to ensure prompt delivery, we ask that you periodically check the address information on your mailing label. If you find any inaccuracies, please contact the Circulation Department immediately. Thank you for your assistance.

About the Cover

PTC uses DSP to narrow the occupied bandwidth of analog voice signals (p 9).

Features

Columns

May/June 2000 *QEX* Advertising Index

THE AMERICAN RADIO RELAY LEAGUE

The American Radio Relay League, Inc, is a noncommercial association of radio amateurs, organized for the promotion of interests in Amateur Radio communication and experimentation, for the establishment of networks to provide communications in the event of disasters or other emergencies, for the advancement of radio art and of the public welfare, for the representation of the radio amateur in legislative matters, and for the maintenance of fraternalism and a high standard of conduct.

ARRL is an incorporated association without capital stock chartered under the laws of the state of Connecticut, and is an exempt organization under Section 501(c)(3) of the Internal Revenue Code of 1986. Its affairs are governed by a Board of Directors, whose voting members are elected every two years by the general membership. The officers are elected or appointed by the Directors. The League is noncommercial, and no one who could gain financially from the shaping of its affairs is eligible for membership on its Board.

"Of, by, and for the radio amateur, "ARRL numbers within its ranks the vast majority of active amateurs in the nation and has a proud history of achievement as the standard-bearer in amateur affairs.

A bona fide interest in Amateur Radio is the only essential qualification of membership; an Amateur Radio license is not a prerequisite, although full voting membership is granted only to licensed amateurs in the US.

Membership inquiries and general correspondence should be addressed to the administrative headquarters at 225 Main Street, Newington, CT 06111 USA.

Telephone: 860-594-0200
Telex: 650215-5052 MCI
MCIMAIL (electronic mail system) ID: 215-5052
FAX: 860-594-0259 (24-hour direct line)

Officers

President: JIM D. HAYNIE, W5JBP
3226 Newcastle Dr, Dallas, TX 75220-1640

Executive Vice President: DAVID SUMNER, K1ZZ

The purpose of *QEX* is to:

1) provide a medium for the exchange of ideas and information among Amateur Radio experimenters,
2) document advanced technical work in the Amateur Radio field, and
3) support efforts to advance the state of the Amateur Radio art.

All correspondence concerning *QEX* should be addressed to the American Radio Relay League, 225 Main Street, Newington, CT 06111 USA. Envelopes containing manuscripts and letters for publication in *QEX* should be marked Editor, *QEX*.

Both theoretical and practical technical articles are welcomed. Manuscripts should be submitted on IBM or Mac format 3.5-inch diskette in word-processor format, if possible. We can redraw any figures as long as their content is clear. Photos should be glossy, color or black-and-white prints of at least the size they are to appear in *QEX*. Further information for authors can be found on the Web at **www.arrl.org/qex/** or by e-mail to **qex@arrl.org**.

Empirically Speaking

A lot is happening in Amateur Radio: licensing reform, discussions of new bands, expanded satellite operation, and so forth. We see fresh inspiration in many parts of the experimental arena, too. Amateur Radio has such diversity that it's difficult to find ways to give it all the coverage it deserves.

Some of you didn't like the few relatively simple projects we ran last time. It is remarkable, though, how little is printed generally about AF through MF. Researchers are discovering some very interesting things about antenna system behavior and wave propagation down there. Over the next year, we will bring you some of their results; we'll also keep you up to date on progress in audio coding, compression and digital transmission. We have a nice collection of HF through microwave antenna articles in the queue, too. We'll continue to emphasize advancement and understanding of frequency-synthesis and power-amplifier techniques. In this issue, correspondents present both background material and newly fashioned points of view on that last subject. Thanks to you writers and reviewers who were so patient while we got "up to speed" on it.

It seems like a good time to look back on the legacies of *QEX*, *Communications Quarterly* and before that, *ham radio*. Now that those publications are effectively consolidated, we'd like to see the combination grow to be more than just the sum of its parts. Ours is a unique opportunity to build a better platform to document progress in our chosen field, celebrate the accomplishments of our colleagues and sustain important discussions. Perhaps we should bring in additional columns or news items. Maybe you would like to see more theoretical articles or instead, more practical applications. The balance we strike depends on you. Please drop us a line.

On March 21st, the FCC issued a Notice of Inquiry regarding software-controlled radios. This notice is on the Web at **www.fcc.gov/Daily_Releases/Daily_Business/2000/db0321/fcc00103.txt**. The commissioners clearly are trying to understand the wide-ranging impact of digital radio technology on their management of spectrum and certification of equipment. In addition, interoperability issues are raised. We will be filing comments and we hope you will, too: This is important! Check it out.

In This Issue

Goals for compression and radio transmission of digitized voice include reduction in occupied bandwidth (bit rate), improvement in quality or both. Charles Brain, G4GUO, and Andy Talbot, G4JNT, have taken the plunge into digital voice over Amateur Radio—and yes, it's legal despite our erroneous warning. We shall listen with interest to hear of results over long-haul paths with their system. It takes advantage of the coding algorithms that have been so successful in digital recording and broadcasting applications, distilled to the chip level. Don't be surprised to hear these signals on the HF phone bands before long.

My own approach involves many of the same DSP principles, but it is transmitted differently: as analog phone. Before committing to a specific technique, I did a fair bit of research on auditory coding. I hope you find the results as interesting as I did.

Johan Forrer, KC7WW, presents a tool that every serious student of propagation should want: a channel simulator. He begins with modeling theory, then describes his practical implementation and test results. Much of this material appears in the *Proceedings of the 18th ARRL and TAPR Digital Communications Conference*, Phoenix, Arizona, September 1999 (ARRL Order No. 7679), as does some of G4GUO's.

L. B. Cebik, W4RNL, studies log-periodic dipole arrays (LPDAs) in the first part of a series. He begins by looking at "short-boom" designs: 60-100 feet! As you can imagine, the next part will cover units requiring a bit more acreage. John Stephensen, KD6OZH, contributes the second installment on his homebrew transceiver. IF, AGC and audio circuits are featured.

Zack Lau, W1VT, presents a no-tune waveguide filter for 10 GHz in his column.—*73, Doug Smith, KF6DX, **kf6dx@arrl.org**.*

Practical HF Digital Voice

High-quality voice communication is possible without exceeding SSB bandwidth or expensive broadcast studio equipment.

By Charles Brain, G4GUO, and Andy Talbot, G4JNT

[Editor's note: We goofed! The transmission of telephony in digital format (emission designator J1E or J2E) is perfectly legal in the phone bands. The restriction placed on transmitted baud rate by §97.307(f)(3) of the FCC rules does not apply. In fact, there is no upper limit on the bit rate for this mode. See the sidebar by ARRL Technical Relations Manager Paul Rinaldo, W4RI. Some of this material is from Charles' paper in the Proceedings of the 18th ARRL/TAPR Digital Communications Conference*, some from Andy's paper in* RadCom*, March 1999.]*

This whole project began with a conversation over the telephone: Andy said that it would be fun to transmit "real-time" digital speech on the amateur bands. Now there was a challenge! As he is located some 70 km away over a fairly obstructed path, it would need to be on HF—even more of a challenge!

For several years, digitized voice has been transmitted in a bandwidth comparable with normal analog voice communications using existing transmitters and receivers. After our phone call finished, Charles then went away and had a long think.

Digital Communication Techniques

To fully appreciate why one data communication technique is employed over another, we need to cover digital communication techniques and the problems of the HF environment. When properly implemented, digital communications can show considerable advantages over their analog counterparts with regard to quality and robustness through noisy transmission media: Consider the quality of CD music recordings over the old vinyl or tape systems and the new digital telephone networks versus the old systems. There are several major issues to be resolved before the conversion is made.

Sampling Rate Selection

To digitize an analog signal such as voice, it first must be sampled; that is, turned into a series of numerical values. Sampling theory dictates that the sampling rate must be at least twice the highest-frequency component present (the Nyquist criterion). Any components at more than half the sampling rate will appear as spurious components at other frequencies, causing distortion. This is called *aliasing*. The high-frequency components need to be removed by conventional filtering before digitization. For a voice signal as transmitted using telephone or SSB, the frequency range of 300-3300 Hz is usually considered important and therefore requires a

7 Elverlands Close
Ferring, West Sussex
BN12 5PL
United Kingdom
chbrain@dircon.co.uk

15 Noble Rd
Hedge End, Southampton
SO30 0PH
United Kingdom
g4jnt@arrl.net

sampling rate of at least 6.6 kHz. In practice, to ease the anti-aliasing filter's design, a sampling rate of 8.0 kHz is often adopted.

Bit-Resolution and Quantization Noise

Since an analog signal has an infinite number of instantaneous amplitude levels, these cannot be represented exactly; it is necessary to choose a suitable number of levels to represent the signal. Instead of levels, it is more convenient to think of the number of bits (N) needed to give the corresponding quantization: 8 bits give 2^8 (256) absolute levels. Sixteen bits per sample give 2^{16} (65,536) levels. The effect of the random instantaneous error at each sampling point is to add a noise component to the signal, referred to as quantization noise.

A simple rule of thumb can be applied here: The best SNR that can be achieved is given by:

$$\text{SNR} \approx (6N-1.75)\ \text{dB} \qquad \text{(Eq 1)}$$

The 1.75 dB is a "fiddle factor" that sometimes has slightly different values in various textbooks, but SNR is approximately $6N$. If a figure of 40 dB is taken as good communications quality, then 8-bit quantization—allowing about 48-dB of SNR—would be adequate. This is the system we adopted—although in slightly modified form—on the public telephone network.

Choosing a Data Rate

We can see that for 8000 samples per second, sampling at 8 bits per sample, a total of (8)(8000) = 64,000 bits per second (b/s) are generated.[1] The digital telephone network has enough bandwidth with optical fiber and microwave links to pass 64 kb/s directly, but a radio communications link does not have this luxury! At HF, we want to pass digital voice over a bandwidth comparable with SSB (3 kHz). At VHF—if NBFM is taken for the standard channel width—we can increase this figure to 12 kHz, but to preserve the enhanced voice quality that good-SNR FM can give, more quantization levels should be used.

Although it is theoretically possible to transmit 64 kb/s in a 3000-Hz bandwidth, the SNR that is required for a sufficiently low error rate is very high—around 64 dB according to Shannon's information theorem. Therefore, other techniques must be adopted to transmit digitized voice signals. A data rate comparable with the RF bandwidth is wanted for optimum transmission at SNRs ratios that would be just acceptable for poor speech quality: around 3000 b/s for 10-15 dB SNR in a 3-kHz bandwidth.

Choosing a Voice Coder (Vocoder)

A number of candidate systems were studied. The vocoder must operate at a low data rate, be inexpensive, stand alone and be reasonably available. The systems considered were: LPC-10e (linear predictive coding), MELP (multiband excited linear-predictive coding), AMBE (advanced multiband excited coding) and various CELP (codebook-excited linear-predictive coding) systems.[2]

We experimented with LPC-10e and even managed to implement a version of it on a Motorola 56002EVM. The speech was understandable but we never did get it to track the pitch correctly. Having listened to a commercial implementation of LPC-10e, we decided that it did not have acceptable speech quality anyway.

We then went on to find an implementation of MELP (the 2.4-kbps DOD standard) on the Internet. We got the code to compile and added some Win95 sound-handling routines. The speech quality was much better, but it consumed about 90% of the CPU resources on Charles' P133 machine. In addition, after contacting the patent holders, we found that they were not at all happy with what we were doing.

We then looked at CELP-based systems. These require large codebooks and clever search algorithms, some things we thought were beyond the ROM capability of the Motorola evaluation module and available programming skills. Finally, we settled on the AMBE vocoder chip manufactured by DVS, Inc.[3] This chip is relatively cheap, has very good sound quality, may use data rates between 2400 and 9600 bps, and the manufacturer would sell us some!

The technique adopted codes the voice to reduce the number of bits/s needed for transmission. There has been a considerable amount of research done on various techniques for doing this over the last decade or so, and some very effective compression schemes are now available. The techniques are too complex to cover in any detail here; they usually involve modeling the human voice tract and coding the various elements, such as voiced and unvoiced sounds, in efficient ways.

As an example, GSM mobile phones

Is Digital Voice Permissible under Part 97?

There has been some discussion about Part 97 of the FCC Rules and whether digital voice is "legal." A careful reading of the Rules will show that digital voice is indeed provided for. Read on.

Q. Is HF digital voice classified as "*Data*," thus subject to the provision in §97.307(f)(3), namely "The symbol rate must not exceed 300 bauds…"

A. No. It is "*Phone,*" also called "*Telephony*." The *Data* symbol-rate limitations do not apply to this mode.

Q. What is the emission designator for HF digital voice?

A. Digital voice is *Phone*, defined in §97.3(c)(5) as: "Speech and other sound emissions having designators with A, C, D, F, G, H, J or R as the first symbol; 1, 2 or 3 as the second symbol; E as the third symbol." (It rambles on…)

The first symbol of the emission symbol depends upon the modulation of the main carrier. Typically, the output of the digital-voice modem would be fed into a single-sideband, suppressed-carrier (SSB-SC) transmitter, in which case the first symbol would be "J." (If the main carrier of the transmitter is modulated in some other way than SSB-SC, then choose from the permissible ones: A, C, D, F, H or R, which are explained in §2.201 in Part 2 of the Rules, readily available in *The ARRL's FCC Rule Book*.)

The second symbol in this case is "2," meaning: "A single channel containing quantized or digital information with the use of a modulating subcarrier, excluding time-division multiplex."

The third symbol is "E" for "Telephony."

So, the most likely HF digital voice emission symbol will be "J2E."

Q. Will other amateur stations think that digital voice stations are unauthorized or even intruders?

A. It's likely that some will, until digital voice is more familiar and accepted. Old timers will recall that, in the days of yesteryear when wall-to-wall full-carrier DSB-AM reigned supreme, the introduction of SSB wasn't without angst. The best approach is to follow **The Amateur's Code** and inform other stations on conventional SSB what you're doing.—*Paul Rinaldo, W4RI, ARRL Technical Relations Manager*

[1]Notes appear on page 8.

use a technique that allows transmission at 13,000 bits/s. Whatever technique is used for voice encoding, there is usually a trade-off between data rate and the quality of the resulting speech. Some of the early systems had a very synthetic-sounding, "Dalek-like" result. Modern variants provide very much better toll-quality speech.

AMBE appears to offer major improvements over earlier systems. It moves away from the concept of modeling the voice tract and instead models the spectrum of the signal every 20 ms. Not many technical details appear to be available to date, as it is still a commercial system. Nonetheless, the results of test programs show the technique to be better than any of the 'ELPs. It has thus been adopted for at least one of the new satellite-based mobile-phone systems. Much more importantly for us, a single-chip solution is available for converting from microphone input to encoded digits. So rather than try to write vocoding DSP software based on published algorithms, we decided to just buy a chip to do the job.

The AMBE1000 chip by DVS implements the whole process and provides the user with extensive tradeoffs between data rate and link quality, as well as forward error correction (FEC). Eventually, the data rate we adopted was 2400 bits/s of voice data plus 1200 b/s of FEC, giving a total of 3600 b/s to be transmitted over the RF link. The IC produces samples every 20 ms and can be regarded as a real-time system in this sense. Any 20-ms samples that get lost just create glitches in the speech that cause minimal disturbance and often go unnoticed.

Programming the Vocoder Module

In use, the AMBE chip must be programmed at turn-on to set the operating conditions, and the easiest way to do this is to include an on-board PIC microprocessor. The digitized output samples at a rate of 3600 bits/s are sent via an EIA-232 interface to the modem—in packets of nine bytes for each 20-ms frame. The data rate for this part of the link is 19.2 kbaud. If you do the math on this, you will find there is a lot of spare capacity for programmers who want to use the development board for their own purposes. An example of this would be for inclusion of data and control signals.

Choosing a Modem

After a literature search, we came to the conclusion that the HF modem must use parallel-tone, PSK technology.[4] (See Fig 1.) It is relatively easy to implement and well proven; it runs on Charles' DSP evaluation module and is more suitable for digital voice transmission than serial-tone modems. Serial-tone modems tend to produce long bursts of errors when the equalizer fails, as opposed to the more random errors produced by a parallel-tone modem. Speech is unlike computer data in that occasional errors do not significantly affect its intelligibility.

PSK

In bipolar phase-shift keying (BPSK), instead of changing the transmission frequency for binary 1s or 0s, the phase is reversed—or effectively, the signal is inverted—between 0 and 1 states. It is possible to show that there is at least a 3-dB improvement in SNR-versus-error-rate performance over frequency-shift keying (FSK) given an "ideal" demodulator for each mode, and very much better than this is possible in practice. PSK has begun to replace keyboard-to-keyboard RTTY on the amateur bands recently in the form of PSK31 (see the articles in December 1998 and January 1999 *RadCom* or July/August 1999 *QEX* by Peter Martinez, G3PLX). For very nearly the same data rate as RTTY, the bandwidth needed has shrunk from around 300 Hz to 30 Hz with a corresponding increase in reliability and error rate. By using four phase states instead of two (90° apart, quaternary phase-shift keying or QPSK), it is possible to encode two bits at once without increasing the bandwidth. This does incur a 3-dB penalty because the transmission power is shared between twice as many bits in a given time.

This technique is available in PSK31, where it is included as an option for adding the extra data needed for FEC in noisy environments. A properly filtered PSK signal has a bandwidth that can approach the baud rate (in fact, PSK31 is optimized to do just this). If it is not implemented correctly—with waveform control and filtering—the bandwidth of the signal can easily spread alarmingly in a manner analogous to CW key clicks.

For the 3600 bits/s needed for the digitized voice experiments, either binary PSK (BPSK) at 3600 baud or QPSK at 1800 baud would be adequate. The QPSK signal at potentially 1800-Hz bandwidth could even be transmitted unmodified over SSB radios. However, while this technique is ideal for UHF or "clean" VHF links, there are particular characteristics on a typical HF transmission path that make simple high-baud-rate signals very prone to errors and frequently unusable.

Designing the Modem

Amateur Radio equipment has very poor filtering compared to military equipment. The filters tend to be quite narrow and have poor group-delay characteristics. This means the modem must use a narrower bandwidth than it would with the equivalent military equipment. This ruled out the MIL-STD-188-110A 39-tone modem.

In the end, we decided on a 36-tone modem, with a baud rate to match the 20-ms frame length of the AMBE vocoder chip. This provides a raw data rate of (36)(2)/(20 ms) = 3600 bits/s and enough time for a 4-ms guard period. The guard period is required to give the modem some multipath tolerance.

Each tone carries two bits of data in each baud interval. Unlike military modems, our modem has no Doppler-correction tone and no slow "sync-on-data" facility. So far, both of these facilities

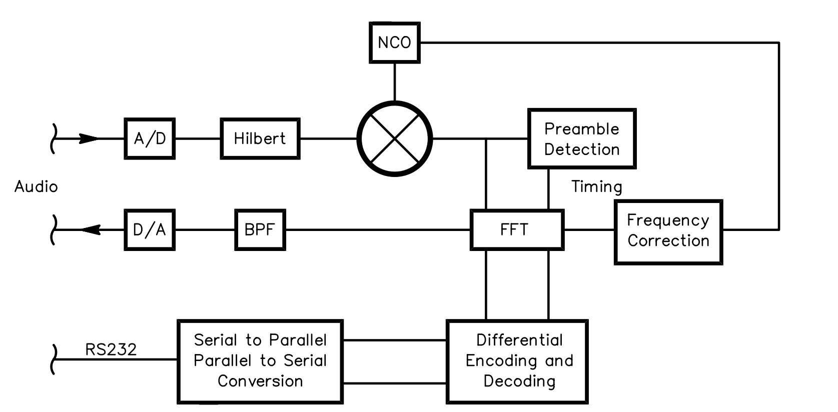

Fig 1—A block diagram of the modem.

have been unnecessary. The modem remains in lock for long periods, well beyond our ability to carry on a dialogue.

We then did some *MATLAB* computer simulations that showed that the modems must be within 5 Hz of the correct frequency to work properly. To achieve initial timing and frequency-offset correction, the modem used three BPSK-modulated preamble tones. It differentially decodes them using a delay of one baud interval. It then integrates the received symbol over that time; from this, it deduces the timing. Then, by looking at the energy in the FFT bins on either side of the preamble tones, it calculates the frequency error and makes a correction by translating the received signal in frequency using a complex mixer. The reason for three tones is to provide some frequency diversity, as on-air testing showed a single tone could get lost during deep fades.

Each symbol consists of 160 samples; the sample rate is 8 ksamples/s. The 36 tones were created by using a 128-point complex FFT. The guard period is added by taking the last 32 samples from the output of the FFT and adding them to the beginning of the FFT samples to form a total of 160 samples. These 32 samples form the 4-ms guard period. The data are differentially coded and mapped to the output phases using Gray coding before transmission.

After the preamble has been sent, the modem sends a reference vector by transmitting a known phase on each of the 36 tones. A "synch" sequence follows this. When the receiving modem detects the synch sequence, it ceases hunting for the preamble and starts passing (we hope!) valid data to the vocoder board.

When the operator releases the PTT, the modem detects the loss of voice data and transmits an EOM (end-of-message) sequence embedded in the data stream. This message is, in fact, the SOM (start-of-message) sequence, inverted. Transmit/receive control of the modem is triggered by the presence/absence of data from the vocoder; there is, at present, no formal protocol between them.

One problem with parallel-tone modems is that they tend to produce signals with very high peak-to-mean ratios. To combat this, our modem uses different initial phases on each of the tones and applies clipping and filtering to the output signal. This allows the transmitter to be driven quite heavily before errors begin to appear in the received signal. The simplest way to set the audio level is to increase the drive level until ALC action occurs, then back it off a bit.

The modem is capable of full-duplex operation. It does not require a feedback channel and so can be used in broadcast operation; that is, with one sender and many listeners. The modem also incorporates a CW-ID feature to comply with UK regulations—the old meets the new. The CW call sign is hand coded into the DSP software, but it can be switched off. It is not sent at the end of each transmission, but after a programmable period.

Fig 2 shows a compressed spectrogram of an off-air transmission. The three preamble tones can be clearly seen along with the selective fading (diagonal stripes), as can the carrier of an AM broadcast station in the background and a burst of interference at the end. The distinct vertical stripes were, in fact, pauses in the speech.

The greatest problem during operation is multipath. Sky-wave signals frequently arrive after several ionospheric hops, with the same instantaneous element of signal arriving at different times after having traveled different distances. For a signal such as SSB voice, these two or more signals will cause alternate cancellation and reinforcement, giving the characteristic multipath fading as a notch passes through the audio passband. Differences in arrival time of typically up to 5 ms are often observed, and in poor propagation conditions, can reach a lot more than this.

The effect on digital signals can be much more catastrophic than it is for analog speech. A particular bit of information arrives at several different points in time, so it can easily land on top of another bit arriving via an alternative path. This mixing up of received information causes *intersymbol interference* and is the major cause of bit errors on what might otherwise appear to be a good link with a strong signal.

There is a way around this. If we can send one symbol in such a way that it remains uncorrupt when mixed with a delayed (say, 0 to 5 ms) version of itself, the error rate due to intersymbol interference can be reduced or even elimi-

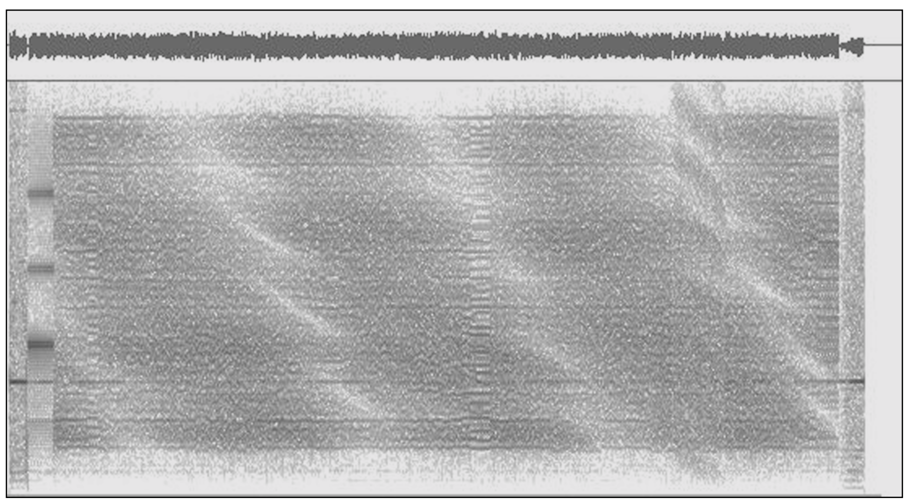

Fig 2—Off-air spectrogram of M36 modem waveform.

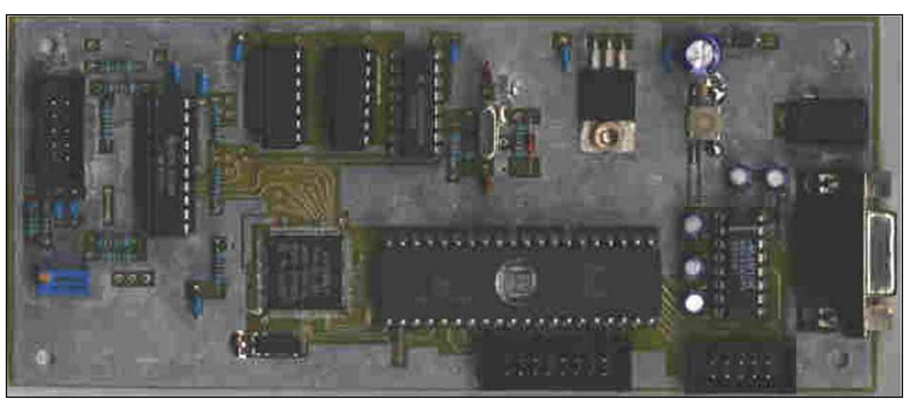

Fig 3—Prototype vocoder board.

nated. One method is to reduce the baud rate so much that the 5-ms multipath period becomes insignificant. A figure of 20 ms is often used in practice, resulting in 50-baud signals. It is no coincidence that the data rate adopted for RTTY signals for many years has been in the 45 to 75-baud region!

To reduce our 3600 bits/s to 50-baud signaling means trying to compress 72 bits into one symbol. While there are some direct techniques of doing this, such as quadrature amplitude modulation, these are prone to other types of errors and inefficiencies. Another system is needed that is more resistant to in-band interference. The technique is as follows.

Instead of using a single carrier modulated with a complex multilevel waveform, we use a large number of multiple carriers, each one modulated with a simple waveform. If there are N carriers, each one independently modulated with 50-baud QPSK, then it is possible to transmit data at $(2)(50N)$ bits/s.

The spacing between each carrier pair must be consistent with the baud rate, and carrier spacing equal to at least the symbol rate is required. If we do a few calculations, it soon becomes evident that many solutions are possible for 3600 bits/s in a voice bandwidth.

Fig 4—Current digital voice station at G4GUO.

FEC

The modem has no inherent FEC capability; instead, it uses the FEC in the AMBE vocoder chip itself. The vocoder tailors the FEC to match the significance of bits in the data stream, so it can probably do a much better job than we can. It is a shame, however, to waste the soft-decision information generated by the modem.

The AMBE chip uses both Golay and Hamming codes for error detection and correction. It follows the normal convention during periods of errors, trying to guess what was sent by looking at previous frames, then ultimately giving up. The format used is 2400 bits/s speech and 1200 bits/s FEC.

The first tests were done without the FEC enabled—whoops! The system worked quite well; but occasionally gave off very loud screeches. After the FEC was enabled, however, fewer strange noises came from the system. When the modem was initially tested without FEC, one third of the tones were in fact transmitting no data whatever and were just wasting energy.

Some experiments were done using a data interleaver, but they were abandoned because the interleaver adds a large delay to the voice. During deep fades or periods of interference this spreads errors over multiple vocoder frames and so prolongs the dropout.

Development of the Vocoder PC Board

The vocoder board consists of a Motorola MC14LC5480P codec using µ-law coding, an AMBE chip, a PIC17C44JW microcontroller, some HC-series glue logic and an EIA-232 interface. The AMBE is a 100-pin surface-mount chip that Charles soldered onto the board by hand. After five boards, he began to get very tired of doing it!

For the PC board, he used the services of ExpressPCB in the US. In hindsight, this was a mistake; their free PC board software is not compatible with anyone else's, so it pretty much locked us into using them once we had started. Their service is very good, however: Charles e-mailed the files on Monday and had the boards back in the UK by Thursday. He also found most of the components from DigiKey[5] in the US as well; it worked out cheaper than buying them in the UK, especially for the microcontrollers.

We used the 17C44 PIC microcontroller for a number of reasons: first, so we could use one crystal to drive both the AMBE and the PIC (the AMBE requires a 27-30 MHz clock); second, the 17C44 PIC has enough ROM available to allow addition of quite complex code at a later date (in fact, Charles has since done a version of his software that can encrypt the speech using triple DES encryption in real-time); finally, because we already had the development tools available. Each board costs us about $150 to make, and we have so far made five.

On-Air Testing

The system has been tested over a 70-km path using frequencies in the 40-meter band. We made our first successful contact at the first attempt on the 27th of March, 1999. This is not a weak-signal mode; it requires about a 25 dB of SNR to function. When working, however, it makes HF sound like a telephone conversation. There is no background noise—total silence—except for the "comfort noise" inserted during gaps in the speech by the vocoder itself. The system can tolerate strong CW interference and the multipath-induced selective fading found on HF. SSB interference is more troublesome—it affects more than one of the tones. If RTTY/CW interference gets too bad, it is possible to switch a DSP notch filter into the circuit: There is enough power in the FEC to cope with the missing tones. The notch filter must be switched out during the preamble phase.

The most effective and impressive demonstration was one evening in April when a QSO lasted for an hour and a half as the sun set. Copy started out as perfect, with no lost preambles or garbled messages. The multipath became worse as dusk arrived so copy worsened slightly, but it wasn't until nearly dark when the link had almost faded out completely that it became unusable.

The weakest part of the modem is the preamble phase. To help remedy this, we added the ability to save the frequency offset correction and timing epoch after each successful preamble synchronization. If, for some reason, the receiving modem misses the start of the transmission, it is then possible to press a button on the front panel and revert to the last set of synch information. In a one-to-one QSO, this works most times.

Another change allows the different tones to be given different amplitudes to compensate for the amplitude response of the transceiver. The group delay in the transceiver does reduce the modem's tolerance to multipath. With The new generation of IF-DSP radios, this will not be a problem as their filter characteristics are much more suited to this kind of operation.

Along with the HF testing, Charles has also used the system on 2 m, both on SSB and FM. There is no reason it would not work via a repeater since there is no ARQ (but we have not tried it).

Conclusion

It is now possible for the home constructor to build—for about $300—a portable, working digital voice system for HF with near-toll-quality audio. This system can be used equally well to experiment with digital speech using different DSP modems on different frequencies. For further information and a full technical description, plus some sound files, surf along to Charles' Web site.[6] Once some boards have been made up in the US, we hope to be able to try some transatlantic tests.

Notes

[1]Consider CD music recording. A sampling rate of 44.1 kHz is chosen to allow a 20-kHz maximum audio frequency; 16- bit quantization is used to give a dynamic range of greater than 90 dB. With two independent channels for stereo, this results in a data rate in excess of 1.4 MB/s.

[2]More information on these technologies may be found in L. R. Rabiner and R. W. Schafer, *Digital Processing of Speech Signals*, (Upper Saddle River, NJ: Prentice-Hall, ISBN 0-13-213603-1); and V. K. Madisetti and D. B. Williams, eds, *The Digital Signal Processing Handbook*, (Boca Raton, FL: CRC Press, ISBN 0-8493-8572-5).

[3]Digital Voice Systems (DVS), Inc may be found on the Web at **http://www.dvsinc.com/**.

[4]It is no coincidence that this low-baud-rate, parallel-tone approach has been adopted for digital TV transmission where 2048 parallel tones are employed in an 8-MHz bandwidth. Multipath on the UHF TV frequencies is typically a few microseconds in duration, and the individual baud rate for each tone is consistent with this. The technique is further refined to minimize bandwidth by using the minimum carrier spacing and ensuring that side lobes from one modulated carrier do not interfere with those adjacent to it. The system is referred to as Coded Orthogonal Frequency Division Multiplexing (COFDM). A similar coding method with 1536 tones of 1-kHz spacing is used for the terrestrial Digital Audio Broadcasting network. Parallel-tone modems are one of the candidate technologies for HF digital broadcasting and there is a lot of professional interest in parallel-tone technology.

[5]Digi-Key Corporation, 701 Brooks Ave S, PO Box 677, Thief River Falls, MN 56701-0677; tel 800-344-4539 (800-DIGI-KEY), fax 218-681-3380; **http://www.digikey.com/**.

[6]G4GUO's Web page is found at **www.chbrain.dircon.co.uk/dvhf.html**. The page includes sample audio and project updates.

PTC: Perceptual Transform Coding for Bandwidth Reduction of Speech in the Analog Domain, Pt 1

A new method for optimizing the bandwidth of phone signals using auditory psychophysics

By Doug Smith, KF6DX

A revolution is afoot in Amateur Radio: An increasing number of operators are producing high-fidelity audio in the narrow bandwidths available to us on HF SSB. Many of us have grown tired of listening to the same old "communications-quality" signals. We have yearned for a more pleasurable sound from our equipment. Coupled with skills learned in professional recording and broadcast studios, the availability of high-quality HF transceivers in the last few years has enabled some startling accomplishments in narrow-band audio quality.

It is remarkable what can be achieved in a bandwidth (BW) of only 3 kHz. Characteristics of speech processing can be manipulated to allow the perception of much greater BW. Properties of human speech can be further exploited to reduce the occupied BW of phone emissions quite significantly. That is the subject of this paper.

PO Box 4074
Sedona, AZ 86340
kf6dx@arrl.org

Drawing on the extensive audio-coding research of others, I will show how certain human speech and hearing attributes lend themselves to analog BW compression of speech. In Part 2, I will demonstrate how a speech signal of 4-kHz BW is compressed to occupy less than 1 kHz and a full-range signal of 15-kHz BW to less than 4 kHz. I will emphasize the technical tradeoffs that influence sound quality. The goal is to retain the perceived quality of the original, uncompressed signal. First, however, please follow me through a little history and background as I lay down the basis for my invention.

A History of Phone Modes

In the days before SSB became popular on our bands, AMers used a lot of plate-modulated vacuum-tube equipment. It was relatively easy to obtain a broad baseband frequency response with this type of gear—perhaps it was too easy to be too broad! It was also easy to sustain lots of interference and noise, since each information-bearing sideband reaches only about 1/6 of the total output power. Although each sideband is a mirror image of the other, selective fading often makes it difficult to recover all of the energy from both sidebands simultaneously. Carrier fades tend to cause severe distortion. Modern methods of exalted-carrier, synchronous detection have largely solved those problems, but the occupied BW of AM has relegated it to some obscurity on the Amateur Radio bands. It is retained for broadcasting because it is detectable with relatively simple equipment.

SSB is popular because all the output power is dedicated to the information and emissions occupy only the BW necessary for perfect reproduction. SSB also does not suffer from the distortion caused by carrier fading. It does impose constraints, however, that result in loss of fidelity. In the filter method of SSB generation, it is usually essential to "roll off" the low-frequency response to ensure adequate suppression of the carrier and opposite sideband. Even with the phasing method, opposite-sideband suppression may suffer if low audio frequencies are not attenuated. These problems have made it difficult to achieve good low-frequency response in SSB. Operators have been frustrated (until recently) by the limitations of IF filters in their transceivers. They can seriously attenuate both low- and high-frequency audio content.

SSB experimenters are well aware of certain speech-processing tools, such as AF and RF compressors. Automatic level control (ALC) is found in every modern rig. ALC is just a form of compressor that prevents drive signals from exceeding the PEP limitations of the transmitter. In a peak-limited system, average output power depends heavily on the nature of the modulation. Some voices produce peak-to-average ratios of up to 15 dB; a station running 1500 W PEP might only produce an average output of about 50 W!

Because of the Hilbert-transform or "repeaking" effect of SSB, AF limiting achieves only a modest intelligibility increase even with large compression ratios. IF or RF compression avoids this problem—6 dB or more improvement in average output power is possible.

For audiophiles, the trouble with any compression scheme is that it adds distortion. Naturally, any departure from linearity involves harmonic distortion (HD) and intermodulation distortion (IMD). At high compression ratios, an AF compressor especially suffers from HD effects that reduce clarity. Formant energy and plosive sounds tend to be sacrificed. IF and RF compressors generate HD that falls outside the band of interest; hence it is easily removed by filtration. These compressors still create in-band IMD, though; this distortion ultimately limits their effectiveness.

While on the subject, let's note that distortion caused by our electronics limits the quality level we can finally attain, no matter what we do. Many receivers produce as much in-band IMD as do transmitters. The phase and amplitude of each IMD product are influenced by many variables. Levels can be measured, however, and the transfer function ascertained. Whether these products augment or diminish intelligibility seems to involve another set of variables that depend on the nature of human speech and hearing systems. As I'll highlight later, these cannot be directly measured.

So the question is, How can we produce better audio quality while using a narrow BW? A lot of work has been done on this problem, especially with respect to digital coding of audio.[1, 2, 3, 4, 5, 6] The impetus for this work has been provided by the recording industry, telephone companies and interest in passing audio over Internet connections at low bit rates. Most of the breakthroughs in such coding have focused on characterizing human speech in ways that are efficiently represented by ones and zeros. Progress on BW compression in the analog domain has been frustrated by increasing emphasis on digital modes. Digital methods may have an advantage in error detection and correction, and in signal-to-noise ratio (SNR), but they likely will never be the most BW-efficient techniques for speech coding.

Linear predictive coding (LPC) and other methods[7, 8, 9] have concentrated on passing parameters that describe features of speech production. They are "lossy" in the sense that they sacrifice perfect reproduction of the input waveform for BW reduction. Perceptual audio coders[10, 11, 12] code in such a way that redundancy and irrelevancy in speech are removed, reducing BW. Both approaches take advantage of the fact that only perceived quality matters. I shall adopt this as my sole criterion for the remainder of this discussion.

Evaluating the Human Hearing System

Speech communication is crucial to our society. It conveys the sense of how someone feels, how they are thinking and some idea of who they are more than any other form. Nothing is more comforting than hearing the voice of a loved one in dire times. I postulate, therefore, that this mode of telecommunications will never be replaced.

Because of that suspicion, I can write that the secondary goal of any speech-coding scheme is to preserve those characteristics of speech that allow us to recognize the speaker, along with the nuances that are so important. In other words, we have to conserve certain distinctive qualities of speech so that we can't tell the speech was coded. Let's examine what those qualities are and what it is about human hearing that influences perception.

Perception vs. Measurement

In the study of the human hearing system, it must be clear that there is no objective means of measurement. All information about what someone hears (or doesn't hear) must be learned subjectively through the responses of the listener. All we can do is ask questions of a subject and attempt to infer something about the nature of sounds. Furthermore, we have no guarantee that a particular stimulus will be perceived in the same way by one subject as another. We therefore define our terms for measurement and perception differently and separately.

Sound *intensity* is a physical measure of air pressure level. Two persons equipped with identically calibrated instruments will measure the same intensity for any given sound. *Loudness* is the corresponding perceptual magnitude. It can be defined as "that attribute of auditory sensation in terms of which

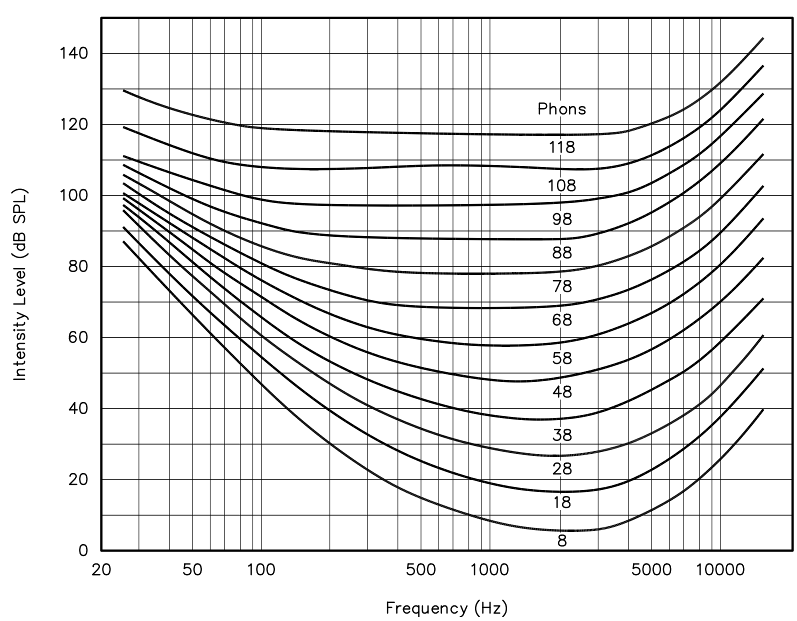

Fig 1—Intensity versus frequency for constant loudness.

[1]Notes appear on page 12.

sounds can be ordered on a scale extending from quiet to loud."[13] The unit of loudness, the *sone*, is defined by subjectively measuring loudness ratios. A stimulus half as loud as a one-sone stimulus has a loudness of 0.5 sones. A 1-kHz tone at 40 dB sound-pressure level (SPL) is arbitrarily defined to have a loudness of one sone.

We might be left to wonder how a unit based solely on individual perceptions can be useful, especially since so much variation exists from person to person. The method of applying stimuli and of obtaining responses from listeners has a large effect on results. Loudness comparison of two equal-frequency tone bursts, however, generally produces reliable and repeatable data. Loudness comparisons between dissimilar stimuli, such as between a pure tone and a polyphonic source, yield unpredictable results because of poorly understood subjective effects. So a quantification of loudness scaling (one sound is half as loud as another) is as good as absolute loudness matching (one sound is the same loudness as another). Additionally, some researchers have observed under many conditions that loudness adds.[14] Binaural presentation of stimuli generally results in loudness doubling and two equally loud sources—if they are far enough apart in frequency—are twice as loud as one alone. Because of other effects described below, this rule must be used with caution, though. There is evidence that loudness addition is far from a perfect description of human perception.[15]

Frequency is a physical measure of a sound's number of cycles per second; each of us can measure frequency identically using similar instruments. We define *pitch* as the perceptual quantity corresponding to frequency. Pitch is to frequency as loudness is to intensity. Note that the relations between loudness/intensity and pitch/frequency are not necessarily linear, nor are the two perceptual measures independent of one another. Under certain conditions, the loudness of a constant-intensity sound can be shown to decrease with decreasing frequency; pitch can be shown to decrease with increasing intensity, even when frequency is held constant.

As ably documented by Fletcher,[16] Stevens and Davis,[17] and others, loudness depends on both frequency and intensity. Fig 1 (after Reference 17) shows some loudness contours. Each curve represents a constant-sone level. These data have been measured countless times, but the basic revelations remain unchanged. The most sensitive frequency region of the ear is between 1.5 and 3.0 kHz and the curves get flatter as the intensity is raised. Further, loudness grows faster with intensity at low frequencies. Finally, the curves reveal the dynamic range of hearing: Single tones below the zero-sone curve are inaudible, while tones above the top line are painful. In fact, we know today that the useful dynamic range of human hearing is substantially less than shown. Extended exposure to sounds well under the top line produces permanent hearing loss in some individuals.[18]

This is Auditory Psychophysics

We're now well into what is called *auditory psychophysics*, or just *psychoacoustics*. Recall that our goal is to exploit the redundancies and irrelevancies in speech to reduce its occupied BW. To identify the irrelevant content, we must discover how well the ear-brain combination discerns differences in intensity and frequency. Moreover, we must try to ascertain the performance of the hearing system in the presence of polyphonic sounds; that is, how certain sonic components tend to dominate others of lesser intensity or of small frequency difference.

I will now expand the discussion to include definitions for various perceptual thresholds, to introduce the idea of *masking*, and to present the concept of *critical bands*.

Thresholds of Hearing

One of the thresholds of hearing, the *intensity threshold*, is defined as the lowest intensity the listener can detect. We cannot directly measure the listener's perception, though; we can only ask whether he or she thinks the sound is audible. This might seem a fine distinction, but the method of measurement determines the threshold as much as the listener's aural gifts.

At or near the intensity threshold, the subject's *criterion level* is in play.[19] He or she might indicate some sound is audible when it *might be* present, or perhaps only when it is *definitely* present. With no incentive to produce correct results (such as large sums of cash), the criterion level is beyond the experimenter's control.

An interesting way of dealing with the uncontrolled criterion-level problem is to use a *criterion-free* experimental model. According to Hall (see Note 19), the simplest of these is the "two-interval, forced-choice" paradigm. In this method, the stimulus is presented at random in one of two observation intervals. The subject is asked to determine in which of the two intervals the stimulus was present. A perfect observer always selects the interval that elicits the larger

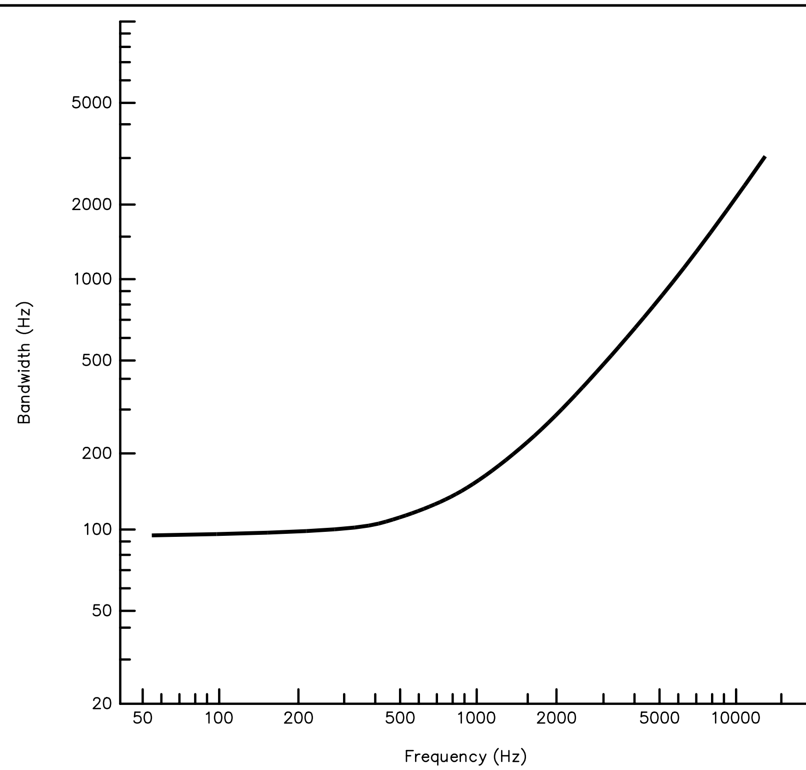

Fig 2—Critical BW versus frequency.

decision variable; thus the criterion level is no longer a factor. He or she has a 50% chance of selecting the correct interval even without actually detecting the stimulus. It can be shown that the *psychometric function* thereby produced solves the criterion-level problem.

I think it interesting to note that all this has a bearing on "A/B" comparisons as commonly done on the air, regardless of the parameter being changed. A measurement criterion such as loudness or signal strength must first be set, then the stimulus presented *at random* to the observer. Any additional information given the observer prior to measurement, such as "A is amplifier off, B is amplifier on," introduces bias in the result. Further discussion of *detection theory* is beyond the scope of this paper.

Getting back to definitions, we may also define *differential intensity threshold* as the ability to detect whether one sound is louder than another. In fact, we may define differential thresholds for other attributes of sounds, such as frequency and duration. A differential threshold is the amount one or more of these attributes must change to allow an observer to detect the change.

In the first half of the last century, German physiologist E. H. Weber gave us the first serious, quantitative depiction of differential thresholds. According to *Weber's Law*, the differential intensity threshold dI is proportional to the stimulus intensity I, or:

$$\frac{dI}{I} = k \qquad \text{(Eq 1)}$$

where k is known as the *Weber fraction*. This alleged constant has also been applied to sensitivity to changes in frequency and BW, as well as nonauditory senses such as color, image sharpness, pain, smell and taste. Very soon after Weber made this "law" known, folks found out it broke down at intensities near absolute thresholds. Physicist G. T. Fechner, also a German, suggested a *modified Weber's Law*:

$$\frac{dI}{(I + I_0)} = k \qquad \text{(Eq 2)}$$

where I_0 is a constant. It's a good approximation, but it apparently doesn't hold exactly.

Masking

Masking is defined as the ability of one sound (the masker) to render another (the desired) inaudible when present simultaneously or closely in time. It is quantified as the difference between the absolute intensity threshold of the desired in the absence of the masker and the elevated intensity threshold of the desired when the masker is present. Fletcher and Munson made a landmark study of the relation between loudness and masking effects.[20] They found that quieter sounds that are close in frequency to dominant sounds are rendered inaudible in proportion to their spectral separation and their relative intensities. They were among the first to use bands of "colored" noise as maskers. An important effect is the relationship between the masker BW and the amount of masking. This relation is most prominent when the desired signal lies within the masker's BW. Noise whose entire BW lies outside the desired signal's frequency does not contribute much to its masking. This is one manifestation of the human hearing system: For many auditory functions, the ear behaves as if it is a set of band-pass filters and energy detectors. These filters are said to occupy critical bands.

Critical Bands and Peripheral Auditory Filters

The above-mentioned relation between BW and masking is only one example of human hearing behavior relevant to the coder I will describe in Part 2. Another example is provided by SSB over HF, where the ear quite often encounters severe phase distortion. The ear seems to tolerate relatively large shifts in the relative phases of speech components without impairing intelligibility, when the components are far enough apart in frequency. Scharf[21] defined the critical bandwidths associated with these theoretical auditory filters as "that bandwidth at which subjective responses rather abruptly change." He measured critical bands using two-tone masking and loudness-summation techniques. Zwicker *et al*[22] measured phase sensitivity using polyphonic sounds. These studies agree fairly well with others performed over the years. Fig 2 is a plot of critical BW versus frequency that averages the Scharf and Zwicker data.

These and other studies support the idea that *differential frequency threshold* increases with frequency. In other words, it is more difficult to discern small frequency differences at high audio frequencies. Since we decided that our perception of things is all that matters, it makes sense to analyze speech signals with a system whose frequency resolution matches that of the human hearing system. It is remarkable that this sort of approach also seems to apply across a broad scale of other things we can classify. The science of image compression and construction, for example, has made extensive use of the methods I will relate in Part 2.

Notes

[1]R. E. Crochiere, S. A. Weber, and J. L. Flanagan, "Digital Coding of Speech in Subbands," *Bell System Technical Journal*, Vol 55, October 1976.

[2]P. P. Vaidyanathan, *Multirate Systems and Filter Banks*, (Englewood Cliffs, NJ: Prentice-Hall, 1992).

[3]M. Vetterli, and J. Kovacevic, *Wavelet and Subband Coding*, (Englewood Cliffs, NJ: Prentice-Hall, 1995).

[4]N. S. Jayant, and P. Noll, *Digital Coding of Waveforms: Principles and Applications to Speech and Video*, (Englewood Cliffs, NJ: Prentice-Hall, 1984).

[5]R. D. Jurgen, "Broadcasting with Digital Audio," *IEEE Spectrum*, March 1996.

[6]P. Noll, "MPEG Digital Audio Coding Standards," *The Digital Signal Processing Handbook*, V. K. Madisetti, and D. B. Williams, editors (Boca Raton, FL: CRC Press LLS, 1998).

[7]L. R. Rabiner, and R. W. Schafer, *Digital Processing of Speech Signals*, (Englewood Cliffs, NJ: Prentice-Hall, 1978).

[8]B. S. Atal, "Predictive Coding of Speech at Low Bit Rates," *IEEE Transactions on Communications*, COM-30, April 1982.

[9]A. Gersho, "Advances in Speech and Audio Compression," *Proceedings of the IEEE*, Vol 82, 1994.

[10]J. D. Johnston, and A. J. Ferreira, "Sum-Difference Stereo Transform Coding," *ICASSP-92 Conf. Rec.*, II, 1992.

[11]D. Sinha, J. D. Johnston, S. Dorward, and S. R. Quackenbush, "The Perceptual Audio Coder (PAC)," *The Digital Signal Processing Handbook*, V. K. Madisetti, and D. B. Williams, editors, (Boca Raton, FL: CRC Press LLS, 1998).

[12]R. V. Cox, "Speech Coding," *The Digital Signal Processing Handbook*, V. K. Madisetti, and D. B. Williams, editors, (Boca Raton, FL: CRC Press LLS, 1998).

[13]B. Moore, *An Introduction to the Psychology of Hearing*, (London: Academic Press, 1989).

[14]H. Fletcher, "Loudness, Masking, and Their Relation to the Hearing Process and Problem of Noise Measurement," *Journal of the Acoustic Society of America*, Vol 45, 1969.

[15]B. Scharf, and D. Fishkin, "Binaural Summation of Loudness: Reconsidered," *Journal of Experimental Psychology*, Vol 86, 1970.

[16]H. Fletcher, *Speech and Hearing in Communication*, ASA Edition, J. B. Allen, editor, American Institute of Physics, New York, New York, 1995.

[17]S. S. Stevens, and H. W. Davis, *Hearing*, (New York: John Wiley & Sons, 1938).

[18]C. M. Harris, editor, *Handbook of Acoustical Measurements and Noise Control*, (New York: McGraw-Hill, 1991).

[19]J. L. Hall, "Auditory Psychophysics for Coding Applications," *The Digital Signal Processing Handbook*, V. K. Madisetti, and D. B. Williams, editors, (Boca Raton, FL: CRC Press LLS, 1998).

[20]H. Fletcher, and W. A. Munson, "Relation between Loudness and Masking," *Journal of the Acoustic Society of America*, Vol 9, 1937.

[21]B. Scharf, "Critical Bands," *Foundations of Modern Auditory Theory*, J. V. Tobias, editor, (New York: Academic Press, 1970).

[22]E. Zwicker, G. Flottorp and S. S. Stevens, "Critical Bandwidth in Loudness Summation," *Journal of the Acoustic Society of America*, Vol 29, 1957.

A Low-Cost HF Channel Simulator for Digital Systems

In the past, HF channel simulators used exotic and expensive computing hardware that was not available to the average amateur experimenter. Here's a simulator based on a low-cost, floating-point DSP evaluation kit.

By Johan B. Forrer, KC7WW

This project was inspired by a desire to develop HF digital communications devices that effectively deal with the variable nature of the ionospheric propagation medium. Simulating the behavior of the ionosphere in real time allows for bench testing of HF modems and other communications devices. In the past, so-called HF channel simulators used exotic and expensive computing hardware that was not available to the average amateur experimenter.

The simulator presented in this article is based on a low-cost, floating-point DSP evaluation kit. It accommodates a wide range of simulated conditions, including CCIR 520-1.[1] The simulation model is an implementation of the Watterson, Gaussian-scatter, HF ionospheric-channel[2] model, which is the *de facto* standard for this kind of work.

The article concludes with a summary of test results for a number of contemporary, forward-error-correcting (FEC) HF digital systems on this HF channel simulator: PSK31, CBPSK and MT63. This simulator is a worthy addition to anyone's array of testing tools for developing DSP data communications algorithms.

The Variable Nature of an HF Channel

HF propagation involves several interrelated phenomena that result in a highly variable propagation medium. This variability is a challenge to anyone designing and implementing effective, high-speed digital communications systems for HF.

The ability to quantitatively evaluate how engineering designs carry through to final implementations often makes the difference between success and failure. Experienced, well-equipped engineers use special tools such as channel simulators to shorten development cycles. These are invaluable, for example, to verify dynamic-range performance, acceptable signal-to-noise ratio (SNR) performance and quite a few other factors such as adjacent-channel interference and frequency/timing tolerances. These are very common

26553 Priceview Dr
Monroe, OR 97456
forrerj@peak.org

[1]Notes appear on page 17.

problems. Protocol performance is of equal importance. This has to do with the efficiency of frame and character synchronization, effectiveness of error control and the success of protocol adaptation.

Although some of these tests may be done on the air, F-layer propagation conditions are almost impossible to repeat; thus, there is no real chance to make comparative tests this way. What we need is a means to create an artificial ionospheric test medium—an "ionosphere in a box"—that can be reproduced at will. Only then is it possible to set up norms and milestones for performance evaluation. Computer simulation is one way to obtain repeatable, quantitative results. A simulation study based on theoretical concepts can provide the basis for establishing expected performance characteristics and may also serve as a guide to requirements for hardware and software. It can provide for continuing development work with minimal risk.

During test and development phases, real-time testing using a HF channel simulator is essential. An understanding of ionospheric behavior and how it impacts communications is key to developing an effective waveform and protocol suitable for high-speed HF digital communications.

Ionospheric Reflection Model

HF communication is typically characterized by multipath propagation and fading. Transmitted signals travel to the receiver over several propagation modes via single or multiple reflections from the E and F ionospheric layers. Because propagation times vary over different paths, signals arriving at the receiver may be spread in time by as much as a few milliseconds.

Ionospheric turbulence causes distortion of both signal amplitude and phase. In addition, different ionospheric layers move up or down, which leads to independent Doppler shift on each propagation mode. In ionospheric sky-wave HF propagation, multipath arises from paths having different numbers of multiple reflections between earth and the ionosphere (multiple-hop paths) and from paths at multiple elevation angles connecting the same end points ("high" or "low" rays). Natural inhomogeneities of the ionospheric layers and polarization-dependent paths caused by magneto-ionic effects also contribute to multipath.

Short-term distortion on the HF channel can therefore be described by parameters that specify the time-spread and frequency-spread characteristics; that is, differential propagation delay between modes, Doppler spread on each mode and the relative signal strengths. Fig 1 shows an actual example of these different mechanisms in action (this illustration provided by courtesy of J. P. Martinez, G3PLX[3]). Martinez experimentally recorded an event on November 9, 1994 by saving a digitized audio tone of a remote broadcast station's carrier in a computer file. The broadcast station's carrier was located on 7.7 MHz and arrived via the ionosphere; the broadcast station was located on the island of Gibraltar, the receiver on the south coast of England. Subsequent processing of the recorded digital data revealed frequency-domain changes over time. For this, the results of 256-point FFTs are presented as pixel-intensity values on the Y-axis, with time plotted on the X-axis.

For the graph shown, each pixel point in time represents approximately 20 seconds of signal with UTC hour "tick" marks shown along the top. The Y-axis represents 0.025 Hz/pixel (256 pixels = 6.25 Hz). This representation effectively shows the history of a very slowly changing process, with most of the finer, random events filtered out to better illustrate the various propagation modes. Because of the frequency in question (7.7 MHz), we are reasonably sure that the propagation mode is via the F-layer. Note that at about 0600 UTC, the signal penetrates the ionosphere and no propagation path to Earth results. Just before this happens, note the high F-layer ray (the so-called Pedersen ray) appears lower in frequency than the main (low) ray. The high ray itself appears to be split in two parts each with distinct Doppler shifts; the upper image probably being the opto-ionic, or O-ray, and the lower image being produced by the extraordinary, or X-ray. The X-ray undergoes further retardation due to interaction with Earth's magnetic field. Note that the high and low rays of the O-trace penetrate first, followed by the X trace. About 0640 UTC the F-layer comes back in again, and the process is seen in reverse: the X-trace appearing first and splitting into high and low, followed by the O-ray. Further, more-diffuse propagation paths open a few minutes later.

The Watterson Gaussian-Scatter HF Ionospheric Channel Model

Watterson et al—using wide-band HF emissions over a path between Boulder, Colorado and Washington—proposed a model for a narrow-band HF channel. This model forms the basis for most modern HF channel-simulation work and often is used for both software and hardware channel simulation. This model, known as the "Watterson Gaussian-scatter HF ionospheric channel" model, assumes that the HF channel is nonstationary in both frequency and time, but that when considered over small bandwidths (<10 kHz) for sufficiently short times (<10 minutes), most channels can be represented by a stationary model.

The HF channel is modeled as a tapped delay line, with one tap for each resolvable propagation mode (or path) in time. The delayed signal is modulated in amplitude and phase by a

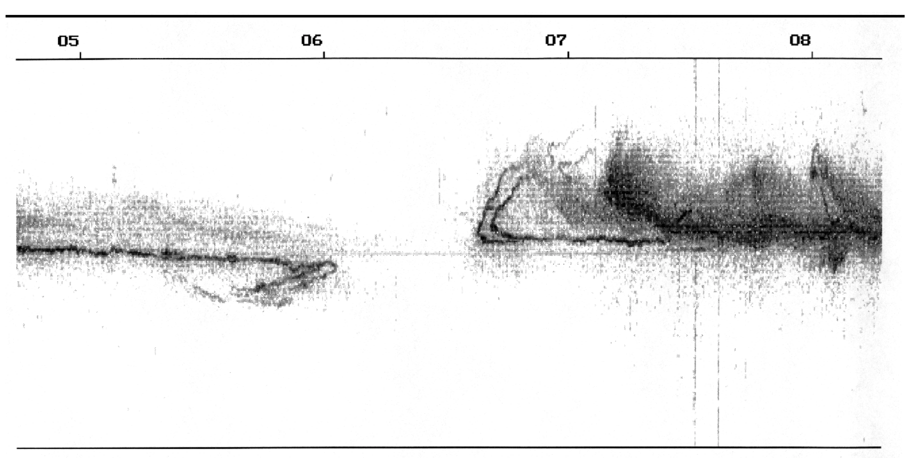

Fig 1—Martinez' Dopplergram illustrating several interesting ionospheric phenomena (see text).

complex, random finite impulse response changing over time. It is described by:

$$G_i(t) = G_{ia}(t)e^{j2\pi f_{ia}t} + G_{ib}(t)e^{j2\pi f_{ib}t} \quad \text{(Eq 1)}$$

Where a and b subscripts denote the i-th element in a time-series representation for two magneto-ionic path components. In this context, $G_{ia}(t)$ and $G_{ib}(t)$ represent two independent, complex, bivariate Gaussian ergodic random processes, each with zero mean and independent real and imaginary components with equal root-mean-square (RMS) values that produce Rayleigh fading. The exponential variables provide frequency shifts f_{ia} and f_{ib} for the magneto-ionic components in the impulse-response spectrum. Each tap coefficient (gain) has a spectrum $H_i(\lambda)$ that, in general, consists of the sum of two magneto-ionic components, each of which is a Gaussian function of frequency, as specified by:

$$H(\lambda) = \frac{e^{\left(\frac{\lambda_{ia}-\lambda}{2\sigma_{ia}^2}\right)}}{A_{ia}\sqrt{2\pi\sigma_{ia}}} + \frac{e^{\left(\frac{\lambda_{ib}-\lambda}{2\sigma_{ib}^2}\right)}}{A_{ib}\sqrt{2\pi\sigma_{ib}}} \quad \text{(Eq 2)}$$

where A_{ia} and A_{ib} are component attenuations, and the frequency spread on each component is determined by $2\sigma_{ia}$ and $2\sigma_{ib}$. The frequency shift on the two components are given by λ_{ia} and λ_{ib}. Coefficient distributions for a two-ray model are shown in Fig 2.

The Watterson model implies the use of equal-power (RMS) paths. This is effectively like a deep notch filter sweeping through the passband, at times obliterating parts of the signal. This often has devastating implications for some modem algorithms. Simulation of simultaneous X and O rays is seldom undertaken; this was suggested by Watterson since they are often unresolvable. Fig 1 shows proof of the existence of these components, especially at band closings and openings. Simulators intended for simulation of CCIR-recommended conditions, implement Rayleigh-faded paths; either a single path for flat fading conditions or two delayed paths for selective-fading conditions. Simulation results represent a "snapshot" of ionospheric conditions. They do not include dynamically changing events like seasonal or diurnal changes.

In attempts to compare performance results of standard equipment against published materials where professional channel simulators have been used, there appears to be some leeway in interpretation of the Watterson model and subsequent discrepancies in results. There have been investigations by researchers on this subject; however, without having access to details on proprietary implementations, these discrepancies remain unresolved.

Generally, published specifications and research results often tend to omit weaknesses that are readily shown by such simulators. More often than not, results obtained by this simulator tend to be interpreted as highly critical or erroneous. This is not the intention; rather, it should be an opportunity that should be exploited to the user's advantage.

Development of a Real-Time HF Channel Simulator

Discussions on developing a low-cost HF channel simulator took place in several forums: TAPR HFSIG list, specifically during 1994; 1995 TAPR Annual Meeting in St. Louis, Missouri; Digital Communications Conferences (DCC), 1995 Arlington, Texas, and 1996 in Seattle, Washington. Early work involving Alexander Kurpiers, DL8AAU, of Darmstadt, Germany, produced code for a TI 320C26-based DSP implementation. I ported this for use on the TAPR DSP93 and demonstrated its use at the 1996 DCC meeting in Seattle. This model has seen service in several projects, however, it has limited performance due to memory and processor considerations.

Several others have shown active interest in this project: Barry Buelow, WA0RJT; Jon Bloom, KE3Z; Eric Silbaugh; Glen Worstell, KG0T; Phil Karn, KA9Q; and especially Tom McDermott, N5EG. Tom presented a paper on theoretical aspects of HF channel simulation at the 1996 DCC HFSIG meeting. The specifics for the implementation of the Watterson Gaussian-scatter HF ionospheric channel model follow. This topic is divided into two sections: the hardware platform and software implementation.

HF Channel-Simulator Hardware

I saw an opportunity when a new floating-point DSP evaluation module (EVM) from Analog Devices[4] became available. The EZ-KIT Lite SHARC is a 40 MIPS processor that can produce 150 MFLOP performance. The SHARC DSP follows modern trends; its instruction set is optimized for use with the C programming language.

The kit is supplied with GNU-based C tools on CDROM that includes the usual compiler, linker and librarian tools. The ability to use a high-level language made the implementation of the Watterson-model mathematics much easier. Even time-critical code, such as interrupt handlers, may be written in C; alternatively, either inline assembly or assembly-language modules may be developed. The EVM contains a 48-kHz stereo codec to handle audio I/O and a UART chip to handle serial communications with the host. The DSP contains a total of 16 k 48-bit words of on-chip memory, part of which is available for user code. The amount of on-chip user memory is adequate for implementing the Watterson-model simulator.

HF Channel-Simulator Software

A paper by Ehrman, et al,[5] provides basic implementation ideas that were

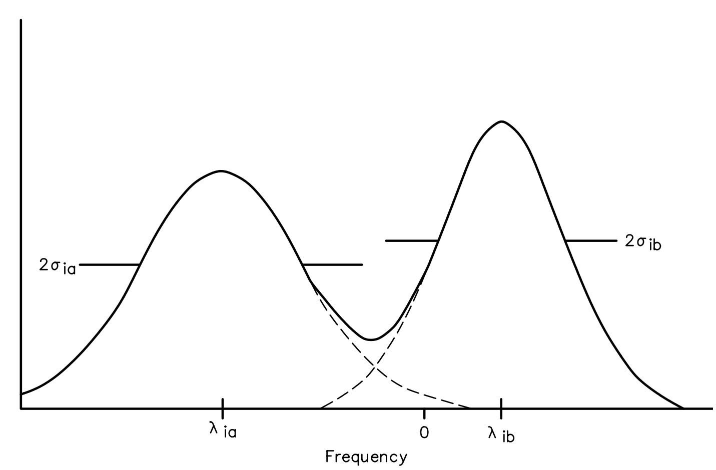

Fig 2—Tap-gain distributions for a two-ray model.

used in this project. Several parallel tasks can be distinguished:

1. Transform and process the baseband input signal, such that its phase and amplitude properties can be manipulated in real time,
2. Simulate, independently and in real time, a predefined HF propagation condition,
3. Apply simulated distortion to the processed input signal,
4. Apply noise perturbations.

Fig 3 shows the interaction between a number of parallel tasks. Input is applied at the top left and output produced at the bottom right of the figure.

The Watterson model only deals with the effects of the ionosphere and the distortion that it introduces; it does not attempt to simulate HF noise perturbations. CCIR 520-1 also does not specify any kind of noise source, however, it does allude to including a noise source in simulation. Let's look at these processing steps in further detail.

Input Signal Processing

The input signal is a real signal. Fading and Doppler effects will be introduced to this signal by mixers. These mixers, however, are *complex* devices requiring in-phase (I) and quadrature (Q) components, and thus requiring that the input signal be an analytic signal. This conversion of the input signal is achieved by using a Hilbert transform.

To simulate multiple rays passing through the ionosphere, dual tapped delay lines are used: one for the I component, another for the Q component. The analytic input signal is then extracted from the appropriate points in the delay lines. The position in the delay line is a function of the input sample rate (typically 8 kilosamples/s) and the required path delay (varies in the range 0.1-10 ms, or 1-80 delay-line taps).

Computing Channel Effects: Doppler Shift and Fading

Watterson, et al, showed that the desired fading and Doppler shift can be introduced by the product of two Gaussian functions; that is, a Rayleigh distribution. Since this multiplication process of the two Gaussian functions is commutative, it does not matter what is generated first, the fading function or the Doppler shift.

The fading function is produced using a random-number generator with Gaussian (white-noise) distribution. This stream of numbers is then passed through an infinite-impulse-response filter (IIR) designed for the appropriate bandwidth; that is, this filter determines the fading bandwidth. Actually, it controls the statistical spread for this Gaussian function, like that shown in Figure 2.

Doppler shift is produced on the fading function using a similar method, except that no filter is used. After performing the complex mixing of the fading and Doppler functions, the resultant signal now has a Rayleigh distribution. That is the desired impulse response (tap-gain function) to be applied to the delayed analytic input signal. In the finish, we take only the real part of this last mixing step.

As an option, noise perturbations with the correct amplitude are then added to set the noise background for the desired SNR level. The computation of the noise background requires further consideration.

Computing Channel Noise Effects and SNR

Gaussian noise models are commonly used in VHF, UHF and microwave work. HF noise behavior, however, has more of an impulsive nature that is more complex and sometimes described in terms of Markov models, rather than stochastic models, in the literature. For purposes of this paper, only Gaussian noise is considered. This simplifies matters, but does not accurately represent HF channel noise.

The exact channel measurements typically used for comparing systems should be carefully considered. Classical reference books use bandwidth-normalized SNR measurements. Instead of simple SNRs, this appears in units of bits/s/W/Hz. When dealing with real communications systems, however, this kind of measurement is difficult, since power measurements need to be accurately correlated with exact bit timings to compute the actual energy per bit. Coding schemes and ARQ protocol issues further complicate this measurement. It is often more convenient to determine throughput rate instead, but it would be difficult to relate this to E_b/N_o, as used in most references.

Computation of SNR has a few pitfalls. At least, it would be impossible to generate wide-band AWGN (additive white Gaussian noise) on a DSP for output through its analog-to-digital converter (ADC)—that will be limited by the Nyquist rate. It is important to design the simulator with a particular bandwidth in mind. The Watterson model is valid over narrow bandwidths (<10 kHz). The audio passband of communications equipment often is <3 kHz wide. When making external measurements of signals generated by the simulator, actual noise bandwidth should be strictly observed. Limited bandwidth results in power loss of potential noise output and this loss must be compensated. Power loss for the design bandwidth is proportional to the ratio of the output bandwidth and the ADC sample rate; it also is affected by decimation and interpolation processes implemented in the DSP code. For this reason, it often is easier to devise an internal noise-power calibration procedure in the DSP software. This procedure is set up to produce a train of noise values that are then processed though the entire filter chain as if it was generated in real time. The RMS value of the resultant data, RMS_n is then computed and saved as a reference for later use during real-time simulation.

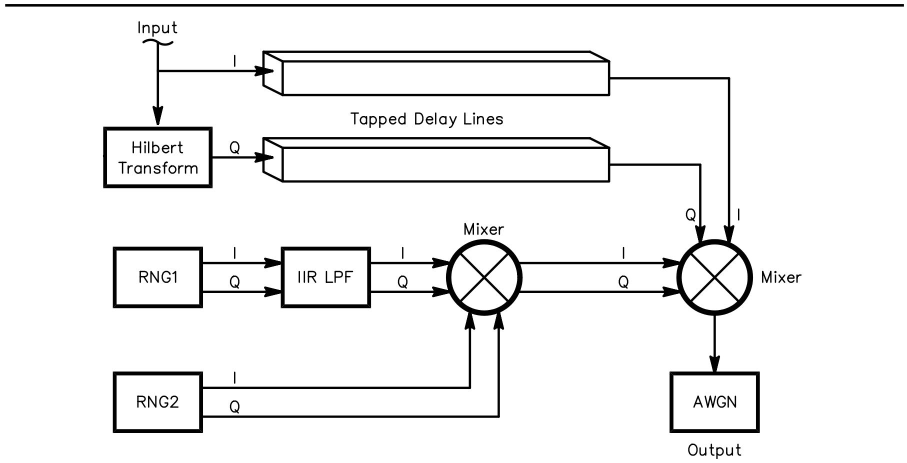

Fig 3—Simulator process flow.

In this regard, Leeland's discussion[6] on methods to determine bit-error rates (BERs) is of interest. In it, BER is advanced as the best basis for evaluation of modem SNR performance: If it doesn't meet BER specifications, it isn't working as expected. That result may imply that defensive actions like dynamic protocol adaptation or tracking algorithms are failing to assess channel properties correctly. BER also allows one to compose classic "waterfall" BER-versus-SNR curves. These sets of curves allow one to check measured performance against theoretical and other published performance data.

Modern modem designs use calculated SNR methods for BER estimation. The SNR is calculated from the measured SNR using the mean, M_x, and the variance, σ_x, of the symbol data as follows:

$$SNR = \frac{M_x^2}{\sigma_x^2} \quad \text{(Eq 3)}$$

where

$$M_x = \sum_{k=0}^{N-1} \frac{x_k}{N} \quad \text{(Eq 4)}$$

and

$$\sigma_x^2 = \sum_{k=0}^{N-1} \frac{(x_k - M_x)^2}{N-1} \quad \text{(Eq 5)}$$

Table 1—CCIR Recommendations for the Use of HF Ionospheric Channel Simulators.

CCIR Recommendation 520-1 gives guidelines for practical values for frequency spread and delay times between ray components:

Condition	*Frequency Spread (Hz)*	*Delay (ms)*
Flat Fading	0.2	0
Flat Fading (extreme)	1.0	0
Good	0.1	0.5
Moderate	0.5	1.0
Poor	1.0	2.0

It is proposed that these parameters be used to validate average and extreme conditions during simulation as well as during actual hardware testing.

Test Results

As examples, simulator tests were performed on three FEC communications modes: PSK31, CBPSK and MT63. In these examples, the test condition used was CCIR "POOR," which comprises the use of two equal-power rays with 2-ms differential path delay and 1-Hz Doppler frequency spread. The SNR level was set at –10 dB. This represents a 3-kHz bandwidth AWGN channel. This test condition represents marginal HF conditions that probably are close or equal to the practical limit for reliable HF communications. Results are shown in the Appendix.

Acknowledgements

This work was made possible by generous contributions from participants of the TAPR HFSIG list and discussions at various DCC meetings. Not only did these forums stimulate the development of this HF channel simulator, but also new HF digital communications modes like PSK31 and MT63.

I gratefully acknowledge the contribution of TAPR in this respect and thank those that participated in the many interesting and educational postings on the HFSIG list. The contributions of Peter Marinez, G3PLX, in is ionospheric Dopplergrams and his work on PSK31 are gratefully acknowledged. A special word of appreciation is due to Pawel Jalocha, SP9VRC, who brought us SLOWBPSK, the granddaddy of PSK31 and MT63. Free demonstration simulator code is available for downloading[7] from my Web site.

Notes

[1]CCIR Recommendation 520-1, *Use of High Frequency Ionospheric Channel Simulators*

[2]C.C. Watterson, J. R. Juroshek and W.D. Bensema, "Experimental confirmation of an HF channel model," *IEEE Transactions on Communications Technology*, Vol COM-18, pp 792-803, Dec1970.

[3]J. P. Martinez, G3PLX, High Blakebank Farm, Underbarrow, Kendal, Cumbria LA8 8BN, United Kingdom. The author gratefully acknowledges J. P. Martinez's permission to reproduce these experimental results.

[4]Super Harvard Architecture Computer (SHARC) EZ-KIT Lite. Part number: ADDS-2106X-EZLITE. Available from Analog Devices distributors. Street price $179. URL: **http://products.analog.com/products/info.asp?product=21000-HARDWARE**.

[5]L. Ehrman, L. B. Yates, and J. F. Eschile, and J. M. Kates, "Realtime Software Simulation of the HF Radio Channel," *IEEE Transactions on Communications*, Aug 1992, p 1809.

[6]S. Leeland, "Digital Signal Processing in Satellite Modem Design," *Communication Systems Design*, June 1998.

[7]URL **http://www.peak.org/~forrerj**; **forrerj@peak.org**

Appendix

Simulator tests results performed using PSK31, CBPSK and MT63 under CCIR "POOR" conditions (two equal-power rays with 2-ms differential path delay, 1-Hz Doppler frequency spread) at –10 dB SNR, 3-kHz bandwidth AWGN.

The contents of the test message is documentation from the *TUNER* program. The results after passing the test message through the simulated channel using the selected HF communications mode are shown. Notice that decoding errors introduced some unprintable control characters that caused the word processor to make substitutions: more often than not, these were line-feed characters. The last test for the 2-kHz bandwidth MT63 used a –5 dB SNR. Here's the test message:

> The Tuner program - TUNER.COM
> 1. This is a tuning aid to help get a received tone exactly on 800.0 Hz. It should accept COM2, COM3, COM4 command line parameters (default is COM1) and report CLIPPING (audio signal too strong for the sigma-delta circuit).
>
> 2. Unfortunately, it takes too many computing cycles to incorporate this in COHERENT, so run TUNER first if necessary, using an 800-Hz sine wave with no modulation on it—a steady carrier, in other words. It may be slightly useful on a carrier that is phase-modulated, but the indicator will jump around trying to follow the modulation, and in any event, the useful frequency range would be limited.
>
> 3. The idea is to get the little yellow line centered between the two green lines, and staying within the green lines at all times. The nominal frequency is 800.0 Hz.
>
> 4. The range of this tuning indicator is 800 Hz plus or minus 20 Hz. If your signal is not ALREADY tuned to within better than 20 Hz, this indicator will be useless and quite likely confusing as hell!
>
> 5. There will be some rejection of other signals outside this range, but if the signal you want is weak and the interfering signals are strong there will no doubt be problems.
>
> 6. If you can hear the tone, there is no substitute for zero-beating it with a good crystal-derived 800 Hz sine-wave sidetone.
>
> 7. *TUNERC.COM* is for anyone who still uses CGA graphics—I slowed down the update rate to accommodate sluggish LCD displays.
>
> VE2IQ—November '95.

Simulator Results: PSK31 with Varicode

The UNER0 on ramD T∂ER.ROO

-r- tiDi—iDe ————ul——

1. Tt=s is a tuning ai t tfhe∂ ge a repotvedi/e l tc&a ∂ 800.0 Hz.

It trould a oc?t Cr M2o COO∂∂r MM cemmand line farao etera

default is ttO01)

nnd report CLIP∂∂ Maudl sign∂-oo stroog for ∂e oigma-deiit circ∂e0∂

2. Unftrtunately 7 takes too many coeeputing cycle∂o

oraorate this

tn CO ERENet, so run AUl ERKirst f ne eessar∂ using8aeD Hz sinewa∂

with vtmosul ti/ on it(a stead t carri=n otrer wordo).

At o aybe slightly u∂ ul on a carier that s pha8-∂dulat d, but

the iodiahto ai oa juee]arount trying-f lrow the modllation, and in

any even th u eeul frequ ncy r a ae wo∂dbe li∂te.

∂ Tme ic a is to get t& littliyellow line cen Ved betweefta2tireen

∂nes, and staying wtthiihhe yreei lines at al∂imesEii he nominal

frequenc io 80gbte ∂.

l4. The ron ne of this tuningyodicator is 800 r∂plus oa ∂nur 2∂Hz. ebf yoeer signae es ntt yieRE∂Y tu ld o wVain betoer taan $g Heret this

indicncr hill be us$ess Ld puite likelm honfusgas helle

5. Theri ailLb

eome re:e∂ioa of othet∂gnals tutsi T this raeg∂ but

im hlsia nal you wtnhis geak and the interferinte signalalrst tng therqwill no doubt be problems.

a. f yol can hea e the eone, thite iDno substT∂e foi >ero tbeatie?w∂ a good cr∂ al-der ved 800 r z si(vave si tetooer

C. TUPE eC.COM ∂ d∂ aoaone i6o stilTZ es c(graphics u l ∂oe e6down

hup tat. te to adcommo rte sluggish PCD dis∂ays.

VE2IQ - Gog]'r '9$.

Thn TUNER program -4TUNER.COM

——————E—————

1. Thiy is a tuning aid to help get a

Ered+i8nd tone exactly on 800.0 Hz.

It should accept COM2, COM3, COM4 c

ommand line paramKtebs (de@aul' is COM1)

and report CLIPPING (audfo sig

nal too strong for the sigmp-delta circuit).t

. Unfortunately it tak

es tooEmant computing cycles to incorporate thsm

n COHERENT, to rcn TUN

ER first if necessary, using an 800 Hz sinewave

citp no modulation on i

t (a steady carrie1 in other words).

It may be slightly useful on a car

rier that

phase-modulated, but

te indicator will jumparound tryidg

4to follow the modulation, Gnd in

any event the usedul frequency range

would be limited.

e

3t The idea is to ge0 the little yel.ow line cente

red between the 2%green

lines,nd sta-ing within the green lines;at al

l times. The nominal

frequency is 800.0 Hz.

4. The range of this t

uning indicator is 80f Hz plus or minos 23 Hz.

If your signal is not AL

READY tmnOd to within better than 20 Hz, this

indicator will be uaeless

and quite likely confusing as hell!

}

5. There will be some rejection

OofEoeher signals outside this range, but

if thesi9nal you4want is weak

and the intrfering signals are strong there

gwill no doube be probleds

.

6. If yod can hear the tone, there is no s#bstitute for zero-beati

ng it

with a geod+crystal-derived 800BHc:sinewave sidetone.

<. mUHE

RC.CE\q5;T7wSzunwg1sW2kT=aRh

es CGA graphics - I slowed Town

the up

datb rate to aTco1modate sluggish LC4 displays.

1VE2IQ - Novemeer '95.

Simulator Results: MT63 - 2kHz, double interleave factor.

The TUNER program - TUNER.COM

———————————

———

1. This is a tuning aId to help geT a received tOne exactly on 800.0 HZ

It should accept COM2, COM3, COM4 command line parameters (defaUlt is CoM1

and report CLIPPInG (aUdio signal too stRong for the sigma-delta circuit).

i

AG5q 2. Unfortunately it takes too many computing cycles to incorPoratE this /kin COHERENT, so run TUNER first if necessary, usiNg an 800 Hz sinewave with no modulatIon on it (a steady carrIer in oTher words).

I _ It may be slightly useful oN a carrierthat is phase-modulated,but the indicator will jump around trying to follow the modulation, and in

* bany event the useful frequency range would be limiteD.

= ?jq3. The idea is to get the little yellXw line centered between the2GReen lines, and staying within the green lines at all times. Thenominal dfrequency is 800.0 Hz-

* x __ 44. The range of this tuning indicator is 800 Hz plus or minus 20 Hz.

9x m If your signAl is not ALREADY tuned to within better than 20 Hz, thIs x - m~lindicator will be useless aNd quite likely confusing as hell!

iQe 5. There will be some rejection oFOtHer signAls outside this range, but if tHe siGnal you wAnT is weak and the interfering signals are strong there LB ut5Jll l_ ll no doubt be problems.

6. If you can Hear the tone, there is No substitute for zero-beatingit u with a goOd crystal-derived 8_0 Hz sInewave sidetone.-

-

6 d2 7. tUNERC.cOM is for anyOnEwho still uses CGA

* the update rate to accommodate slUggisH LCD disPlaYS.

~ iP __VE2IQ - November '95.

Simulator Results: MT63 - 2kHz, double interleave factor
(Test at -5dB SNR, 3kHz Bandwidth AWGN.)

The TUNER program - TUNER.COM

———————————————

1. This is a tuning aid to help get a received tone exactly on 800.0 Hz.

It should accept COM2, COM3, COM4 command line parameters (default is COM1)

and report CLIPPING (audio signal too strong for the sigma-delta circuit).

2. Unfortunately it takes too many computing cycles to incorporate this

in COHERENT, so run TUNER first if necessary, using an 800 Hz sinewave

with no modulation on it (a steady carrier in other words).

It may be slightly useful on a carrier that is phase-modulated, but

the indicator will jump around trying to follow the modulation, and in

any event the useful frequency range would be limited.

3. The idea is to get the little yellow line centered between the 2 green

lines, and staying within the green lines at all times. The nominal

frequency is 800.0 Hz.

4. The range of this tuning indicator is 800 Hz plus or minus 20 Hz.

If your signal is not ALREADY tuned to within better than 20 Hz, this

indicator will be useless and quite likely confusing as hell!

5. There will be some rejection of other signals outside this range, but

if the signal you want is weak and the interfering signals are strong there

will no doubt be problems.

6. If you can hear the tone, there is no substitute for zero-beating it

with a good crystal-derived 800 Hz sinewave sidetone.

7. TUNERC.COM is for anyone who still uses CGA graphics - I slowed down

the update rate to accommodate sluggish LCD displays.

VE2IQ - November ‘95.

□□

Notes on Standard Design HF LPDAs, Pt 1: "Short" Boom Designs

"Short" is a relative term here. These 3 to 30-MHz wide-band antennas have a 167-ft longest element on a 100-ft boom. Definitely a job for computer modeling!

By L. B. Cebik, W4RNL

Hams have heard of 3-30 MHz dream antennas of log-periodic dipole array (LPDA) design since their advent. While wide-band LPDAs are common in governmental and commercial circles, little performance or specification data on the antennas has filtered into amateur publications. LPDAs for 14-20 MHz are much more common. Because modeling software (*NEC-4*) exists to assess the potential for 3.5-octave LPDAs, and because curiosity must ultimately be served, I began a preliminary modeling study, the first two parts of which appear in this series.

1434 High Mesa Dr
Knoxville, TN 37938-4443
cebik@utk.edu

The first part of this preliminary study looks at standard LPDA designs of the order produced by *LPCAD* for three 3-30 MHz antennas:

- 60-ft boom with 20 elements
- 100-ft boom with 20 elements
- 100-ft boom with 26 elements

The 60-foot boom length is not recommended because of difficulties in obtaining an SWR of less than 2:1 across the passband relative to some common impedance and because of very significant pattern anomalies at numerous frequencies.

More feasible is a 100-ft boom using either 20 or 26 elements, if a free-space forward gain of less than 6.0 dBi is acceptable across the passband. Except at the lowest frequencies, the front-to-back ratio is acceptable (more than 18 dB from 9 MHz upward), although rear lobes are broader than would be expected for an LPDA of narrower frequency range. By careful selection of the interelement transmission-line value and the use of an antenna line terminating stub, an SWR of under 2:1 can be obtained for the entire passband with only small (and likely correctable) exceptions.

For some designs—especially the 100-ft boom, 20-element version—element diameter tapering according to the value of Tau shows significant improvements across the passband. However, this technique results in unrealistically large diameters for the tubular elements. A possible wire simulation of the large elements is proposed, along with a simple mechanism for shortening the physical length of the element while preserving its resonant frequency.

Preliminary Design and Modeling Considerations

Flat-plane LPDAs are normally designed in accord with well-published design equations. There are several LPDA design programs employing these equations, of which *LPCAD* by Roger Cox may be the best known and most widely distributed. The 3-30 MHz LPDAs described here were initially designed using *LPCAD*. Since the theory and equations for standard LPDA designs appear in so many publications, they will be only briefly noted here.

Tau is the ratio between element lengths. It is, as Fig 1 shows, also the ratio of element distances from the center of a circle such that the element lengths define an arc having a constant angle. Since the angle, which is twice Alpha, is often difficult to work with, we may also define a spacing constant, Sigma. Sigma can be defined, as shown in the diagram, in terms of Tau and Alpha, but often it is more convenient to calculate it by taking the spacing of any two elements and dividing that distance by twice the length of the longer element.

For dipole arrays, there is an optimal value for Sigma:

$\text{Sigma}_{opt} = (0.243\ \text{Tau}) - 0.051$ (Eq 1)

Suppose we opt for a Tau value of 0.94. The optimal value of sigma will be 0.1774. Plugging this value back into the equation by which we determine Alpha yields an angle of about 4.833°; this results, in turn, in a very long boom. For a 3-30 MHz LPDA with a longest element of 167.28 ft, the boom length becomes about 989 ft.

For most applications, much shorter lengths are physically required for LPDAs. The immediate consequence is a reduction in gain, along with irregularities in gain across the design passband of the array. When the length becomes too short, pattern shaping also tends to become irregular and often unusable at many frequencies within the passband of the LPDA design. Finally, obtaining a relatively constant source impedance across the passband becomes nigh well impossible.

One of the initial goals of this preliminary study was to determine the approximate shortest length that would be feasible for a 3-30 MHz LPDA. Since antenna gain has not been specified in advance, the criteria for an acceptable length included the ability of the antenna to achieve a 2:1 SWR across the passband relative to some specific impedance value. In addition, free-space azimuth patterns must achieve reasonable shapes for all test frequencies, with no spurious forward or rearward lobes of consequence.

An additional goal of this preliminary study was to look at the effect of element diameter upon antenna performance. Standard (but simplified) tubing diameter progressions would be compared to element diameters increased for each element by the value of Tau used in the element-length schedule. The latter schedule of element diameters would result in a constant length-to-diameter ratio for the entire array.

The designs resulting from *LPCAD* inputs were modeled on *NEC-4* (*EZNEC*) using aluminum elements throughout. The environment selected was free space, so that all values reported would be comparable and not subject to variations due to height above ground. The resulting models were sizable: 836 segments for 20-element versions and 1184 segments for 26-element versions of the LPDA. Even on a 400-MHz computer, the run time for the models—especially for frequency sweeps from 3 to 30 MHz in 1-MHz increments—limited the number of variations possible. Consequently, there are design modification possibilities that have not been explored in these preliminary notes. Moreover, instead of a survey of boom lengths in small increments, only two selected boom lengths could be initially checked: 60 and 100 ft. Whether an intermediate length realizes the improvements found in the 100-ft boom length was not determined.

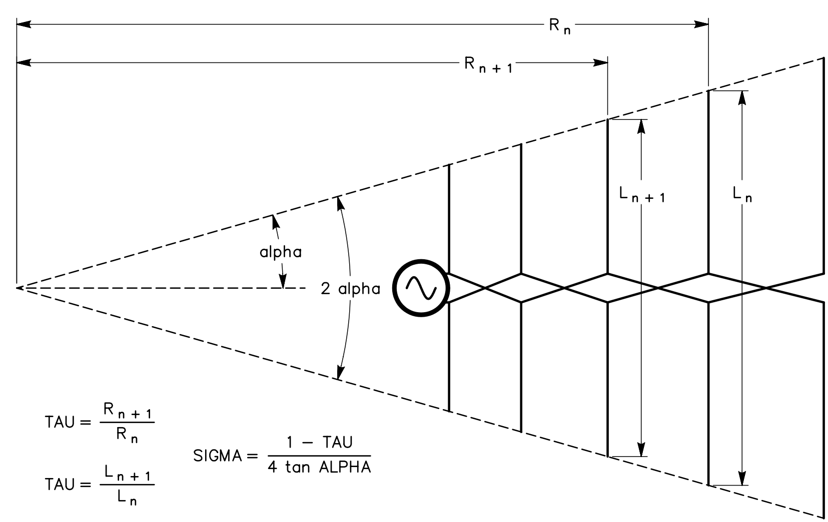

Fig 1—Some of the basic relations used in standard LPDA design [adapted from Richard C. Johnson, Ed., *Antenna Engineering Handbook*, 3rd ed. (New York: McGraw-Hill, 1993), p 14-36.]

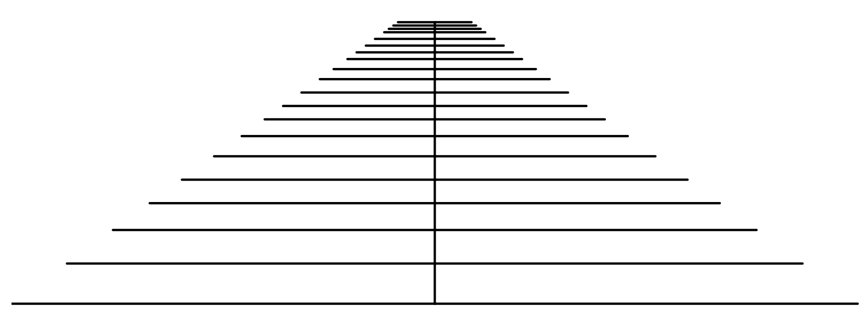

Fig 2—Outline of the 60-ft, 20-element 3-30 MHz LPDA.

The models themselves are further limited by the use of the TL facility in NEC—the mathematical modeling of transmission lines used to interconnect elements. Physical models of LPDAs with transmission lines are not feasible due to certain limitations in NEC, most notably the angular junction of wires of dissimilar diameter. However, mathematical transmission lines do not account for losses in these lines, and therefore, all performance figures may be very slightly off the mark.

Within these limitations, certain trends are notable and reported in the following.

A 60-ft, 20-Element LPDA

The first model developed used a 60-ft boom length with 20 elements ranging from 2.0 inches in diameter at the rear to 0.5 inch in diameter for the shortest element. Based on initial modeling tests for a "best" SWR curve, the interelement transmission line was set at 150 Ω. The *EZNEC* model description is appended at the end of the report to show the facets of design, including the tubing schedule. In general, each diameter divisible by 1/4 inch is used twice, while those divisible only by 1/8 inch are used only once in the element progression.

Fig 2 displays the generalized outline of the 60 ft, 20-element LPDA used in this study. The longest element is 2007 inches (or about 167 ft), while the shortest is 155 inches (or about 13 ft). See Table 1 for a listing of element half-lengths and cumulative spacing for the final model design. For this design, overall length and the number of elements were specified, with the values of Tau (0.87) and Sigma (0.02) becoming the results of the calculations. It is interesting that *LPCAD* initially predicted a free-space forward gain of about 6.5 dBi, with front-to-back ratios ranging from 13 to 19 dB. Only the front-to-back ratios met the prediction. Although a 150-Ω transmission line was finally used, *LPCAD* recommended a 200-Ω line and predicted that the antenna input resistance would be about 85 Ω.

Apparently, the 60-ft boom length is categorically unable to yield a SWR under 2:1 for any particular reference impedance value. Using 1-MHz increments from 3 to 30 MHz, impedance values varied widely. The range of the resistive component was from a 24 Ω low to a 168 Ω high. Reactance varied between –68 Ω and +71 Ω. The SWR curve for the 3-30 MHz passband, shown in Fig 3, reveals only a couple of minor excursions below 2:1 relative to a 75-Ω reference value. Other reference values will yield more values below 2:1, but the peak values of SWR climb proportionately. The result is a design that is unlikely to be matchable to standard feed lines by any straightforward means.

In addition to an unacceptable set of SWR values across the passband, the 60-ft, 20-element design also shows numerous pattern anomalies. Often, an LPDA design will show a small frequency region of unacceptable pattern shape. Such problems are sometimes amenable to input-stub correction. However, the present design shows anomalies at many frequencies.

Table 2 samples performance values at 3-MHz intervals across the passband and reveals the general performance trends for the antenna. The table reveals some strong difficulties at the lower and upper ends of the passband. The gain and front-to-back ratio at 3 MHz is exceptionally low and only slowly improves as the frequency progresses toward 9 MHz. At the upper end of the passband, the source impedance reaches very low values. The gain shows large excursions throughout the 3 to 30 MHz range.

Some selected free-space azimuth patterns for 3, 9, 15 and 30 MHz can

Table 1—Element half-lengths and cumulative spacing of the 60-ft, 20-element 3-30 MHz LPDA model

Element	*Half Length (inches)*	*Cumulative Spacing (inches)*
1	1003.68	0.00
2	876.93	98.50
3	766.19	184.56
4	669.44	259.75
5	584.90	325.45
6	511.04	382.85
7	446.50	433.00
8	390.12	476.82
9	340.85	515.11
10	297.81	546.56
11	260.20	577.79
12	227.34	603.32
13	198.65	625.63
14	173.55	645.13
15	151.63	662.16
16	132.49	677.04
17	115.76	690.04
18	101.14	701.40
19	88.37	711.33
20	77.21	720.00

Table 2 —Performance of the 60-ft, 20-element model LPDA at 3-MHz increments from 3-30 MHz

Frequency (MHz)	*Free-Space Gain (dBi)*	*Front-to-Back Ratio (dB)*	*Source Impedance (R ± jX Ω)*	*SWR (75-Ω)*
3	3.66	3.6	120 –*j*68	2.30
6	5.93	10.2	168 +*j*40	2.39
9	4.88	16.1	108 +*j*63	2.16
12	5.50	16.4	162 +*j*11	2.18
15	6.00	18.7	35 +*j*12	2.24
18	5.36	19.0	86 +*j*60	2.09
21	6.08	18.7	124 +*j*50	2.04
24	6.01	18.7	81 +*j*50	1.89
27	5.18	17.5	25 +*j*27	3.47
30	5.64	18.7	27 –*j*24	3.05

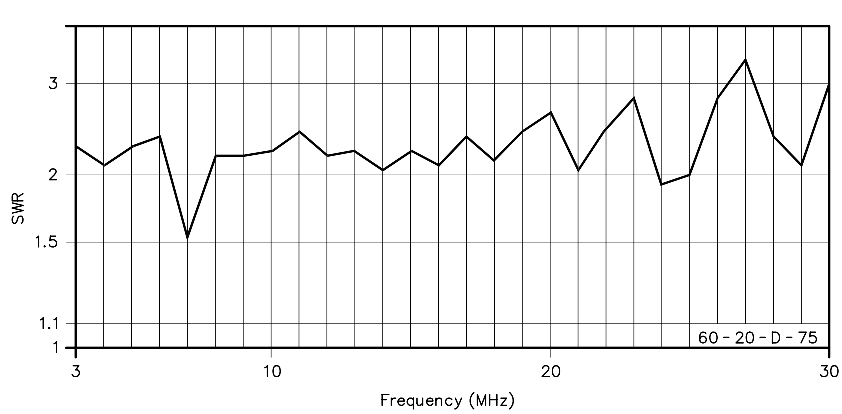

Fig 3—3-30 MHz SWR sweep of the 60-ft, 20-element LPDA model referenced to 75 Ω.

reveal other weaknesses in the design. The 3-MHz pattern in Fig 4 reveals clearly the very weak directional pattern for the design at its lowest frequency. Although gain and front-to-back ratio improve as frequency is increased, the size of the rear lobes at 9 MHz is still very much larger than is desirable for most operation.

The 15-MHz pattern in Fig 4 reveals a double forward lobe, along with added side lobes in both the forward and rearward quadrants. Although this pattern might be corrected to some degree by compensatory loading, the fact that a similar set of problems attach to the 30-MHz pattern largely precludes this course of action. There would still be sets of frequencies with unacceptable azimuth patterns.

The general conclusion to be reached from this exploration is that the standard LPDA design—as produced by *LPCAD*—yields unacceptable results. Moreover, the problematical performance numbers are unlikely to be overcome by compensatory actions on the design. In the end, a 60-ft boom is simply too short for a standard LPDA design to achieve any set of desired goals.

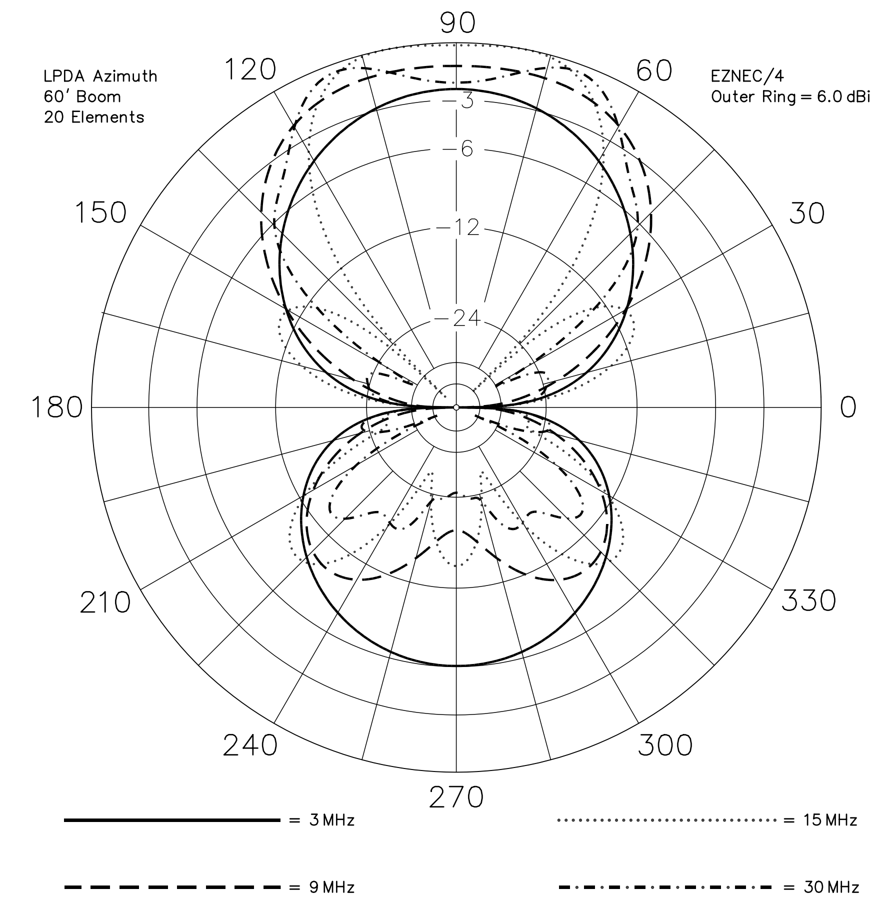

Fig 4—Free-space azimuth pattern of the 60-ft, 20-element LPDA model at 3, 9, 15 and 30 MHz.

100-ft, 20-Element LPDA

Since the model sizes precluded incremental investigation with the goal of finding the shortest acceptable boom, a longer boom was arbitrarily selected for modeling. A 100-ft length was chosen because it seemed sufficiently longer than the 60-ft boom (167%) to offer significantly modified antenna behavior. The parameters were presented to *LPCAD*, which produced a design with the same element lengths as used in the 60-ft design, but with a new spacing schedule. Fig 5 shows the general outline of the longer design, while Table 3 provides element half-lengths and cumulative spacing for the model. Initially, the tubing diameter schedule used in the 60-ft-boom model was

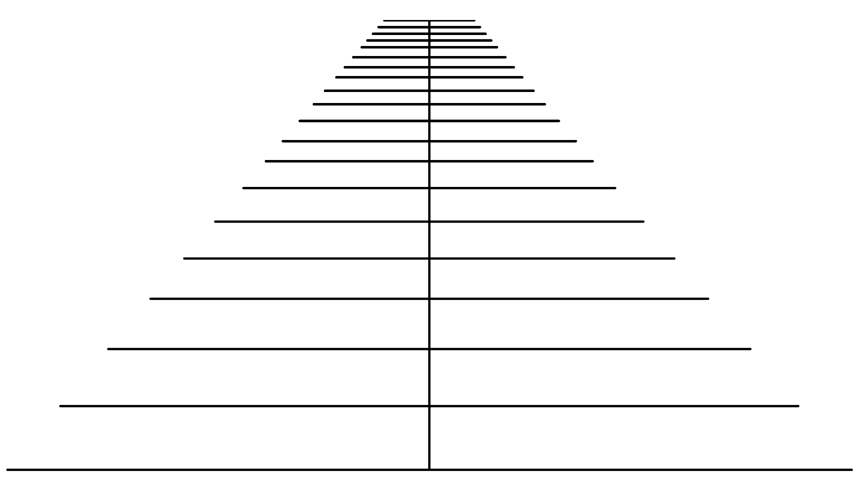

Fig 5—Outline of the 100-ft, 20-element 3-30 MHz LPDA.

Table 3—Element half-lengths and cumulative spacing of the 100-ft, 20-element 3-30 MHz LPDA model

Element	*Half Length (inches)*	*Cumulative Spacing (inches)*
1	1003.68	0.00
2	876.93	164.17
3	766.19	307.60
4	669.44	432.92
5	584.90	542.42
6	511.04	638.09
7	446.50	721.68
8	390.12	794.71
9	340.85	858.52
10	297.81	914.28
11	260.20	962.98
12	227.34	1005.54
13	198.65	1042.72
14	173.55	1075.21
15	151.63	1103.60
16	132.49	1128.40
17	115.76	1150.07
18	101.14	1169.00
19	88.37	1185.55
20	77.21	1200.00

transferred to the new 100-ft version.

The interelement transmission line impedance was set at 200 Ω, in accord with *LPCAD* recommendations. To this and all subsequent models in Part 1 of these notes, I added a 90-inch shorted stub at the end of the line at the longest element to effect a transmission-line termination. In all cases, this stub has the same characteristic impedance as the interelement line. Again, because models are so large, varying the length of this stub might produce small improvements in the projected performance of some of the models. However, it is unlikely that major changes will be created.

As revealed in Fig 6, the 100-ft boom, 20-element LPDA is capable of a quite good SWR curve relative to a reference value of 95 Ω (in contrast to the *LPCAD* predicted input resistance of 103 Ω). Only once (in the 1-MHz increment scan) does the SWR value just barely exceed 2.0. Consequently, the antenna design passes one of the major criteria of acceptability.

LPCAD predicted that the antenna free-space gain would be about 6.5 dBi, with front-to-back ratios ranging from 13 to 19 dB. In some performance categories, the antenna shows a few serious shortcomings, especially with respect to gain. Table 4 presents selected frequency performance figures, which reveal some of the design's weakness. The notation "BFL" records a judgment that the antenna at the given frequency exhibits a *broad forward lobe*. However, even where technically double, the difference between the forward direction and the peak is under 0.5 dB and therefore is more accurately called a broad lobe than a double lobe.

The gain at the lower end of the passband remains low, but slightly better than that of the 60-ft model. Numerous test frequencies show broad frontal lobes, with equally wide rear lobes, although the front-to-back ratio is very consistent from 12 MHz upward. Moreover, the gain figures, while lower on some bands than those of the 60-ft model, are far more consistent from one test frequency to the next. All in all, the 100-ft, 20-element version of the LPDA shows distinct improvements over the 60-ft model.

Although the model uses a set of element diameters that increase as frequency decreases, the rate of increase does not match the inverse of Tau (0.87). Table 5 gives a comparison of the initially modeled and the "Tau-tapered" element diameters, counting from element 20 at the highest frequency downward toward element 1 at the lowest frequency.

The element diameters remain roughly the same for the shortest seven elements. Then the rigorous "Tau-tapering" schedule increases the element diameter much more rapidly, reaching a final value of 6.5 inches for the longest element. Although this element diameter may be impractical in a tubular design, there may be a way of simulating such elements. One possibility will be suggested in the final section of these notes.

To test whether the "Tau-taper" element set would make a difference in the performance predicted by *NEC-4*, the 100-ft model was reset using the new element diameters. For the initial test, I retained the 200-Ω interelement feed line, the 90-inch terminating stub and the SWR reference impedance of 95 Ω. The resulting SWR curve in Fig 7 remains quite good, with only one slight excursion above 2:1.

Table 6 reveals the performance improvements that occur at the lower end of the antenna passband. Relative to the original 100-ft model, the "Tau-tapered" model shows improved front-to-back ratio at every frequency. Gain at 3 MHz is improved so that it never drops below 5 dBi throughout the entire frequency range for the frequencies tested. Only at 18, 27 and 30 MHz is the gain of the new model slightly lower than for its companion. However, the frequencies at which we encounter broad forward lobes (BFL) remain constant between the two models. The

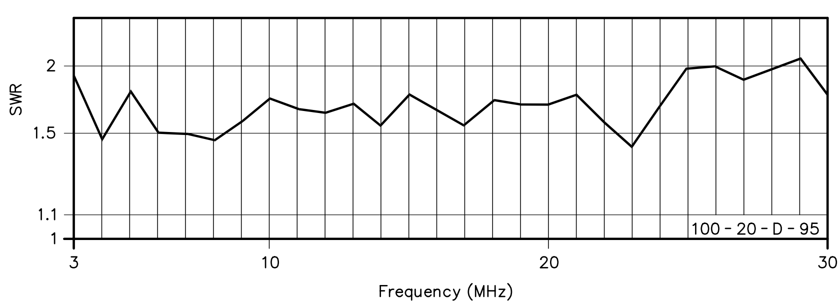

Fig 6—3-30 MHz SWR sweep of the 100-ft, 20-element LPDA model referenced to 95 Ω.

Table 4—Performance of the 100-ft, 20-element model LPDA at 3-MHz increments from 3-30 MHz "BFL" means broad forward lobe (see text).

Frequency (MHz)	Free-Space Gain (dBi)	Front-to-Back Ratio (dB)	Source Impedance (R ± jX Ω)	SWR (95-Ω)	
3	4.70	6.9	148 –j57	1.91	
6	6.02	15.2	67 –j18	1.52	
9	5.60	17.7	71 –j29	1.58	
12	4.95	19.1	61 –j17	1.64	BFL
15	5.56	21.8	167 –j11	1.77	
18	5.32	18.7	80 –j46	1.73	BFL
21	5.27	22.0	71 –j40	1.75	BFL
24	5.07	22.7	81 –j43	1.68	BFL
27	5.21	20.9	166 +j37	1.87	BFL
30	5.23	20.9	55 +j16	1.78	

Table 5 —Comparison of the element diameters for the initial and "Tau-tapered" versions of the 100-ft, 20-element LPDA model. Diameters are in inches.

Element	Initial	Tau-Taper
20	0.50	0.50
19	0.50	0.57
18	0.625	0.66
17	0.75	0.75
16	0.75	0.86
15	0.875	0.98
14	1.00	1.12
13	1.00	1.29
12	1.125	1.47
11	1.25	1.69
10	1.25	1.93
9	1.375	2.21
8	1.50	2.53
7	1.50	2.89
6	1.625	3.31
5	1.75	3.79
4	1.75	4.34
3	1.875	4.96
2	2.00	5.68
1	2.00	6.50

improvements at the lowest frequencies alone strongly suggest that the longest elements may benefit from increased diameter.

100-ft, 26-Element LPDA

If 20 elements provide a baseline of performance for the 100-ft long standard LPDA, would more elements yield further improvements? Additional elements would reduce the separation of resonant frequencies from one element to the next.

A 26-element model, outlined in Fig 8, was created using an extension of the original element-diameter scheme so that the longest elements are 2.5 inches in diameter. Despite the increased diameter of the longest element (still 167 ft long), there is considerable disparity of length-to-diameter ratio between it and the shortest element. Table 7 lists the element half-lengths and cumulative spacing for the model. *LPCAD* predicted a gain of 7 dBi, with front-to-back ratios ranging from 17 to 23 dB. The Tau for the model is 0.90, with a Sigma of 0.03. With a recommended 200-Ω interelement feed line, *LPCAD* predicted the feed-point impedance to be 93 Ω.

Modeling of the antenna on *NEC-4* suggested the use of a 150-Ω interelement feed line, with retention of the 90-inch terminating stub. The resulting SWR curve, referenced to 75 Ω as shown in Fig 9, is quite good. Excursions above 2:1 SWR values occur only at the high end of the passband.

Relative to the comparable 20-element model, the 26-element model shows detectable improvements in performance at virtually every test frequency. Gain is up by perhaps 0.25 dB on average, and the front-to-back ratio exceeds 20 dB more consistently. In almost all cases, the 26-element model also shows improvements over the "Tau-tapered" version of the 20-element model.

Nonetheless, as Table 8 demonstrates, the gain of the standard-design LPDA rarely reaches 6 dBi, a figure common to monoband two-element

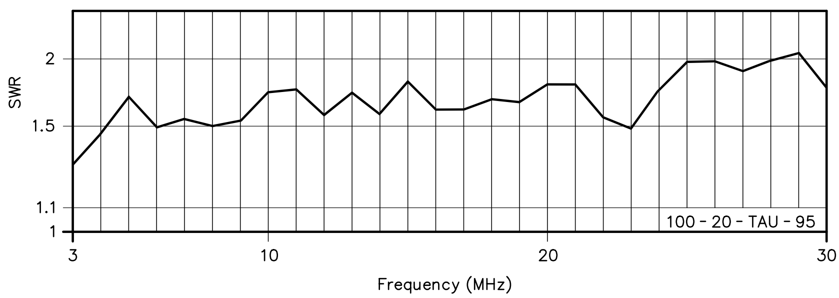

Fig 7—3-30 MHz SWR sweep of the 100-ft, 20-element LPDA model (with "Tau-tapered" element diameters) referenced to 95 Ω.

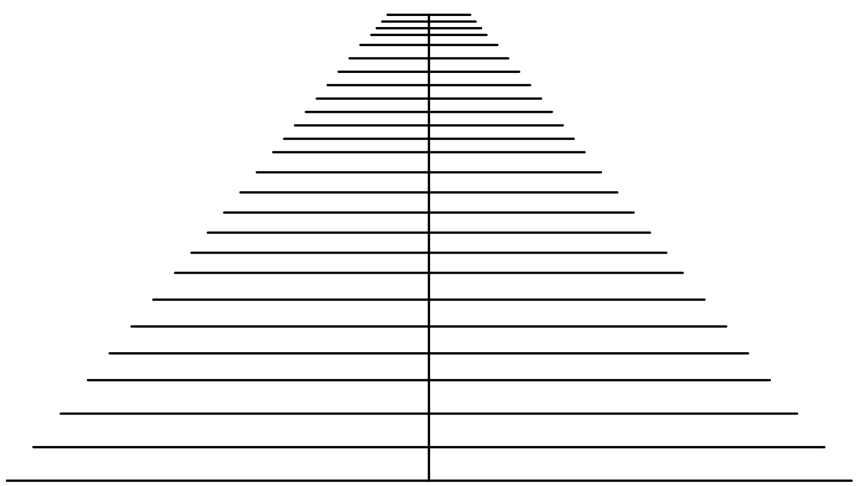

Fig 8—Outline of the 100-ft, 26-element 3-30 MHz LPDA.

Table 6—Performance of the 100-ft, 20-element model LPDA with "Tau-tapered" element diameters at 3-MHz increments from 3-30 MHz "BFL" means broad forward lobe (see text)

Frequency (MHz)	*Free-Space Gain (dBi)*	*Front-to-Back Ratio (dB)*	*Source Impedance (R ±jX Ω)*	*SWR (95-Ω)*	
3	5.05	8.3	85 –*j*22	1.31	
6	6.14	15.9	66 +*j*5	1.50	
9	5.61	18.4	64 –*j*15	1.54	
12	5.06	20.8	61 –*j*9	1.57	BFL
15	5.61	22.8	170 –*j*15	1.81	
18	5.20	19.3	80 –*j*44	1.69	BFL
21	5.41	23.1	71 –*j*42	1.79	BFL
24	5.15	22.8	86 –*j*50	1.74	BFL
27	5.01	21.3	159 +*j*47	1.89	BFL
30	5.18	22.1	55 +*j*12	1.76	

Table 7—Element half-lengths and cumulative spacing of the 100-ft, 26-element 3-30 MHz LPDA model

Element	*Half Length (inches)*	*Cumulative Spacing (inches)*
1	1003.68	0.00
2	905.81	126.76
3	817.49	241.17
4	737.77	344.41
5	655.83	437.59
6	600.91	521.69
7	542.31	597.58
8	489.43	666.07
9	441.71	727.89
10	398.64	783.64
11	359.76	834.02
12	324.68	879.46
13	293.02	920.47
14	264.45	957.47
15	238.66	990.87
16	215.39	1021.01
17	194.39	1048.22
18	175.43	1072.77
19	158.33	1094.93
20	142.89	1114.93
21	128.96	1132.97
22	116.38	1149.26
23	105.03	1163.96
24	94.79	1177.22
25	85.55	1189.20
26	77.21	1200.00

Yagis. The standard design predictions for gain, as reflected in the *LPCAD* implementation, overestimate gain by a full decibel. It likely would require a considerably longer boom to achieve the predicted 7 dBi figure in *NEC-4* models.

Except for diminished performance at the lowest test frequencies, this LPDA shows good consistency for most of the passband. The number of test frequencies at which we encounter broad forward lobes (BFL) is reduced relative to the 20-element model. If the modest forward gain figures are acceptable, this model or a variant would likely meet both the SWR and pattern-shape criteria set forth earlier in this study.

The 26-element model uses 2.5-inch diameter elements for the lowest frequencies—a significant increase over the largest diameter used in the 20-element model. Whether a "Tau-taper" element set might effect any improvements became the next question. With a Tau of 0.903, the requisite element set showed the sizes listed in Table 9, once more set against the element-diameter schedule for the initial 26-element model.

The resulting model uses the same 150 Ω inter-element transmission line as used in the initial 26-element model. The SWR curve is well behaved, with excursions into values above 2:1 occurring only at the upper frequencies. If we set the reference impedance to 65 Ω, the maximum SWR is about 2.17:1 at 28 and 29 MHz, as shown in Fig 10. Use of this reference value results in a rougher curve for other frequencies than it might otherwise be.

If we select 75 Ω as the reference impedance for the SWR curve, as was done for Fig 11, values for frequencies under 20 MHz show a lower SWR, but the peak SWR value at 28 MHz rises to 2.49:1. Of course, the actual source impedances have not changed, but the choice of reference impedance may have a bearing on the selection of means to match the antenna to a specific main feed line for the system.

Except for the lowest frequencies, the gain performance of the "Tau-tapered" version of this model is slightly under that of the initial model. The result owes partially to the greater diameter of the rear elements (2.5 inches) in the initial 26-element model. Table 10 is instructive. SWR values are referenced to 65 Ω. Except perhaps for 3 MHz, there is nothing overall to choose between the two 26-element models. The number of cases of "broad forward

Table 8—Performance of the 100-ft, 26-element model LPDA at 3-MHz increments from 3-30 MHz "BFL" means broad forward lobe (see text)

Frequency (MHz)	*Free-Space Gain (dBi)*	*Front-to-Back Ratio (dB)*	*Source Impedance (R ±jX Ω)*	*SWR (75-Ω)*	
3	5.08	8.5	71 –*j*7	1.12	
6	6.24	16.4	64 –*j*31	1.61	
9	5.97	18.4	92 –*j*34	1.58	
12	5.90	20.5	95 +*j*26	1.62	
15	5.65	19.8	117 +*j*15	1.61	BFL
18	5.95	21.2	51 +*j*21	1.68	
21	5.44	21.8	108 –*j*16	1.50	
24	5.80	22.4	67 –*j*37	1.69	BFL
27	5.66	21.8	49 –*j*30	1.91	BFL
30	5.69	20.6	106 –*j*49	1.89	

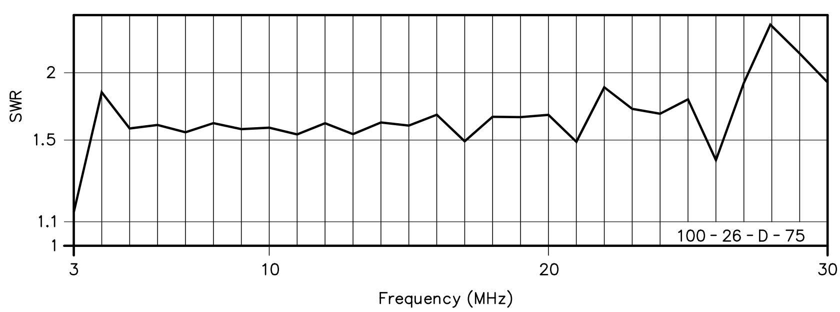

Fig 9—3-30 MHz SWR sweep of the 100-ft, 26-element LPDA model referenced to 75 Ω.

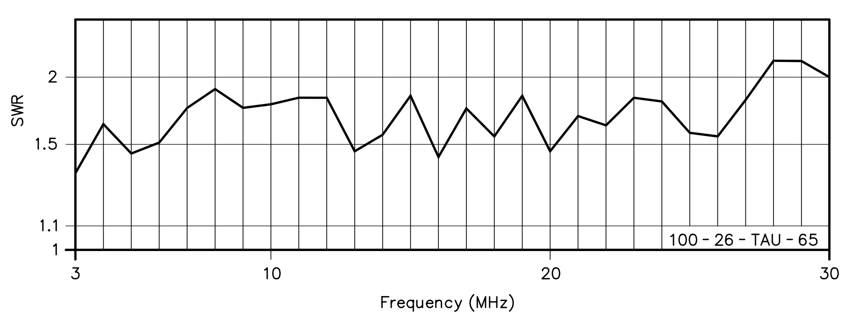

Fig 10—3-30 MHz SWR sweep of the 100-ft, 26-element LPDA model (with "Tau-tapered" element diameters) referenced to 65 Ω.

Table 9—Comparison of the element diameters for the initial and "Tau-tapered" versions of the 100-ft, 26-element LPDA model Diameters are in inches.

Element	*Initial*	*Tau-Taper*
26	0.50	0.50
25	0.50	0.56
24	0.625	0.62
23	0.75	0.69
22	0.75	0.76
21	0.875	0.85
20	1.00	0.94
19	1.00	1.04
18	1.125	1.15
17	1.25	1.27
16	1.25	1.41
15	1.375	1.56
14	1.50	1.73
13	1.50	1.91
12	1.625	2.12
11	1.75	2.34
10	1.75	2.59
9	1.825	2.87
8	2.00	3.18
7	2.00	3.52
6	2.125	3.90
5	2.25	4.32
4	2.25	4.79
3	2.375	5.30
2	2.50	5.87
1	2.50	6.50

lobe" (BFL) continues to diminish with each improved model.

However, the entire progression of models at the 100-ft length has shown significant improvements over the 60-ft model. How much improvement we have made can be judged by the following series of free-space azimuth patterns taken at 3, 9, 15 and 30 MHz. These are the same frequencies used for patterns of the 60-ft model. Directly comparing the patterns in Fig 12 with those in Fig 4 provides a measure of the improvements made by increasing the boom length and number of elements.

The 3-MHz pattern in Fig 12 shows the same circularity of the forward and rear lobes as does the 3 MHz 60-ft model pattern. However, the improved gain and front-to-back ratio are readily apparent. The 9-MHz pattern for the "Tau-tapered" 100-ft, 26-element model shows far better control (relative to the 60-ft model) of the rear lobe, despite its broadness.

The 60-ft model showed a many-lobed pattern at 15 MHz. In Fig 12, the 26-element model shows only forward and rearward lobes at the same frequency. The forward lobe is technically a double lobe, but the center-point is down only a fraction of a decibel, far too little to be detected in operation. Nonetheless, this lobe, like the lobes at many frequencies, continues to be somewhat broader than those associated with monoband Yagi antennas. At 30 MHz, the 26-element "Tau-tapered" model shows a similar pattern, although technically having only a single peak value. The irregularities on the sides of the forward lobe and all around the rear lobe are incipient secondary lobes created by the cumulative effects of the elements behind the shortest elements. Although current magnitudes in the longer elements are low, together they add remnant multiwavelength, multilobe facets to the 30-MHz pattern.

Fuller Frequency Sweeps

There are dangers associated with performing only spot performance checks at 3-MHz intervals. Therefore, I ran some 0.5-MHz-increment frequency sweeps of the tubing and the "Tau-tapered" element versions of the 100-ft, 26-element design. The purpose was to determine whether there were any hidden oddities of performance in either design. Although superior to checks at 3-MHz intervals,

Table 10—Performance of the 100-ft, 26-element model LPDA with "Tau-tapered" element diameters at 3-MHz increments from 3-30 MHz "BFL" means broad forward lobe (see text)

Frequency (MHz)	*Free-Space Gain (dBi)*	*Front-to-Back Ratio (dB)*	*Source Impedance (R ±jX Ω)*	*SWR (65 Ω)*	
3	5.38	9.9	71 +*j*17	1.30	
6	6.29	16.6	55 –*j*24	1.54	
9	5.80	18.5	85 –*j*38	1.75	
12	5.85	21.0	100 +*j*36	1.83	
15	5.56	19.5	117 +*j*20	1.87	BFL
18	5.80	21.1	48 +*j*17	1.56	
21	5.44	21.8	110 –*j*10	1.70	
24	5.76	22.6	72 –*j*41	1.81	BFL
27	5.57	22.4	51 –*j*32	1.83	
30	5.47	21.2	101 –*j*45	1.99	

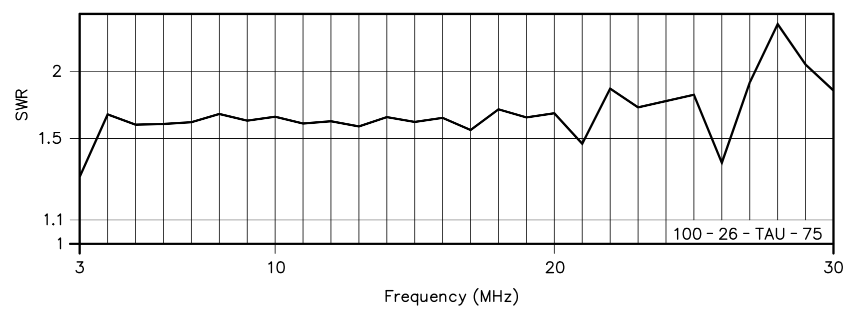

Fig 11—3-30 MHz SWR sweep of the 100-ft, 26-element LPDA model (with "Tau-tapered" element diameters) referenced to 75 Ω.

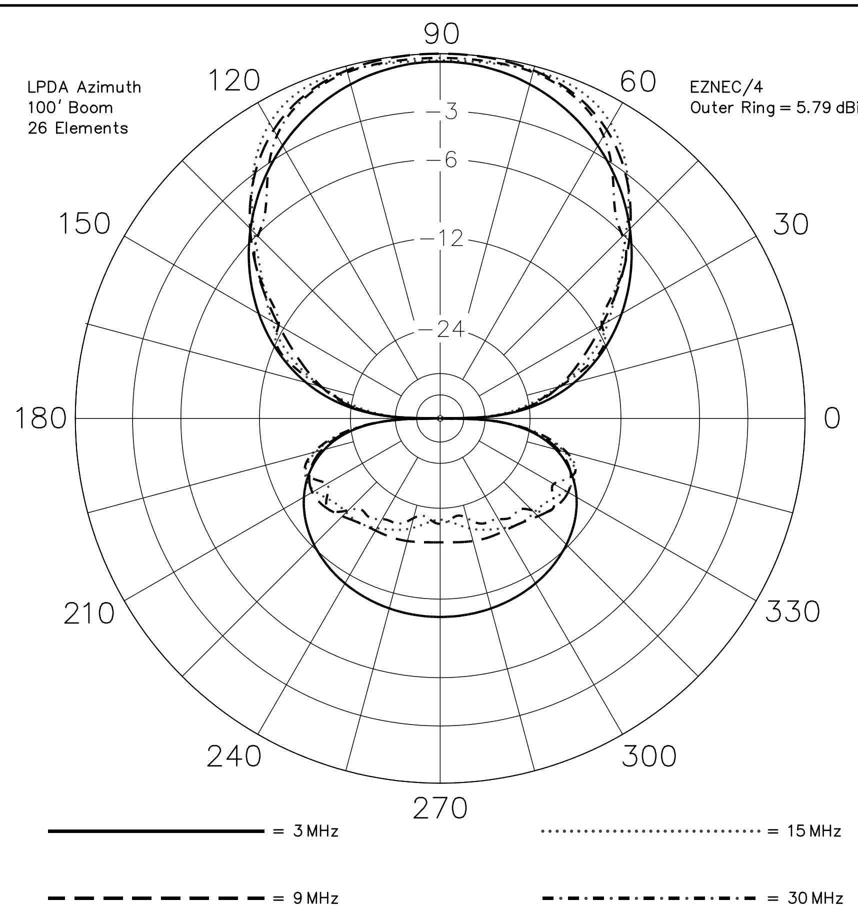

Fig 12—Free-space azimuth pattern of the 100-ft, 26-element LPDA model at 3, 9, 15 and 30 MHz.

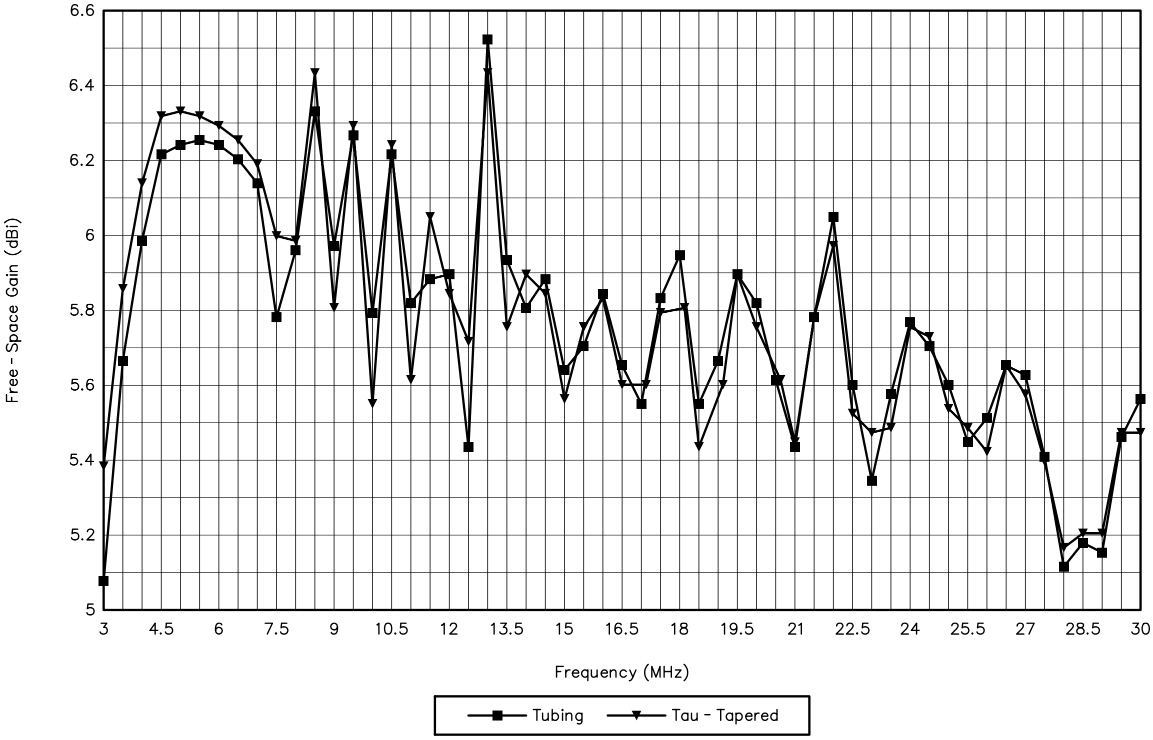

Fig 13—Frequency sweep at 0.5 MHz intervals of free-space gain (dBi) for both versions of the 100-ft, 26-element LPDA model.

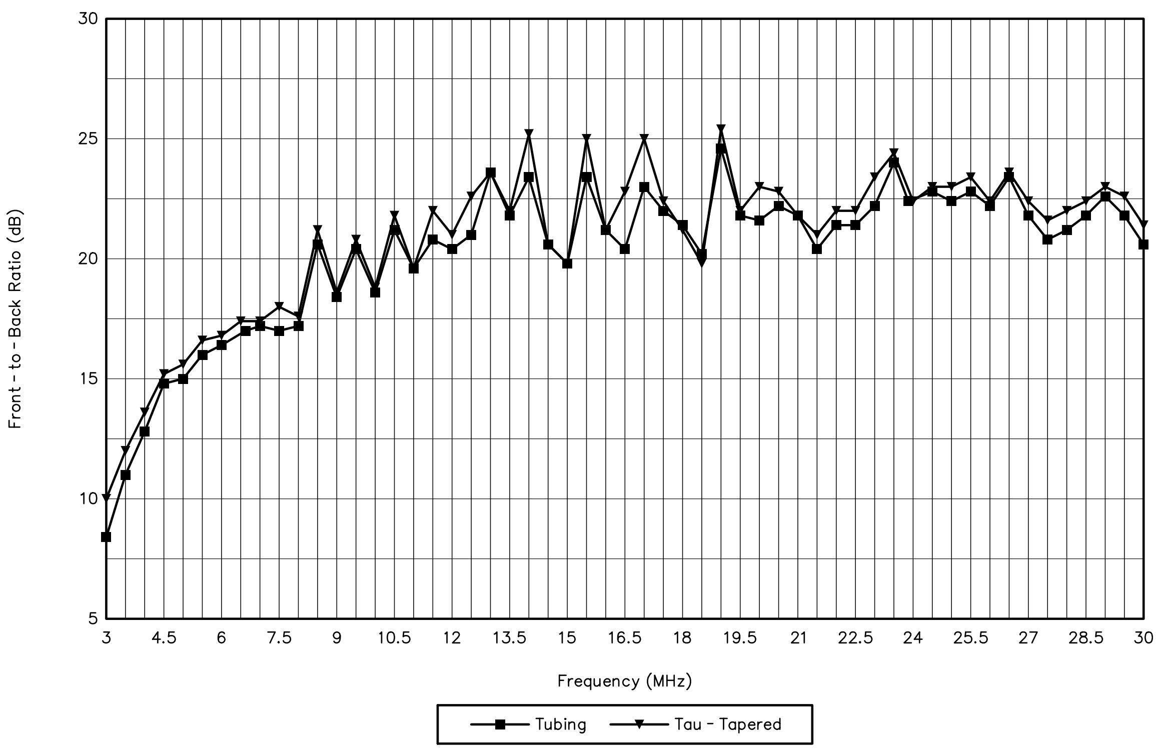

Fig 14—Frequency sweep at 0.5 MHz intervals of the front-to-back ratio (in dB) for both versions of the 100-ft, 26-element LPDA model.

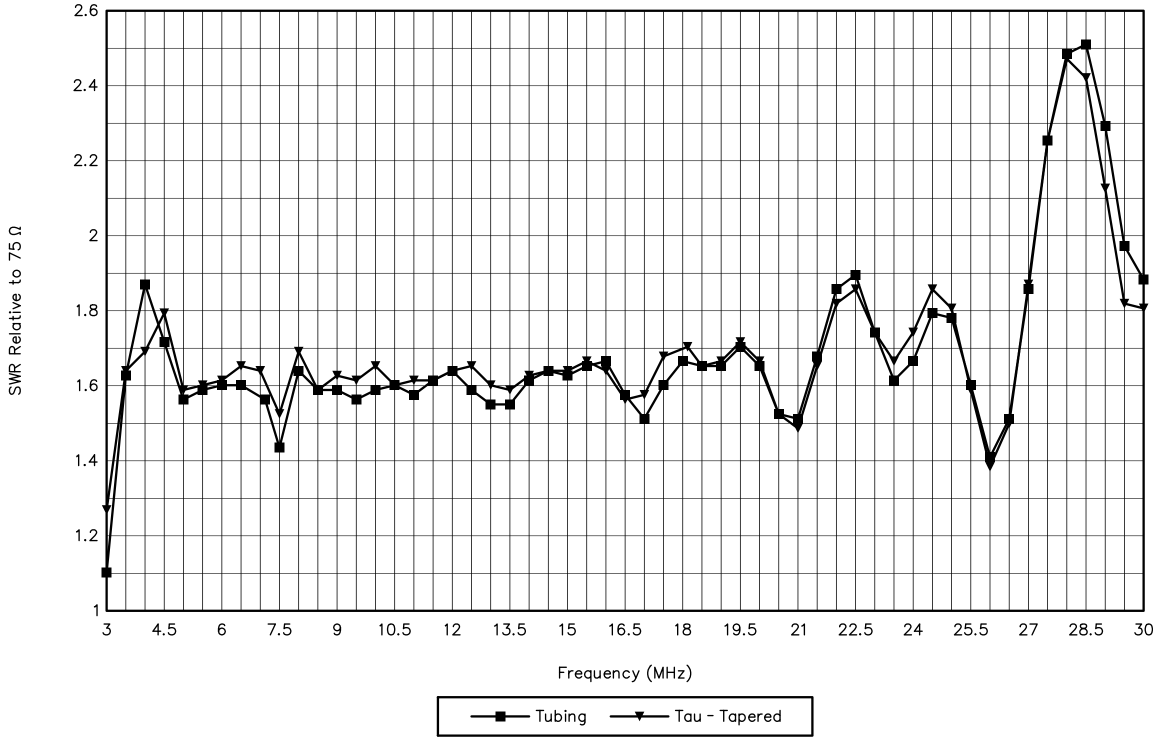

Fig 15—Frequency sweep at 0.5 MHz intervals of the 75-Ω SWR for both versions of the 100-ft, 26-element LPDA model.

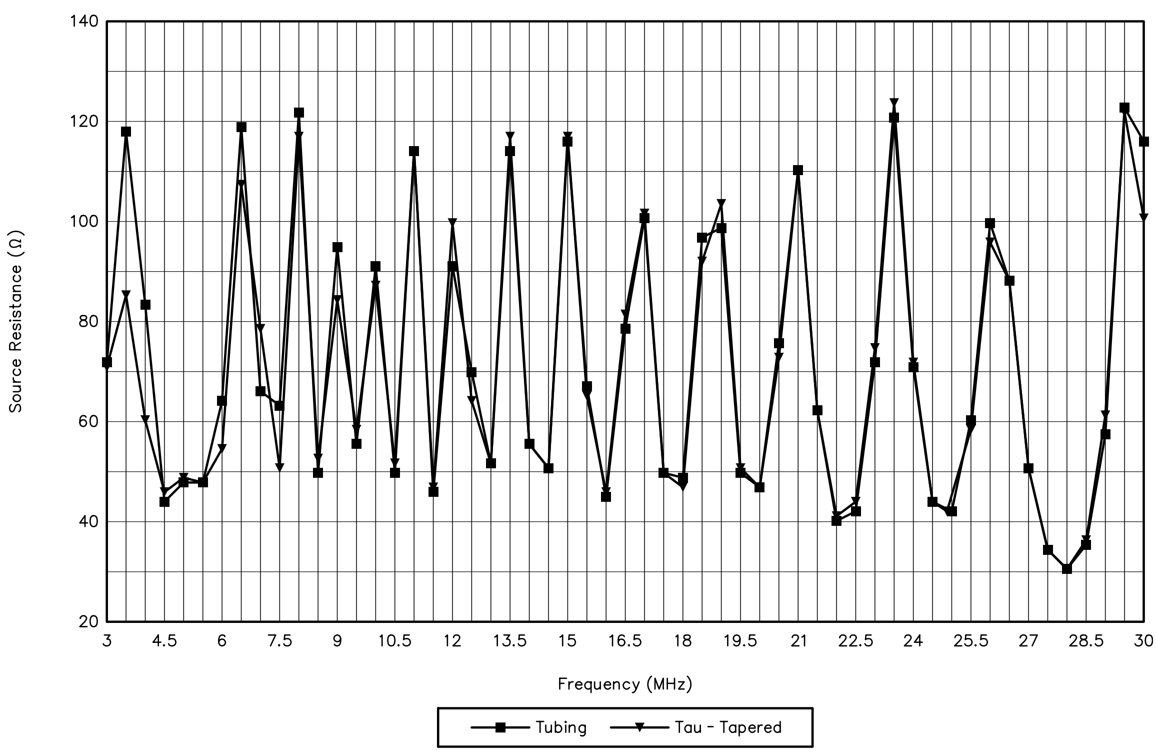

Fig 16—Frequency sweep at 0.5-MHz intervals of the feedpoint resistance (Ω) for both versions of the 100-ft, 26-element LPDA model.

even 0.5-MHz increments can miss some properties. Therefore, every LPDA design of interest should be swept at smaller intervals across every portion of the spectrum at which operation is contemplated.

The free-space gain graph in Fig 13 shows relatively good coincidence between the two design variants. However, in the lower third of the passband, the tubing version, which is limited to a maximum element diameter of 2.5 inches, shows greater excursions of free-space gain, including significantly lower values at 3 and 12.5 MHz.

The 180° front-to-back curves in Fig 14 are remarkably coincident across the entire passband. The 90-inch 150-Ω shorted stub used on both models smoothes the curve below 8.5 MHz, above which frequency the familiar sawtooth LPDA progression of values re-emerges.

The three final graphs should be read in this order: 75-Ω SWR (Fig 15), Source Resistance (Fig 16) and Source Reactance (Fig 17). The SWR curve in Fig 15 is quite smooth through at least 20 MHz, average a little over 1.6:1 relative to a 75-Ω standard. The illusion created by this curve is that the source impedance has a fairly constant value across this range. As the following Source Resistance graph (Fig 16) shows, the actual resistive impedance varies over a range greater than 4:1. What holds the SWR values to a narrow range is the reactance associated with each resistance value, which appears in Fig 17. Resistance values near the impedance standard of 75 Ω are accompanied by high inductive or capacitive reactance values. Resistive values more distant from the standard have associated reactance values that are much lower. The exception is in the 27.5 to 29 MHz range, where low resistance values are accompanied by high reactance values.

Indeed, the fuller frequency sweeps did uncover some interesting properties of the 100-ft, 26-element LPDAs that the wider-interval checks left obscure. Initially, the curves were developed to compare the tubing and the "Tau-tapered" element designs, but the interesting properties that emerged applied equally to both models.

Tentative Conclusions

Of the models evaluated in this part of the preliminary study, the 100-ft, 26-element versions provide the best overall performance. Additional elements within the 100-ft length are unlikely to add significantly to performance. Only additional boom length—to provide a more satisfactory value of Sigma—would show increases in gain. However, the gain advantage may be offset by a reduction in lower-frequency performance if the element density is not maintained. With the element density set to at least 20 elements per 100 ft of boom and up to 26 elements per 100 ft, obtaining a satisfactory SWR curve and well-controlled pattern shapes for the array should pose no major problem.

Some modification of low-frequency performance can be obtained by adjustments to the terminating stub. In all cases, the final length should be obtained by experiment on the physical antenna in order to make all due allowance for interelement transmission-line losses, which the *NEC-4* models cannot take into account. As well, the shortest elements active in the formation of the 27 to 30 MHz patterns should be experimentally adjusted to obtain the best patterns and the most satisfactory impedance values. However, such empirical adjustments may also throw off the feedpoint impedance,

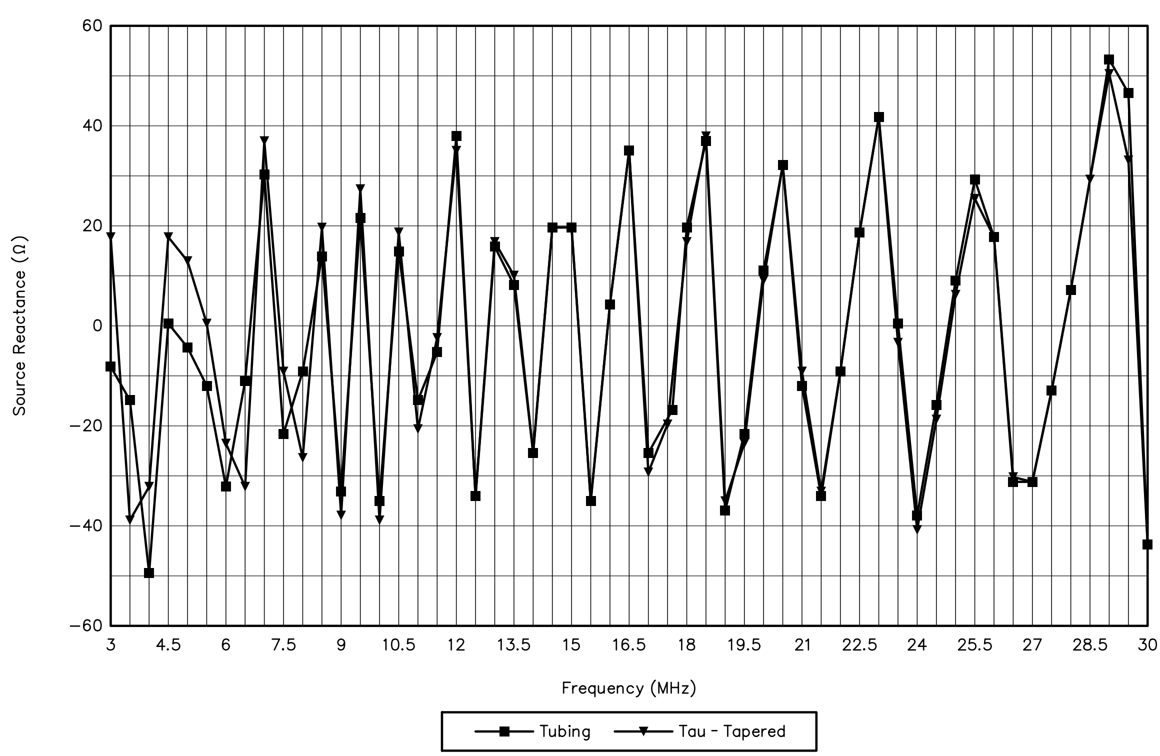

Fig 17—Frequency sweep at 0.5-MHz intervals of the feedpoint reactance (Ω) for both versions of the 100-ft, 26-element LPDA model.

even at frequencies distant from the ones for which element lengths and spacings are changed.

All of the models examined in these preliminary notes are of standard LPDA design. No attempt to use periodic element length techniques or other suggested enhancements has been attempted. Moreover, there are apparently some proprietary alternative algorithms said to provide improved performance across the 3-30 MHz spectrum. These algorithms are not accessible to me at present and therefore the designs that might result from them cannot be evaluated. Nonetheless, the general trends of standard LPDA designs have proven instructive in themselves.

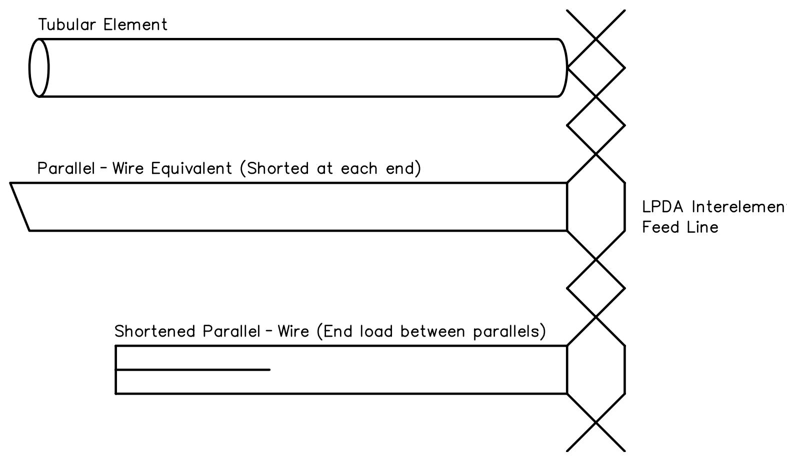

Fig 18—Evolution from tubular elements to equivalent wire elements to possible shortened-wire elements.

Tau-Tapered Element Design

True "Tau-tapered" elements result in impractical element diameters. However, an alternative construction method might use wire instead of tubing.

For a given element with an assigned tubular diameter, there will be a self-resonant frequency. One may construct the same element in skeleton form from wire. The length can be made equal to the original element and the spacing between wires adjusted until the wire element is resonant on the same frequency as the original tubular element. The principle is illustrated in Fig 18.

As a practical—although still hypothetical—example, let us take the longest element of the 100-ft, 20-element "Tau-tapered" array. This element in tubular form is 6.5 inches in diameter. The element is 2007.36 inches (167.28 ft) long. Isolated, it is resonant at 2.796 MHz, with a source impedance of 72.00 $-j0.02$ Ω. An equivalent #10-aluminum-wire element of the same length requires that the pair of wires be shorted at both their outer ends and at the feed point. Under these conditions, a spacing of 14 inches yields a resonant element at 2.796 MHz with an impedance of 70.53 + $j0.08$ Ω. There is a 0.02-dB deficit in gain owing to the slightly higher loss of the wire element.

Now let us shorten the wire element to 1680 inches (140 ft) or 840 inches each side of center. If we run a wire from the center of the outer end shorting wire toward the feed point to a position 67.4 inches away from the feed point, we again achieve resonance at 2.796 MHz. The loading effect reduces the element impedance to 46.50 + $j0.88$ Ω, and the gain is further decreased 0.25 dB. The seven-inch spacing between wires is sufficient to prevent arcing between wires for any power level.

Whether the shortened element would yield acceptable performance at the lower end of the 3-30 MHz passband has not been determined with models. However, the technique represents one of the simplest methods of shortening elements and preserving much of the current distribution on the element's center in an all-wire LPDA design.

A Final Question: Gain

The low gain of the LPDA models we have so far examined likely has two causes. First is the short boom length used, which results in borderline values for Sigma, in the 0.03 region. Ideal values for Sigma result in wider-spaced elements on much longer booms.

A second cause for the low gain, especially as it tapers off below 9 MHz, lies in the use of thin elements. Programs like *LPCAD* calculate element lengths based on a length-to-diameter ratio of 125, whereas even in the "Tau-tapered" models, the ratio is about 300:1. In general, as frequency increases, there is no gain problem, since the effective region of activity can simply move rearward for any frequency relative to what the active region would be for an idealized design. For the lowest frequencies, the longest element sets the limit of how far back the active region can move.

However, gain at the lowest design frequency is not solely a function of the longest element. It is also a function of the number and arrangement of elements forward of the longest element. Whichever way one wishes to achieve more gain, there is no escaping the need for a longer boom. We shall examine some longer designs in Part 2.

Antenna Model Descriptions

You can download this package from the ARRL Web site http://www.arrl.org/files/qex/. Look for LPDAPT1.ZIP.

60' 20-Element 3-30 MHz LPDA Frequency = 3 MHz.

Wire Loss: Aluminum Resistivity = 4E08 ohm, Rel. Perm. = 1

WIRES

Wire	Conn.	End 1 (x,y,z : in)	Conn.	End 2 (x,y,z : in)	Dia(in)	Segs
1		1003.7, 0.000,	0.000	1003.68, 0.000, 0.000	2.00E+00	105
2		876.93, 98.500,	0.000	876.930, 98.500, 0.000	2.00E+00	87
3		766.19,184.560,	0.000	766.190,184.560, 0.000	1.87E+00	75
4		669.44,259.750,	0.000	669.440,259.750, 0.000	1.75E+00	69
5		584.90,325.450,	0.000	584.900,325.450, 0.000	1.75E+00	57
6		511.04,382.850,	0.000	511.040,382.850, 0.000	1.62E+00	49
7		446.50,433.000,	0.000	446.500,433.000, 0.000	1.50E+00	43
8		390.12,476.820,	0.000	390.120,476.820, 0.000	1.50E+00	39
9		340.85,515.110,	0.000	340.850,515.110, 0.000	1.38E+00	37
10		297.81,546.560,	0.000	297.810,548.560, 0.000	1.25E+00	35
11		260.20,577.790,	0.000	260.200,577.790, 0.000	1.25E+00	33
12		227.34,603.320,	0.000	227.340,603.320, 0.000	1.12E+00	31
13		198.65,625.630,	0.000	198.650,625.630, 0.000	1.00E+00	29
14		173.55,645.130,	0.000	173.550,645.130, 0.000	1.00E+00	27
15		151.63,662.160,	0.000	151.630,662.160, 0.000	8.75E01	25
16		132.49,677.040,	0.000	132.490,677.040, 0.000	7.50E01	23
17		115.76,690.040,	0.000	115.760,690.040, 0.000	7.50E01	21
18		101.14,701.400,	0.000	101.140,701.400, 0.000	7.50E01	19
19		88.370,711.330,	0.000	88.370,711.330, 0.000	6.25E01	17
20		77.210,720.000,	0.000	77.210,720.000, 0.000	5.00E01	15

SOURCES

Source	Wire Seg.	Wire #/Pct From End 1 Actual	(Specified)	Ampl.(V, A)	Phase(Deg.)	Type
1	8	20 / 50.00	(20 / 50.00)	1.000	0.000	V

TRANSMISSION LINES

Line	Wire #/% From End 1 Actual	(Specified)	Wire #/% From End 1 Actual	(Specified)	Length	Z0 Ohms	Vel Fact	Rev/ Norm
1	1/50.0	(1/50.0)	2/50.0	(2/50.0)	Actual dist	150.0	1.00	R
2	2/50.0	(2/50.0)	3/50.0	(3/50.0)	Actual dist	150.0	1.00	R
3	3/50.0	(3/50.0)	4/50.0	(4/50.0)	Actual dist	150.0	1.00	R
4	4/50.0	(4/50.0)	5/50.0	(5/50.0)	Actual dist	150.0	1.00	R
5	5/50.0	(5/50.0)	6/50.0	(6/50.0)	Actual dist	150.0	1.00	R
6	6/50.0	(6/50.0)	7/50.0	(7/50.0)	Actual dist	150.0	1.00	R
7	7/50.0	(7/50.0)	8/50.0	(8/50.0)	Actual dist	150.0	1.00	R
8	8/50.0	(8/50.0)	9/50.0	(9/50.0)	Actual dist	150.0	1.00	R
9	9/50.0	(9/50.0)	10/50.0	(10/50.0)	Actual dist	150.0	1.00	R
10	10/50.0	(10/50.0)	11/50.0	(11/50.0)	Actual dist	150.0	1.00	R
11	11/50.0	(11/50.0)	12/50.0	(12/50.0)	Actual dist	150.0	1.00	R
12	12/50.0	(12/50.0)	13/50.0	(13/50.0)	Actual dist	150.0	1.00	R
13	13/50.0	(13/50.0)	14/50.0	(14/50.0)	Actual dist	150.0	1.00	R
14	14/50.0	(14/50.0)	15/50.0	(15/50.0)	Actual dist	150.0	1.00	R
15	15/50.0	(15/50.0)	16/50.0	(16/50.0)	Actual dist	150.0	1.00	R
16	16/50.0	(16/50.0)	17/50.0	(17/50.0)	Actual dist	150.0	1.00	R
17	17/50.0	(17/50.0)	18/50.0	(18/50.0)	Actual dist	150.0	1.00	R
18	18/50.0	(18/50.0)	19/50.0	(19/50.0)	Actual dist	150.0	1.00	R
19	19/50.0	(19/50.0)	20/50.0	(20/50.0)	Actual dist	150.0	1.00	R

Ground type is Free Space

100' 20-Element 3-30 MHz LPDA Frequency = 10 MHz.

Wire Loss: Aluminum Resistivity = 4E08 ohm, Rel. Perm. = 1

WIRES

Wire	Conn.	End 1 (x,y,z : in)	Conn.	End 2 (x,y,z : in)	Dia(in)	Segs
1		1003.7, 0.000,	0.000	1003.68, 0.000, 0.000	2.00E+00	105
2		876.93,164.170,	0.000	876.930,164.170, 0.000	2.00E+00	87
3		766.19,307.600,	0.000	766.190,307.600, 0.000	1.87E+00	75
4		669.44,432.920,	0.000	669.440,432.920, 0.000	1.75E+00	69
5		584.90,542.420,	0.000	584.900,542.420, 0.000	1.75E+00	57
6		511.04,638.090,	0.000	511.040,638.090, 0.000	1.62E+00	49
7		446.50,721.680,	0.000	446.500,721.680, 0.000	1.50E+00	43
8		390.12,794.710,	0.000	390.120,794.710, 0.000	1.50E+00	39
9		340.85,858.520,	0.000	340.850,858.520, 0.000	1.38E+00	37
10		297.81,914.280,	0.000	297.810,914.280, 0.000	1.25E+00	35
11		260.20,962.980,	0.000	260.200,962.980, 0.000	1.25E+00	33
12		227.34,1005.54,	0.000	227.340,1005.54, 0.000	1.12E+00	31
13		198.65,1042.72,	0.000	198.650,1042.72, 0.000	1.00E+00	29
14		173.55,1075.21,	0.000	173.550,1075.21, 0.000	1.00E+00	27
15		151.63,1103.60,	0.000	151.630,1103.60, 0.000	8.75E01	25
16		132.49,1128.40,	0.000	132.490,1128.40, 0.000	7.50E01	23
17		115.76,1150.07,	0.000	115.760,1150.07, 0.000	7.50E01	21
18		101.14,1169.00,	0.000	101.140,1169.00, 0.000	7.50E01	19
19		88.370,1185.55,	0.000	88.370,1185.55, 0.000	6.25E01	17
20		77.210,1200.00,	0.000	77.210,1200.00, 0.000	5.00E01	15

```
                 SOURCES
Source    Wire      Wire #/Pct From End 1    Ampl.(V, A)  Phase(Deg.)  Type
          Seg.     Actual      (Specified)
1           8    20 / 50.00   ( 20 / 50.00)      1.000       0.000       V

                   TRANSMISSION LINES
Line  Wire #/% From End 1   Wire #/% From End 1    Length       Z0   Vel Rev/
      Actual  (Specified)   Actual  (Specified)               Ohms Fact Norm
1      1/50.0  (  1/50.0)    2/50.0  (  2/50.0)  Actual dist  200.0  1.00  R
2      2/50.0  (  2/50.0)    3/50.0  (  3/50.0)  Actual dist  200.0  1.00  R
3      3/50.0  (  3/50.0)    4/50.0  (  4/50.0)  Actual dist  200.0  1.00  R
4      4/50.0  (  4/50.0)    5/50.0  (  5/50.0)  Actual dist  200.0  1.00  R
5      5/50.0  (  5/50.0)    6/50.0  (  6/50.0)  Actual dist  200.0  1.00  R
6      6/50.0  (  6/50.0)    7/50.0  (  7/50.0)  Actual dist  200.0  1.00  R
7      7/50.0  (  7/50.0)    8/50.0  (  8/50.0)  Actual dist  200.0  1.00  R
8      8/50.0  (  8/50.0)    9/50.0  (  9/50.0)  Actual dist  200.0  1.00  R
9      9/50.0  (  9/50.0)   10/50.0  ( 10/50.0)  Actual dist  200.0  1.00  R
10    10/50.0  ( 10/50.0)   11/50.0  ( 11/50.0)  Actual dist  200.0  1.00  R
11    11/50.0  ( 11/50.0)   12/50.0  ( 12/50.0)  Actual dist  200.0  1.00  R
12    12/50.0  ( 12/50.0)   13/50.0  ( 13/50.0)  Actual dist  200.0  1.00  R
13    13/50.0  ( 13/50.0)   14/50.0  ( 14/50.0)  Actual dist  200.0  1.00  R
14    14/50.0  ( 14/50.0)   15/50.0  ( 15/50.0)  Actual dist  200.0  1.00  R
15    15/50.0  ( 15/50.0)   16/50.0  ( 16/50.0)  Actual dist  200.0  1.00  R
16    16/50.0  ( 16/50.0)   17/50.0  ( 17/50.0)  Actual dist  200.0  1.00  R
17    17/50.0  ( 17/50.0)   18/50.0  ( 18/50.0)  Actual dist  200.0  1.00  R
18    18/50.0  ( 18/50.0)   19/50.0  ( 19/50.0)  Actual dist  200.0  1.00  R
19    19/50.0  ( 19/50.0)   20/50.0  ( 20/50.0)  Actual dist  200.0  1.00  R
20     1/50.0  (  1/50.0)  Short ckt (Short ck)   90.000 in   200.0  1.00
Ground type is Free Space
```

```
100' 20-Element 3-30 MHz LPDA, "Tau-tapered" elements    Frequency = 10  MHz.

Wire Loss: Aluminum  Resistivity = 4E08 ohmm, Rel. Perm. = 1

               WIRES
Wire Conn.  End 1 (x,y,z : in)    Conn.    End 2 (x,y,z : in)       Dia(in)     Segs
1           1003.7,  0.000,       0.000    1003.68,  0.000,  0.000  6.50E+00     105
2           876.93,164.170,       0.000    876.930,164.170,  0.000  5.68E+00      87
3           766.19,307.600,       0.000    766.190,307.600,  0.000  4.96E+00      75
4           669.44,432.920,       0.000    669.440,432.920,  0.000  4.33E+00      69
5           584.90,542.420,       0.000    584.900,542.420,  0.000  3.79E+00      57
6           511.04,638.090,       0.000    511.040,638.090,  0.000  3.31E+00      49
7           446.50,721.680,       0.000    446.500,721.680,  0.000  2.89E+00      43
8           390.12,794.710,       0.000    390.120,794.710,  0.000  2.53E+00      39
9           340.85,858.520,       0.000    340.850,858.520,  0.000  2.20E+00      37
10          297.81,914.280,       0.000    297.810,914.280,  0.000  1.93E+00      35
11          260.20,962.980,       0.000    260.200,962.980,  0.000  1.69E+00      33
12          227.34,1005.54,       0.000    227.340,1005.54,  0.000  1.47E+00      31
13          198.65,1042.72,       0.000    198.650,1042.72,  0.000  1.29E+00      29
14          173.55,1075.21,       0.000    173.550,1075.21,  0.000  1.12E+00      27
15          151.63,1103.60,       0.000    151.630,1103.60,  0.000  9.80E01       25
16          132.49,1128.40,       0.000    132.490,1128.40,  0.000  8.60E01       23
17          115.76,1150.07,       0.000    115.760,1150.07,  0.000  7.50E01       21
18          101.14,1169.00,       0.000    101.140,1169.00,  0.000  6.60E01       19
19          88.370,1185.55,       0.000    88.370,1185.55,  0.000   5.70E01       17
20          77.210,1200.00,       0.000    77.210,1200.00,  0.000   5.00E01       15

                 SOURCES
Source    Wire      Wire #/Pct From End 1    Ampl.(V, A)  Phase(Deg.)  Type
          Seg.     Actual      (Specified)
1           8    20 / 50.00   ( 20 / 50.00)      1.000       0.000       V

                   TRANSMISSION LINES
Line  Wire #/% From End 1   Wire #/% From End 1    Length       Z0   Vel Rev/
      Actual  (Specified)   Actual  (Specified)               Ohms Fact Norm
1      1/50.0  (  1/50.0)    2/50.0  (  2/50.0)  Actual dist  200.0  1.00  R
2      2/50.0  (  2/50.0)    3/50.0  (  3/50.0)  Actual dist  200.0  1.00  R
3      3/50.0  (  3/50.0)    4/50.0  (  4/50.0)  Actual dist  200.0  1.00  R
4      4/50.0  (  4/50.0)    5/50.0  (  5/50.0)  Actual dist  200.0  1.00  R
5      5/50.0  (  5/50.0)    6/50.0  (  6/50.0)  Actual dist  200.0  1.00  R
6      6/50.0  (  6/50.0)    7/50.0  (  7/50.0)  Actual dist  200.0  1.00  R
7      7/50.0  (  7/50.0)    8/50.0  (  8/50.0)  Actual dist  200.0  1.00  R
8      8/50.0  (  8/50.0)    9/50.0  (  9/50.0)  Actual dist  200.0  1.00  R
9      9/50.0  (  9/50.0)   10/50.0  ( 10/50.0)  Actual dist  200.0  1.00  R
10    10/50.0  ( 10/50.0)   11/50.0  ( 11/50.0)  Actual dist  200.0  1.00  R
11    11/50.0  ( 11/50.0)   12/50.0  ( 12/50.0)  Actual dist  200.0  1.00  R
12    12/50.0  ( 12/50.0)   13/50.0  ( 13/50.0)  Actual dist  200.0  1.00  R
13    13/50.0  ( 13/50.0)   14/50.0  ( 14/50.0)  Actual dist  200.0  1.00  R
14    14/50.0  ( 14/50.0)   15/50.0  ( 15/50.0)  Actual dist  200.0  1.00  R
15    15/50.0  ( 15/50.0)   16/50.0  ( 16/50.0)  Actual dist  200.0  1.00  R
16    16/50.0  ( 16/50.0)   17/50.0  ( 17/50.0)  Actual dist  200.0  1.00  R
17    17/50.0  ( 17/50.0)   18/50.0  ( 18/50.0)  Actual dist  200.0  1.00  R
18    18/50.0  ( 18/50.0)   19/50.0  ( 19/50.0)  Actual dist  200.0  1.00  R
19    19/50.0  ( 19/50.0)   20/50.0  ( 20/50.0)  Actual dist  200.0  1.00  R
20     1/50.0  (  1/50.0)  Short ckt (Short ck)   90.000 in   200.0  1.00
Ground type is Free Space
```

100' 26-Element 3-30 MHz LPDA   Frequency = 10 MHz.

Wire Loss: Aluminum Resistivity = 4E08 ohmm, Rel. Perm. = 1

WIRES

Wire	Conn.	End 1 (x,y,z : in)	Conn.	End 2 (x,y,z : in)		Dia(in)	Segs
1		1003.7, 0.000,	0.000	1003.68, 0.000,	0.000	2.50E+00	107
2		905.81,126.760,	0.000	905.810,126.760,	0.000	2.50E+00	97
3		817.49,241.170,	0.000	817.490,241.170,	0.000	2.38E+00	87
4		737.77,344.410,	0.000	737.770,344.410,	0.000	2.25E+00	79
5		655.83,437.590,	0.000	655.830,437.590,	0.000	2.25E+00	71
6		600.91,521.690,	0.000	600.910,521.690,	0.000	2.12E+00	65
7		542.31,597.580,	0.000	542.310,597.580,	0.000	2.00E+00	57
8		489.43,666.070,	0.000	489.430,666.070,	0.000	2.00E+00	53
9		441.71,727.890,	0.000	441.710,727.890,	0.000	1.87E+00	47
10		398.64,783.640,	0.000	398.640,783.640,	0.000	1.75E+00	43
11		359.76,834.020,	0.000	359.760,834.020,	0.000	1.75E+00	39
12		324.68,879.460,	0.000	324.680,879.460,	0.000	1.62E+00	35
13		293.02,920.470,	0.000	293.020,920.470,	0.000	1.50E+00	31
14		264.45,957.470,	0.000	264.450,957.470,	0.000	1.50E+00	29
15		238.66,990.870,	0.000	238.660,990.870,	0.000	1.38E+00	25
16		215.39,1021.01,	0.000	215.390,1021.01,	0.000	1.25E+00	23
17		194.39,1048.22,	0.000	194.390,1048.22,	0.000	1.25E+00	21
18		175.43,1072.77,	0.000	175.430,1072.77,	0.000	1.12E+00	19
19		158.33,1094.93,	0.000	158.330,1094.93,	0.000	1.00E+00	17
20		142.89,1114.93,	0.000	142.890,1114.93,	0.000	1.00E+00	15
21		128.96,1132.97,	0.000	128.960,1132.97,	0.000	8.75E01	15
22		116.38,1149.26,	0.000	116.380,1149.26,	0.000	7.50E01	13
23		105.03,1163.96,	0.000	105.030,1163.96,	0.000	7.50E01	11
24		94.790,1177.22,	0.000	94.790,1177.22,	0.000	6.25E01	11
25		85.550,1189.20,	0.000	85.550,1189.20,	0.000	5.00E01	9
26		77.210,1200.00,	0.000	77.210,1200.00,	0.000	5.00E01	9

SOURCES

Source	Wire Seg.	Wire #/Pct From End 1 Actual	(Specified)	Ampl.(V, A)	Phase(Deg.)	Type
1	5	26 / 50.00	(26 / 50.00)	1.000	0.000	V

TRANSMISSION LINES

Line	Wire #/% From End 1 Actual	(Specified)	Wire #/% From End 1 Actual	(Specified)	Length	Z0 Ohms	Vel Fact	Rev/ Norm
1	1/50.0	(1/50.0)	2/50.0	(2/50.0)	Actual dist	150.0	1.00	R
2	2/50.0	(2/50.0)	3/50.0	(3/50.0)	Actual dist	150.0	1.00	R
3	3/50.0	(3/50.0)	4/50.0	(4/50.0)	Actual dist	150.0	1.00	R
4	4/50.0	(4/50.0)	5/50.0	(5/50.0)	Actual dist	150.0	1.00	R
5	5/50.0	(5/50.0)	6/50.0	(6/50.0)	Actual dist	150.0	1.00	R
6	6/50.0	(6/50.0)	7/50.0	(7/50.0)	Actual dist	150.0	1.00	R
7	7/50.0	(7/50.0)	8/50.0	(8/50.0)	Actual dist	150.0	1.00	R
8	8/50.0	(8/50.0)	9/50.0	(9/50.0)	Actual dist	150.0	1.00	R
9	9/50.0	(9/50.0)	10/50.0	(10/50.0)	Actual dist	150.0	1.00	R
10	10/50.0	(10/50.0)	11/50.0	(11/50.0)	Actual dist	150.0	1.00	R
11	11/50.0	(11/50.0)	12/50.0	(12/50.0)	Actual dist	150.0	1.00	R
12	12/50.0	(12/50.0)	13/50.0	(13/50.0)	Actual dist	150.0	1.00	R
13	13/50.0	(13/50.0)	14/50.0	(14/50.0)	Actual dist	150.0	1.00	R
14	14/50.0	(14/50.0)	15/50.0	(15/50.0)	Actual dist	150.0	1.00	R
15	15/50.0	(15/50.0)	16/50.0	(16/50.0)	Actual dist	150.0	1.00	R
16	16/50.0	(16/50.0)	17/50.0	(17/50.0)	Actual dist	150.0	1.00	R
17	17/50.0	(17/50.0)	18/50.0	(18/50.0)	Actual dist	150.0	1.00	R
18	18/50.0	(18/50.0)	19/50.0	(19/50.0)	Actual dist	150.0	1.00	R
19	19/50.0	(19/50.0)	20/50.0	(20/50.0)	Actual dist	150.0	1.00	R
20	20/50.0	(20/50.0)	21/50.0	(21/50.0)	Actual dist	150.0	1.00	R
21	21/50.0	(21/50.0)	22/50.0	(22/50.0)	Actual dist	150.0	1.00	R
22	22/50.0	(22/50.0)	23/50.0	(23/50.0)	Actual dist	150.0	1.00	R
23	23/50.0	(23/50.0)	24/50.0	(24/50.0)	Actual dist	150.0	1.00	R
24	24/50.0	(24/50.0)	25/50.0	(25/50.0)	Actual dist	150.0	1.00	R
25	25/50.0	(25/50.0)	26/50.0	(26/50.0)	Actual dist	150.0	1.00	R
26	1/50.0	(1/50.0)	Short ckt	(Short ck)	90.000 in	150.0	1.00	

Ground type is Free Space

```
100' 26-Element 3-30 MHz LPDA, “Tau-tapered” elements    Frequency = 10  MHz.

Wire Loss: Aluminum  Resistivity = 4E08 ohmm, Rel. Perm. = 1

               WIRES
Wire Conn. End 1 (x,y,z : in)   Conn.    End 2 (x,y,z : in)       Dia(in)     Segs
1          1003.7,  0.000,      0.000    1003.68,  0.000, 0.000   6.50E+00     107
2          905.81,126.760,      0.000    905.810,126.760, 0.000   5.87E+00      97
3          817.49,241.170,      0.000    817.490,241.170, 0.000   5.30E+00      87
4          737.77,344.410,      0.000    737.770,344.410, 0.000   4.79E+00      79
5          655.83,437.590,      0.000    655.830,437.590, 0.000   4.32E+00      71
6          600.91,521.690,      0.000    600.910,521.690, 0.000   3.90E+00      65
7          542.31,597.580,      0.000    542.310,597.580, 0.000   3.52E+00      57
8          489.43,666.070,      0.000    489.430,666.070, 0.000   3.18E+00      53
9          441.71,727.890,      0.000    441.710,727.890, 0.000   2.87E+00      47
10         398.64,783.640,      0.000    398.640,783.640, 0.000   2.59E+00      43
11         359.76,834.020,      0.000    359.760,834.020, 0.000   2.34E+00      39
12         324.68,879.460,      0.000    324.680,879.460, 0.000   2.12E+00      35
13         293.02,920.470,      0.000    293.020,920.470, 0.000   1.91E+00      31
14         264.45,957.470,      0.000    264.450,957.470, 0.000   1.73E+00      29
15         238.66,990.870,      0.000    238.660,990.870, 0.000   1.56E+00      25
16         215.39,1021.01,      0.000    215.390,1021.01, 0.000   1.41E+00      23
17         194.39,1048.22,      0.000    194.390,1048.22, 0.000   1.27E+00      21
18         175.43,1072.77,      0.000    175.430,1072.77, 0.000   1.15E+00      19
19         158.33,1094.93,      0.000    158.330,1094.93, 0.000   1.04E+00      17
20         142.89,1114.93,      0.000    142.890,1114.93, 0.000   9.40E01       15
21         128.96,1132.97,      0.000    128.960,1132.97, 0.000   8.40E01       15
22         116.38,1149.26,      0.000    116.380,1149.26, 0.000   7.60E01       13
23         105.03,1163.96,      0.000    105.030,1163.96, 0.000   6.90E01       11
24         94.790,1177.22,      0.000    94.790,1177.22, 0.000    6.20E01       11
25         85.550,1189.20,      0.000    85.550,1189.20, 0.000    5.60E01        9
26         77.210,1200.00,      0.000    77.210,1200.00, 0.000    5.00E01        9

               SOURCES
Source    Wire      Wire #/Pct From End 1    Ampl.(V, A)  Phase(Deg.)  Type
          Seg.     Actual      (Specified)
1           5    26 / 50.00   ( 26 / 50.00)      1.000       0.000       V

                 TRANSMISSION LINES
Line  Wire #/% From End 1   Wire #/% From End 1    Length       Z0   Vel Rev/
      Actual   (Specified)  Actual   (Specified)               Ohms Fact Norm
1      1/50.0  (  1/50.0)    2/50.0  (  2/50.0)  Actual dist  150.0  1.00  R
2      2/50.0  (  2/50.0)    3/50.0  (  3/50.0)  Actual dist  150.0  1.00  R
3      3/50.0  (  3/50.0)    4/50.0  (  4/50.0)  Actual dist  150.0  1.00  R
4      4/50.0  (  4/50.0)    5/50.0  (  5/50.0)  Actual dist  150.0  1.00  R
5      5/50.0  (  5/50.0)    6/50.0  (  6/50.0)  Actual dist  150.0  1.00  R
6      6/50.0  (  6/50.0)    7/50.0  (  7/50.0)  Actual dist  150.0  1.00  R
7      7/50.0  (  7/50.0)    8/50.0  (  8/50.0)  Actual dist  150.0  1.00  R
8      8/50.0  (  8/50.0)    9/50.0  (  9/50.0)  Actual dist  150.0  1.00  R
9      9/50.0  (  9/50.0)   10/50.0  ( 10/50.0)  Actual dist  150.0  1.00  R
10    10/50.0  ( 10/50.0)   11/50.0  ( 11/50.0)  Actual dist  150.0  1.00  R
11    11/50.0  ( 11/50.0)   12/50.0  ( 12/50.0)  Actual dist  150.0  1.00  R
12    12/50.0  ( 12/50.0)   13/50.0  ( 13/50.0)  Actual dist  150.0  1.00  R
13    13/50.0  ( 13/50.0)   14/50.0  ( 14/50.0)  Actual dist  150.0  1.00  R
14    14/50.0  ( 14/50.0)   15/50.0  ( 15/50.0)  Actual dist  150.0  1.00  R
15    15/50.0  ( 15/50.0)   16/50.0  ( 16/50.0)  Actual dist  150.0  1.00  R
16    16/50.0  ( 16/50.0)   17/50.0  ( 17/50.0)  Actual dist  150.0  1.00  R
17    17/50.0  ( 17/50.0)   18/50.0  ( 18/50.0)  Actual dist  150.0  1.00  R
18    18/50.0  ( 18/50.0)   19/50.0  ( 19/50.0)  Actual dist  150.0  1.00  R
19    19/50.0  ( 19/50.0)   20/50.0  ( 20/50.0)  Actual dist  150.0  1.00  R
20    20/50.0  ( 20/50.0)   21/50.0  ( 21/50.0)  Actual dist  150.0  1.00  R
21    21/50.0  ( 21/50.0)   22/50.0  ( 22/50.0)  Actual dist  150.0  1.00  R
22    22/50.0  ( 22/50.0)   23/50.0  ( 23/50.0)  Actual dist  150.0  1.00  R
23    23/50.0  ( 23/50.0)   24/50.0  ( 24/50.0)  Actual dist  150.0  1.00  R
24    24/50.0  ( 24/50.0)   25/50.0  ( 25/50.0)  Actual dist  150.0  1.00  R
25    25/50.0  ( 25/50.0)   26/50.0  ( 26/50.0)  Actual dist  150.0  1.00  R
26     1/50.0  (  1/50.0)  Short ckt (Short ck)   90.000 in   150.0  1.00

Ground type is Free Space
```

□□

The ATR-2000: A Homemade, High-Performance HF Transceiver, Pt 2

Part 2 describes the IF and audio sections, including IF amplifier, product detector/balanced modulator, RF compressor, AGC and PC-interface circuits.

By John B. Stephensen, KD6OZH

This article series describes my homebrew HF transceiver. Part 1 described the general architecture and the front end, including the synthesized local oscillator and BFO, mixer and RF band-pass filter.[1] This part describes the IF and audio sections of the transceiver, including IF amplifier, product detector/balanced modulator, RF compressor, AGC and PC-interface circuits.

Dynamic-Range Considerations

Gain distribution is an important facet of transceiver design.[2] Gain ahead of the main band-pass filter should be minimized, so signals on adjacent frequencies do not cause serious intermodulation distortion (IMD). With the IF Preamplifier/Noise Gate module switched out, the ATR-2000 has no gain ahead of the main crystal filter, but rather a loss of 12 dB. As described in Part 1 of this article, noise figure is 18-22 dB depending on which filter is selected, and the 1-dB compression point is +23 dBm. The mixer is not terminated in an ideal load, so we expect at least 3 dB of degradation for a +35 dBm third-order intercept point (IP3).

When the IF Preamplifier/Noise Gate module is switched in, it adds 11 dB of gain, bringing total gain ahead of the main crystal filter up to –1 dB. The noise figure of this module is 4 dB, bringing the system noise figure down to 16 dB. The 1-dB compression point is reduced because of the additional gain. It is determined primarily by the compression point of the IF preamplifier itself, which is +13 dBm at the output to the crystal filter. This is intentionally limited to prevent destruction of the crystals by strong signals. The receiver's input compression point is therefore +14 dBm.

When the incoming signal is within the main filter bandwidth, the compression point is determined by the first few stages of the IF amplifier when it is running at minimum gain. This is the condition when a strong signal is present and AGC is on. This transceiver uses the Analog Devices AD603 low-noise, 90-MHz variable-gain amplifier. Its advantages include

[1]Notes appear on page 51.

153 Gretna Green Wy
Los Angeles, CA 90049
kd6ozh@amsat.org

a +13 dBm 1-dB input compression point and a gain reduction mechanism that does not reduce input signal-handling capability. A post-filter amplifier is included to maintain noise figure; it reduces the 1-dB input compression point to –1 dBm. A 4-dB loss in the SSB crystal filter and 12-dB loss in the front end result in a +15 dBm 1-dB compression point at the antenna terminals without the IF preamplifier, and +4 dBm with it. The resulting dynamic ranges for various input frequencies are shown in Table 1.

IF Preamplifier/ Noise Gate Module

Fig 1 shows the IF preamplifier and noise-gate module. It consists of a diplexer, band-pass filter, low-noise amplifier and noise gate. The diplexer provides a termination for the mixer at the LO and image frequencies. The Q is low and insertion loss is 0.4 dB.

When not in use, power is removed and K1 and K2 bypass all stages after the diplexer. Mechanical relays are used to ensure low IMD as this circuit precedes the main filter. The Omron relays are designed for RF use; they have more than 60 dB of isolation between contacts. At least 80 dB of isolation between input and output is required when the noise blanker is operating.

When the preamplifier is in operation, a two-pole monolithic crystal filter with a 15 kHz bandwidth filters incoming signals and noise. L1, L2 and associated capacitors provide transformation to and from 50 Ω. Because impedance of the KVG XF-910 monolithic crystal filter is very high (6000 Ω), two-thirds of the 1.5 dB loss in this circuit actually comes from the matching networks. High-Q toroidial coils are used to minimize the loss. Note that the filter bandwidth must be several times the information bandwidth (to ensure minimum spreading of pulses), but narrow enough to delay the arrival of noise pulses until after blanking is in effect.

The amplifier consists of a Motorola MRF581 configured as a low-noise

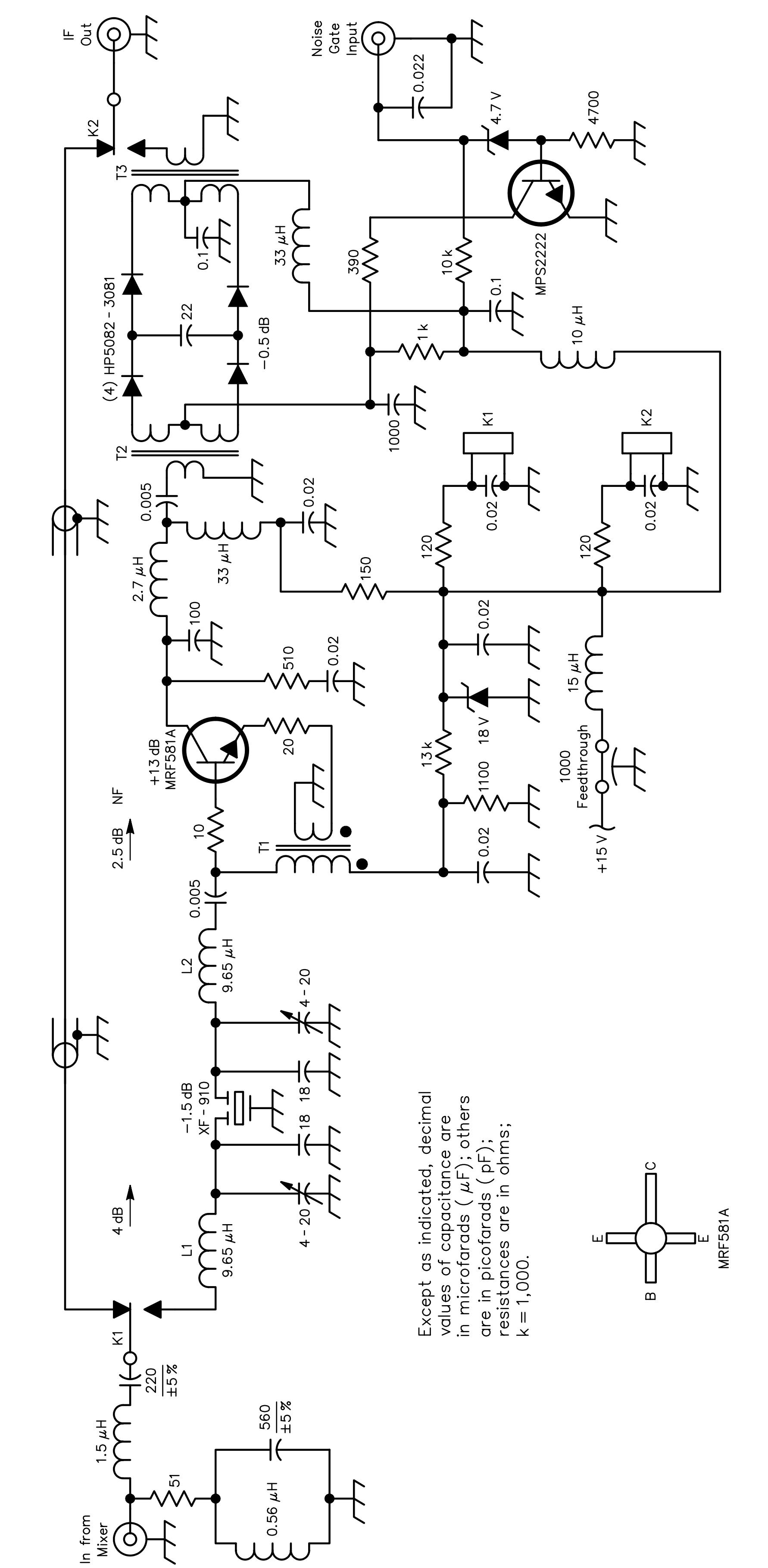

Fig 1—IF preamplifier and noise gate. Unless otherwise specified, use 1/4 W, 5%-tolerance carbon composition or film resistors.
K1, K2—Omron G6Y-1 relay.
L1, L2—43 turns #26 AWG on a T50-2 powdered-iron toroid core.
T1—3 t #26 AWG primary, 1 t #24 AWG secondary on a BLN-43-2402 binocular ferrite core.
T2, T3—6 t #24 AWG (trifilar) on an FT37-43 ferrite toroid core.

amplifier with a 50-Ω input impedance and 13 dB of gain. Unlike many other "noiseless feedback" circuits, this particular circuit has the advantage of providing high isolation between input and output. The MRF581 is biased at 20 mA to provide a low noise figure; the resulting +13-dBm compression level provides some protection for the following crystal filters. The 510-Ω resistor in the collector circuit sets the output impedance of the amplifier at 50 Ω to provide a proper termination for the main crystal filters.

Following the amplifier is the noise gate. A balanced circuit is used to minimize switching noise at the output. HP 5082-3081 PIN diodes are used to minimize IMD and transient generation during turn-on and turn-off. Four PIN diodes are used in the circuit to achieve a high attenuation when the gate is off. The 22-pF capacitor resonates broadly with the inductance of the two transformers at the IF. When the gate is off, it provides shunt reactance to form an "H" attenuator with the junction capacitance of the PIN diodes. This achieves 78 dB of attenuation.

The circuit at Q2 is a time-delay circuit. Normally, the 0.022-µF capacitor is charged through the 10-kΩ resistor, causing the 4.7-V Zener diode and the MPS2222 transistor to con-

Table 1—Predicted Receiver Dynamic Range with 2.4 kHz bandwidth

Frequency Offset	*Total Noise Figure*	*1-dB Compression*	*Receiver IP3*	*Dynamic Range*
IF Preamplifier/Noise Gate out				
> 1.5 kHz	18 dB	+23 dBm	+35 dBm	104.7 dB
0-1.5 kHz	18 dB	+15 dBm	—	—
IF Preamplifier/Noise Gate in				
> 10.0 kHz	16 dB	+23 dBm	+35 dBm	106.0 dB
1.5-10.0 kHz	16 dB	+14 dBm	+29 dBm	102.0 dB
0-1.5 kHz	16 dB	+4 dBm	—	—

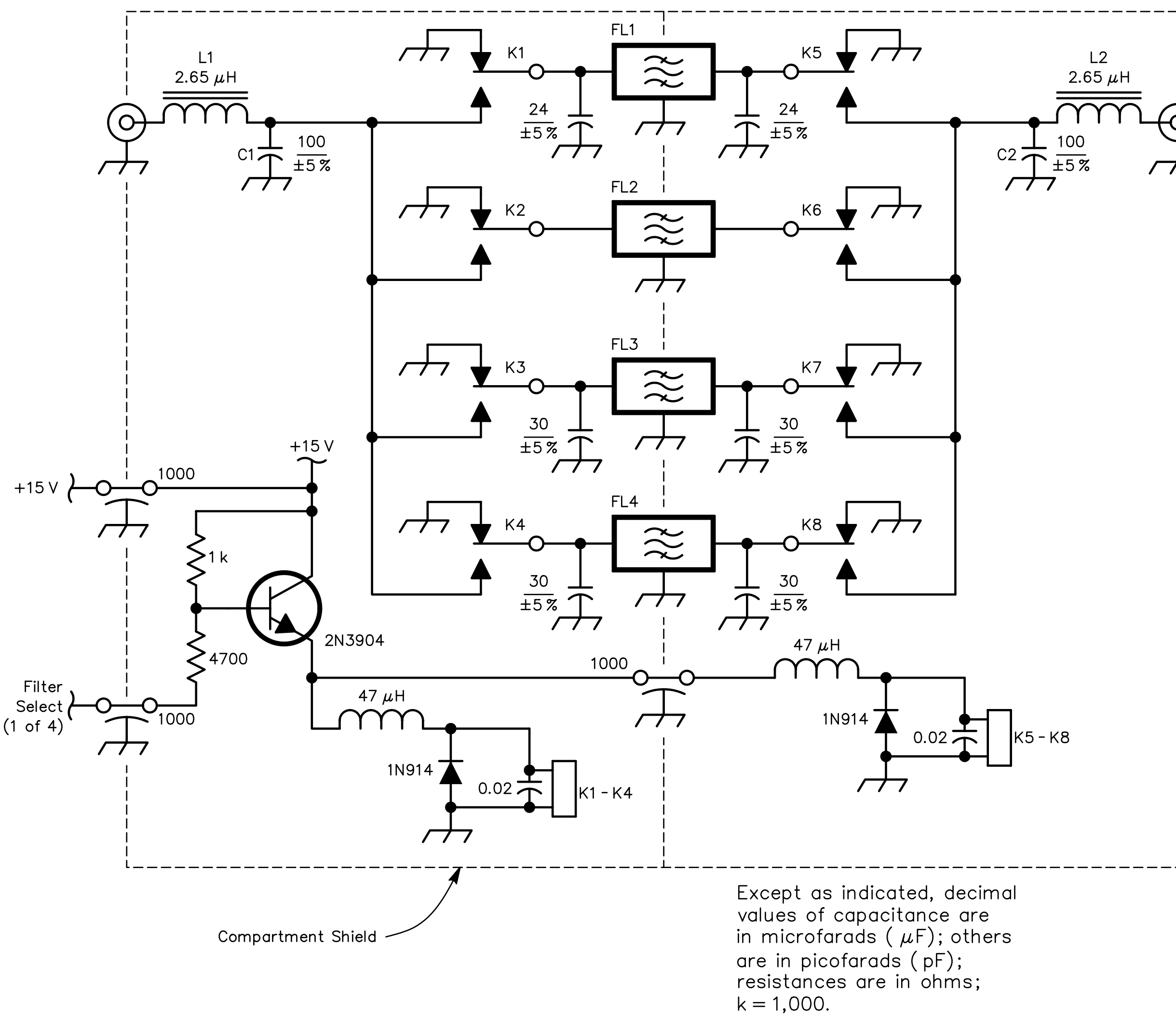

Fig 2—Crystal-filter selection and matching circuits. Only one relay control circuit is shown; the others are identical. Unless otherwise specified, use 1/4 W, 5%-tolerance carbon composition or film resistors.

FL1—KVG XF-9810, 2400 Hz bandwidth.
FL2—International Radio 2308, 1800 Hz bandwidth.
FL3—KVG XF-9NB, 500 Hz bandwidth.
FL4—KVG XF-9P, 250 Hz bandwidth.
K1-K8—RS-241 SPDT relay, 12-V coil.
L1, L2—19 t #24 AWG on a T50-6 powdered-iron toroid core.

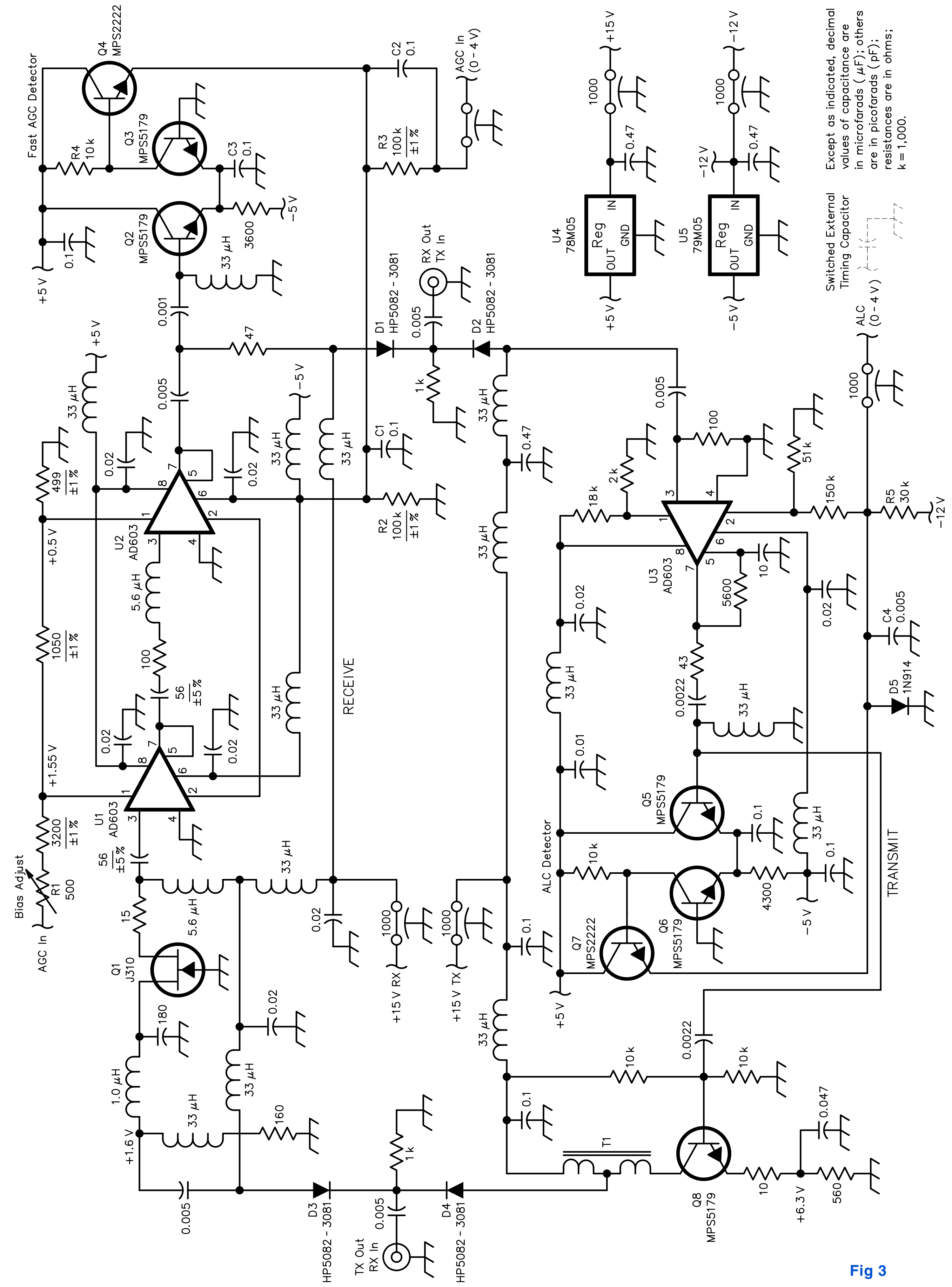
Fast AGC Detector
Q4 MPS2222
Q3 MPS5179
Q2 MPS5179
R4 10 k
C3 0.1
3600
−5 V
+5 V
0.1
33 µH
0.001
C2 0.1
AGC In (0 - 4 V)
R3 100 k ±1%
RX Out TX In
D1 HP5082 - 3081
D2 HP5082 - 3081
0.005
47
1k
33 µH
+5 V
0.005
0.02
499 ±1%
U2 AD603
+0.5 V
5.6 µH
100
56 ±5%
1050 ±1%
+1.55 V
U1 AD603
3200 ±1%
Bias Adjust
R1 500
AGC In
56 ±5%
15
5.6 µH
Q1 J310
180
1.0 µH
+1.6 V
33 µH
160
0.005
D3 HP5082 - 3081
TX Out RX In
D4 HP5082 - 3081
1k
RECEIVE
C1 0.1
R2 100 k ±1%
−5 V
1000
+15 V RX
+15 V TX
0.47
U3 AD603
18 k
2k
100
51 k
150 k
R5 30 k
−12 V
ALC (0 - 4 V)
5600
10
43
0.0022
0.01
ALC Detector
Q5 MPS5179
Q6 MPS5179
Q7 MPS2222
4300
10 k
C4 0.005
D5 1N914
TRANSMIT
T1
Q8 MPS5179
10
+6.3 V
560
0.047
U4 78M05
U5 79M05
Reg
OUT
GND
IN
+15 V
−12 V
−5 V
Switched External Timing Capacitor
Except as indicated, decimal values of capacitance are in microfarads (µF); others are in picofarads (pF); resistances are in ohms; k = 1,000.

Fig 3

duct, turning on the noise gate. When a noise pulse is detected, an external transistor discharges the capacitor. This turns off Q2 and the noise gate. The time required to recharge the capacitor ensures that the noise pulse (stretched by the 15 kHz filter) has ended before the noise gate is re-enabled.

Crystal Filters

The main crystal filter immediately follows the IF preamplifier. This receiver has four selectable filters with 250, 500, 1800 and 2400 Hz bandwidths for PSK, FSK and SSB. (See Fig 2.) The filters' 500-Ω input and output impedances are matched by two L-networks: C1/L1 and C2/L2. Since the Q is only three, these are fixed-tuned using 5%-tolerance components. Additional capacitors are placed near each filter to provide the proper termination. Some filters require a pure 500-Ω source and load impedance while others require 15 or 30 pF of parallel capacitance.[3]

The filters are selected by mechanical relays with unused filter inputs and outputs grounded to minimize feed-through. Power for the relays is filtered to ensure that no coupling occurs via power leads or capacitance to the solenoid coil. The filter-selection relays are controlled from the PC-Interface module via four PNP transistors Q1-Q4. This allows one end of the relay coils to be grounded in order to minimize cross coupling via the power supply.

To preserve the stopband attenuation characteristics of these filters, good mechanical design is required. Unwanted coupling between the filter input and output must be minimized. The filters are mounted directly to the chassis with the input and output pins separated by a shield that partitions the chassis into two compartments. I found that small aluminum boxes didn't work here—they only gave 70 dB of isolation. An old-fashioned 4×5×2-inch welded chassis with a bottom plate gave 90 dB of isolation, which doesn't compromise the 80-dB stopband attenuation of the narrow SSB filter.

Fig 3—There are separate IF amplifiers for receive (upper circuitry) and transmit (lower circuitry) paths. Unless otherwise specified, use 1/4 W, 5%-tolerance carbon composition or film resistors. All capacitors are ±20% and RF chokes are ±10% tolerance unless labeled otherwise.
T1—8 t #28 AWG bifilar wound on an FT23-43 ferrite toroid core.

IF Amplifier

The IF amplifier is shown in Fig 3. Independent circuits are used for transmit and receive, with the signal flow controlled by PIN-diode switches (D1-D4) for low distortion. The first amplifier in the receiver IF strip and the last amplifier in the transmitter IF strip are switched off when not in use by removal of the power-supply voltage.

The receive path consists of a low-noise amplifier followed by two variable-gain amplifiers and an AGC detector. Q1 is a J310 FET in a common-gate circuit with low-Q L networks for input and output matching. The circuit has a gain of 12 dB and brings the IF amplifier noise figure to 3 dB. A 3-MHz-wide series-tuned band-pass filter between the two variable-gain amplifiers limits the broadband noise at the AGC detector.

U1 and U2 are Analog Devices AD603 amplifiers having logarithmic gain control. They are capable of handling 3 V (pk-pk) input signal levels. Gain is variable over a 40-dB range with 1 V of control signal variation. The AGC voltage is applied differentially between pins 1 and 2 of each device; over 80-dB of total gain variation is achieved. The network of 1% resistors connected to pin 1 of each device biases them so that gain is controlled sequentially. R1 is adjusted to provide the correct bias voltages as shown in the schematic and compensates for any variation in the voltage from U4. As the AGC voltage increases, the gain of U2 is reduced from 30 dB to –10 dB before any reduction in the gain of U1. This maximizes the signal-to-noise ratio of the IF strip.

Receive IF gain is controlled from two sources. The control voltage for the slow AGC loop is applied to the 2:1 voltage divider formed by R2, R3, C1 and C2, resulting in a 0-to-4-V AGC range. Note that there is no long time-constant associated with driving the divider since the capacitors balance each other.

Q2 and Q3 form an envelope detector for the fast AGC loop. Q2 acts as a rectifier. It is cut off when the base voltage falls below the sum of the emitter voltage and base-emitter barrier voltage. Q3 is a common-base amplifier that provides dc gain and compensates for temperature variations in Q2's emitter-base voltage in a manner similar to a differential amplifier. The compensation is not perfect because the currents through the two transistors are not identical. The actual variation in detector gain, however, was less than 1-dB from 16°C to 38°C (room temperature) and was all concen-trated at the low end, where there is little operational effect. The detector's rise and fall times are determined by the emitter resistance and C3 to be about 6 µs. The voltage developed across R4 is buffered by Q4, an emitter follower, then applied to the AGC pins of the IF amplifiers, U1 and U2. The advantages of this detector are that it responds to low-level signals and that the output is logarithmic—within 1 dB—over a range of input voltages from 70 mV (pk-pk) to 250 mV (pk-pk). This results in a reasonably constant AGC loop gain and good transient response.

Additional AGC filtering is provided by R2, R3, C1 and C2, amounting to 50 kΩ of resistance and 0.2 µF of capacitance as seen from the emitter follower. This provides a 6-µs attack and 10-ms exponential decay time for the fast AGC. Any voltage from the slow AGC loop that is more than twice the fast AGC detector's output will override the output of Q4 and take control of the IF amplifier gain.

The transmit path contains a variable-gain amplifier (U3) that drives the ALC detector (Q5, Q6 and Q7) and a fixed-gain amplifier (Q8). These circuits amplify the SSB signal from the product detector/balanced modulator module and compress it. The input to this module can range from –10 dBm to –58 dBm depending on the amount of audio applied to the balanced modulator. The output is leveled to a ±4 dBm range.

The ALC detector is identical to that used in the receiver's AGC detector. It generates 0 to 4 V of ALC with a logarithmic response. The ALC is applied to U3; it varies U3's gain from +43 to +3 dB as signal levels rise. This compresses the transmitted signal by a factor of six or more, translating the original 48-dB range to 8-dB. Most voices only vary by 20 dB during normal speech. This range is compressed to 3 dB and the rest of the control range compensates for variations in the dis-tance from the operator to the micro-phone.

The ALC attack time is approximately 6 µs, but the release time is variable. The minimum of 1 dB/µs is determined by C4 and R5. R5 provides a constant discharge current of approximately 0.5 mA. D5 prevents the ALC voltage from going below –0.6V. Since the ALC line is brought out of the module, additional filter capacitors can be placed across the line to increase the time constant. The short time constant provides an action like an RF clipper, but with less in-band distortion. Intermediate time constants on the order of 2-5 dB/ms provide RF syllabic compression. Long time constants of 25-100 dB/s set the RF output to the correct level but do not modify the modulation.

To limit the maximum gain and place background noises below the compression range, the PC Interface module can set a minimum ALC voltage. It can also be used to eliminate the ALC action on normal audio levels, but ALC is left on all the time so that the power amplifier cannot be accidentally over-driven and generate splatter.

The leveled signal at the output of U3 is amplified by Q8 and routed to the main crystal filter. This additional filtering is necessary to remove any out-of-band distortion products caused by rapid gain variations before transmission. It also provides additional carrier suppression when audio levels are low.

Product Detector/ Balanced Modulator

This module was the most straightforward to design. (See Fig 4.) The crystal filter and mixer are both bilateral and so are used for both SSB generation and detection. Q1 is an amplifier that increases the +4 dBm from the DDS BFO up to +10 dBm. This is a common-emitter amplifier with emitter degeneration to set the gain and a low-Q fixed-tuned L-network in the collector circuit for impedance matching. The BFO signal is attenuated 3 dB before application to the level-7 mixer (Z1).

The received signal first passes through a crystal filter (FL1) to strip away excess noise from the wide-band IF strip and eliminate the audio image. This filter need not have tremendous selectivity. I used a five-pole, 2.5-kHz-bandwidth filter from KVG, which has a minimum stopband attenuation of 50 dB. (This is about the minimum required.) Combined with the 80-dB minimum stopband attenuation of the filters ahead of the IF amplifier, at least 130 dB of attenuation is presented to out-of-band signals. This is the minimum necessary for a receiver with 120 dB of AGC range. Two L networks, C1/L1 and C2/L2, provide impedance matching. If an International-Radio

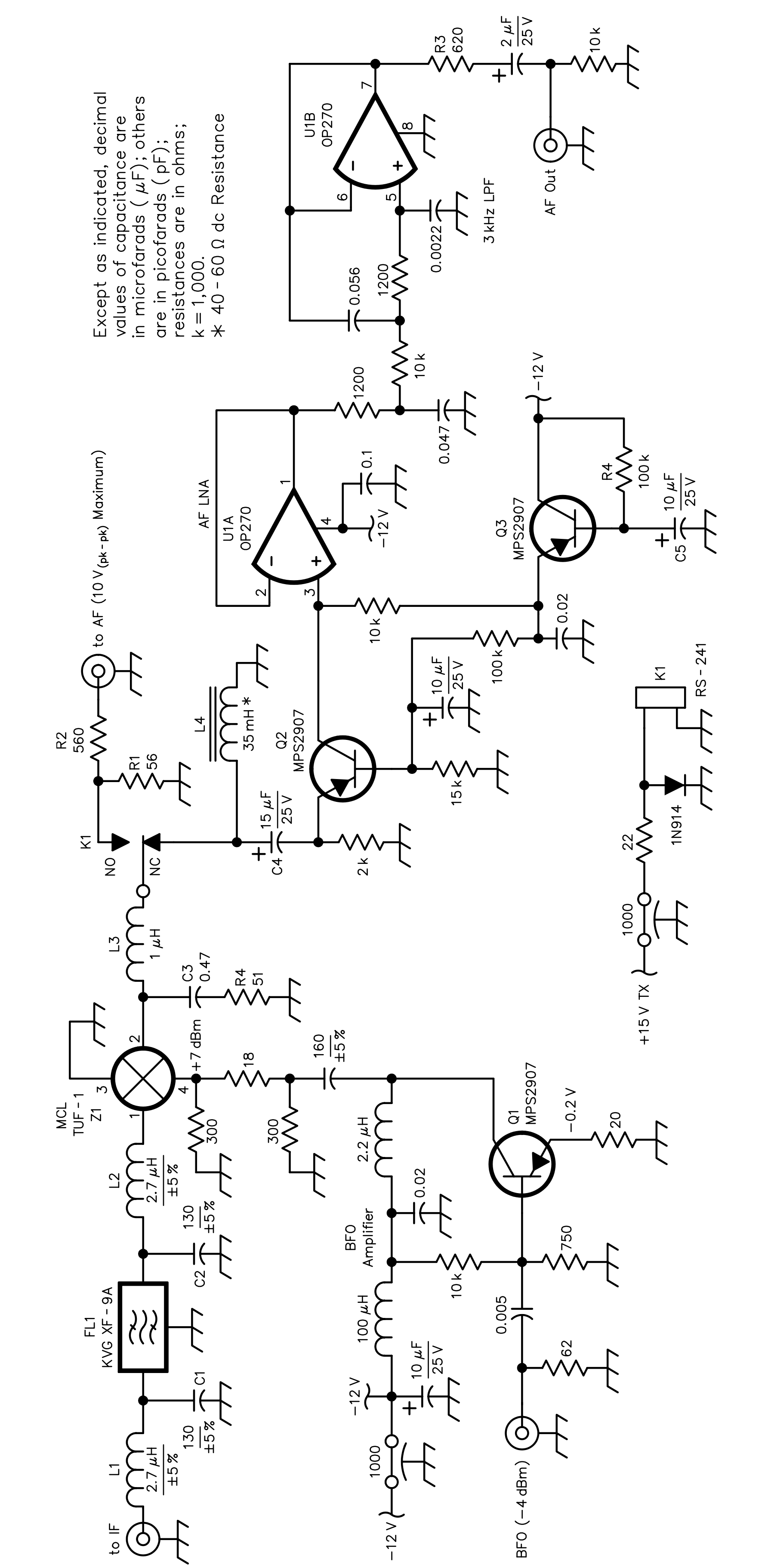

Fig 4—Product detector/balanced modulator circuit. Unless otherwise specified, use 1/4 W, 5%-tolerance carbon composition or film resistors.

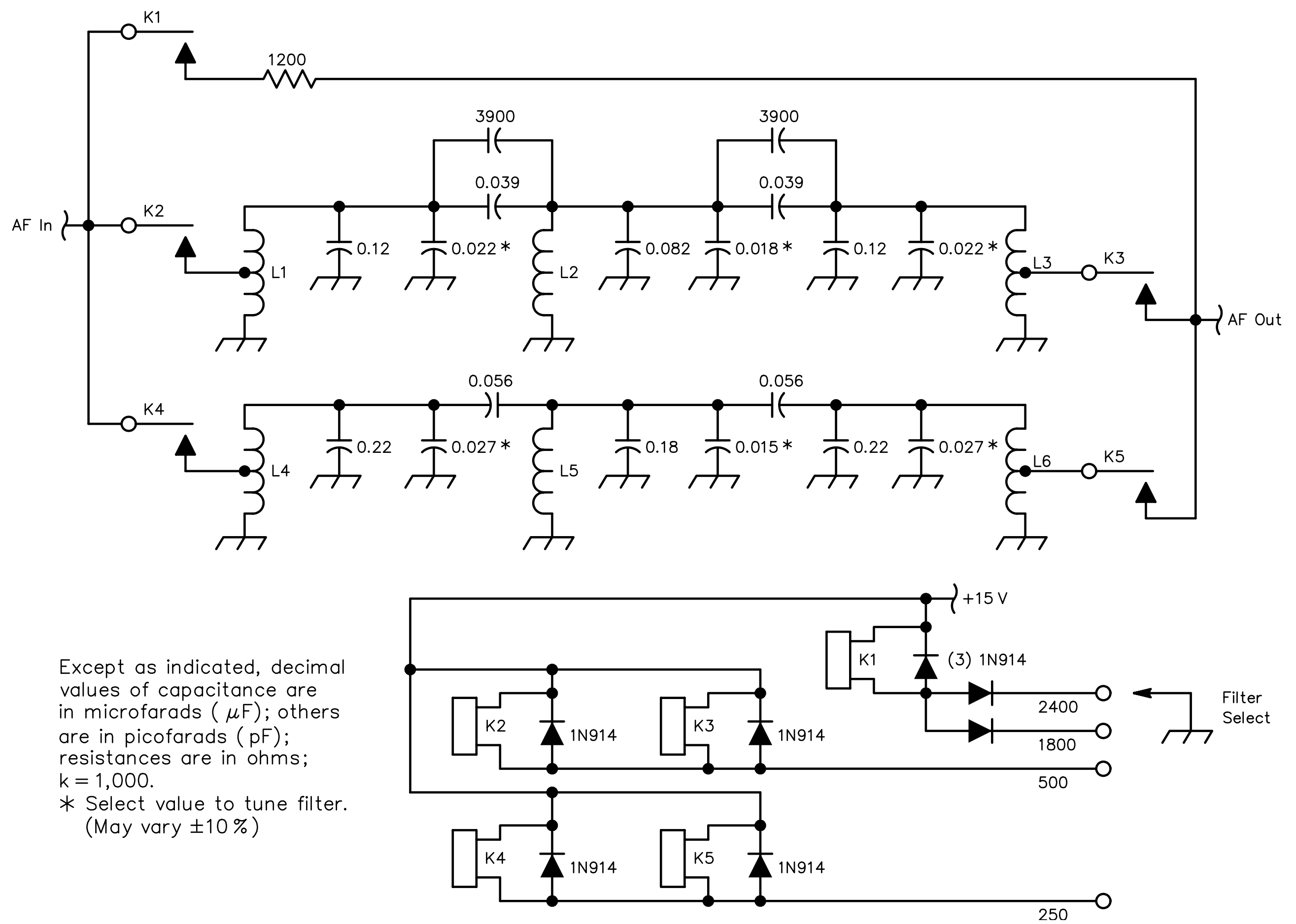

Fig 5—AF filter schematic diagram. Unless otherwise specified, use 1/4 W, 5%-tolerance carbon composition or film resistors. All capacitors are ±5% tolerance mylar components.

K1-K5—Reed relay, SPST, 12-V dc coil.

L1-L6—88 mH toroid inductor, center tapped.

filter is substituted, C1 and C2 must be reduced to 100 pF each.

The double-balanced mixer (DBM) that follows the filter is used as the product detector. Since the IF level at this point is –77 to –37 dBm, low IMD is assured. The DBM is followed by L3, C3 and R4, which form a diplexer with a 6-kHz transition frequency. This is followed by a relay to switch between incoming transmitter audio and the receive audio-amplifier chain.

While receiving, a low-noise audio amplifier follows the relay. L4 provides a dc return for the DBM and forms a 220-Hz high-pass diplexer with C4. Q2 is used as a common-base amplifier and is biased to have a 50-Ω input impedance. An operational amplifier, U1A, configured as a voltage follower, buffers the output. This is followed by U1B, configured as a low-pass filter to attenuate high-frequency audio hiss. The filter is a three-pole Chebyshev with 0.5 dB of ripple and a cutoff frequency of 3 kHz. R3 establishes the output impedance. The voltage gain through the amplifier and filter is 40 dB.

Transmit audio is applied to the DBM through R1 and R2, which form a matching network and attenuator. The maximum audio input of 10 V (pk-pk) results in +3 dBm at the IF port of

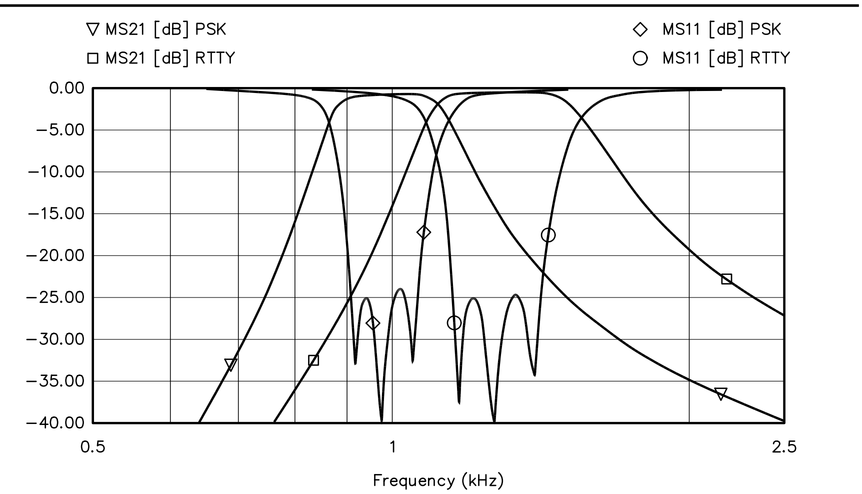

Fig 6—AF filter attenuation (S21) and return loss (S11).

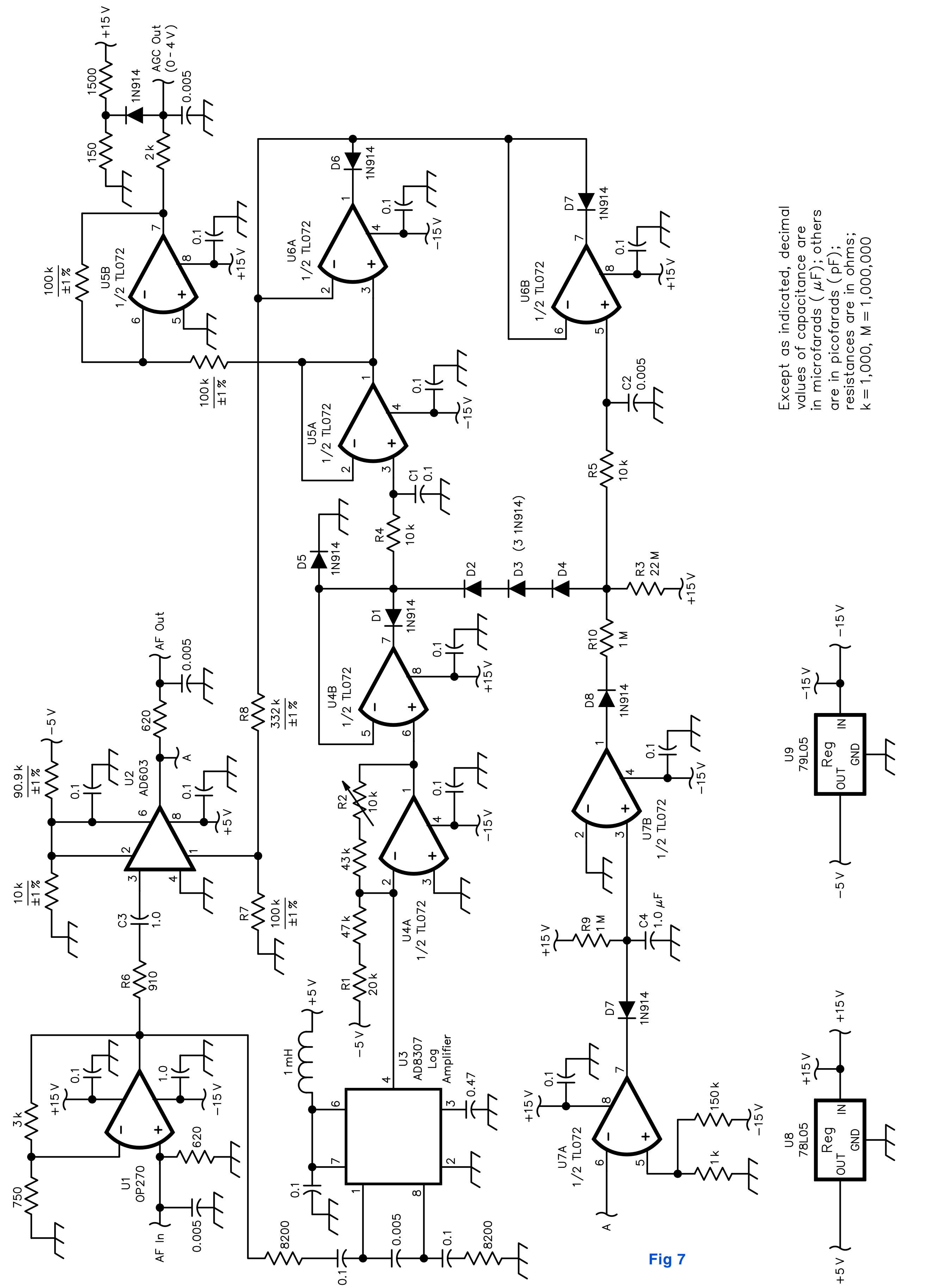
Except as indicated, decimal values of capacitance are in microfarads (μF); others are in picofarads (pF); resistances are in ohms; k = 1,000, M = 1,000,000
AF In
U1 OP270
U2 AD603
AF Out
AGC Out (0 - 4 V)
U3 AD8307 Log Amplifier
U4A 1/2 TL072
U4B 1/2 TL072
U5A 1/2 TL072
U5B 1/2 TL072
U6A 1/2 TL072
U6B 1/2 TL072
U7A 1/2 TL072
U7B 1/2 TL072
U8 78L05
U9 79L05
Reg
(3 1N914)

Fig 7

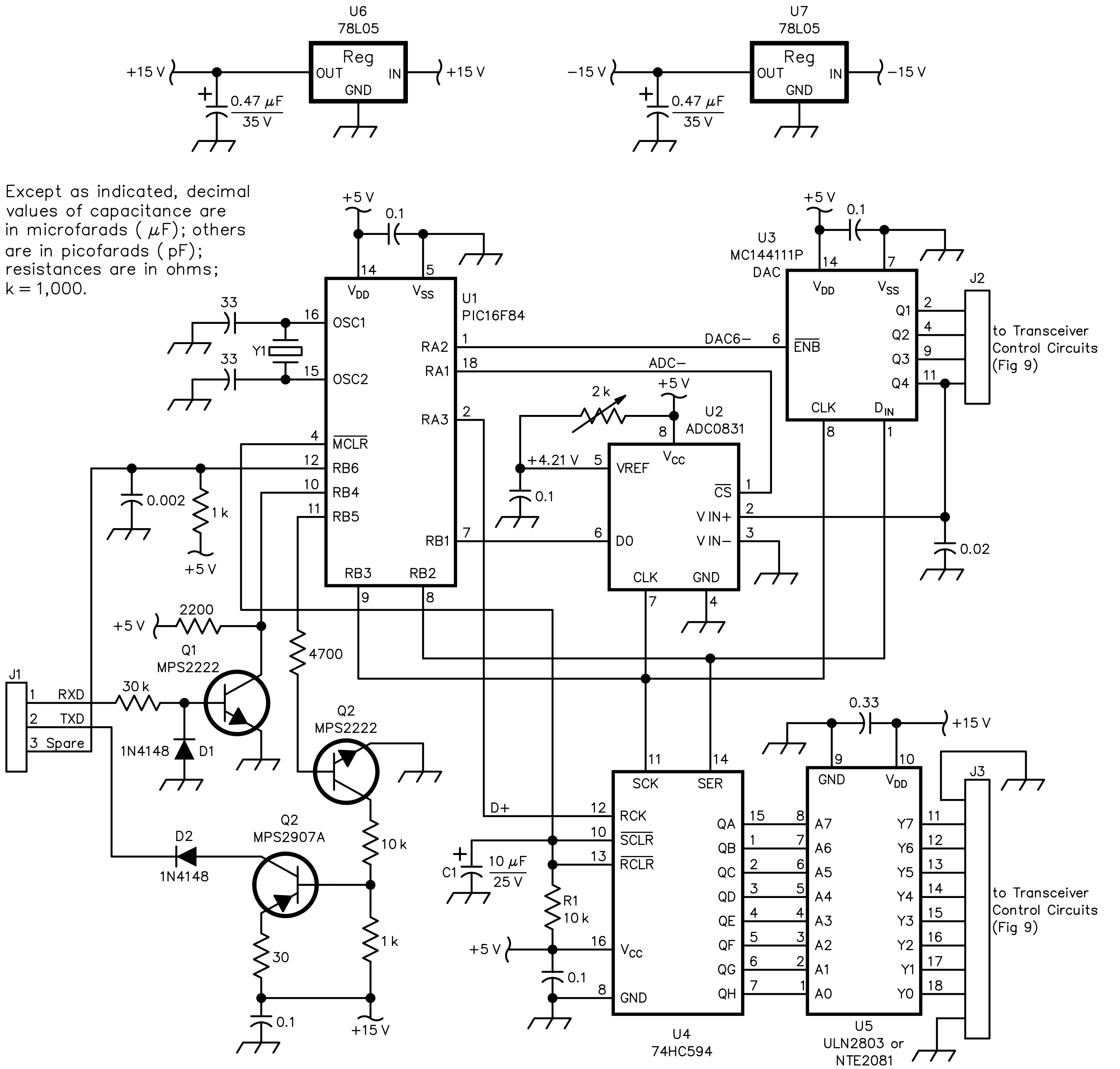

Fig 8—PC interface schematic diagram. Unless otherwise specified, use 1/4 W, 5%-tolerance carbon composition or film resistors.

J1-J3—Molex plug, 0.1-inch spacing in line.

Y1—7.3728 MHz crystal, 20 pF parallel resonant.

Z1. This signal level should result in IMD of –36 dBm or less; the audio level is usually much lower and results in less IMD. Z1 has a minimum LO/RF isolation of 50 dB and provides adequate carrier suppression without adjustment. FL1 suppresses the unwanted sideband before speech processing.

Fig 7—AF amplifier/AGC schematic diagram. Unless otherwise specified, use 1/4 W, 5%-tolerance carbon composition or film resistors.

Audio Filtering

Audio filters may be used more effectively here than in other designs because the IF-amplifier gain is relatively low, the audio image has been stripped by the tail-end filter and the main AGC loop uses an audio detector. The narrow-band crystal filters have 4:1 shape factors and 90 dB ultimate attenuation, so relatively little filtering is needed. The main purpose is to remove IF amplifier noise outside the crystal-filter passband and increase ultimate attenuation.

The filters use 88-mH toroidal inductors[4] with capacitive coupling to minimize the type and number of inductors. (See Fig 5.) The PSK filter is 270 Hz wide at –3 dB and is centered on 1000 Hz. The RTTY filter is 460 Hz wide at –3 dB and centered on 1360 Hz for use with a demodulator using 1275/1445 Hz tones. Fig 6 shows both the PSK and RTTY filter characteristics. When the filters are not in use, a 1200-Ω resistor provides 6 dB of attenuation to compensate for the lower loss of the SSB filters in the IF.

AF Amplifier and AGC

Fig 7 shows the AF amplifier and AGC circuitry. U1 amplifies the received audio signal by 17 dB to present the proper levels to the variable-gain audio amplifier. Connected to the output of U1 is U3, an Analog Devices AD307 logarithmic amplifier. U3 and U4A are used as the AF AGC detector. R2 sets the slope to –100 mV/dB and R1 sets the power level at which the output is zero. This level is set to –107 dBm or 1 µV RMS at the antenna terminals with the noise blanker bypassed. This is 5 dB above the minimum noise level. The upper end of the AGC range is 1 V RMS. The IF AGC detector was designed to give a slightly lower AGC voltage with the same input signal level, so the amount of adjustment required by the slower audio-derived AGC is minimal. However, the audio AGC provides the final, more-accurate control that is reflected by the S-meter. The AD8307 and AD603 are each accurate to ±1 dB over the operating temperature range. The meter reading is accurate to ±2 dB or 1/3 S-unit.

U4B and D1 form a gate that charges the AGC filters to the peak negative level of the detector output. Two AGC filters are provided. A slow filter drives the IF amplifier AGC line. The IF amplifier gain cannot be adjusted rapidly because of delay in the crystal filter preceding the product detector. A fast filter is used to develop AGC for the variable-gain AF amplifier. The fast and slow AGC voltages are compared and the most negative voltage is applied to the amplifier. The fast AGC voltage compensates for excess IF amplifier gain during transient conditions by decreasing AF amplifier gain.

The circuit is somewhat complex. R3 provides a constant-current discharge path for the slow and fast filter capacitors, C1 and C2. The resulting decay times produce a gain increase of 20 dB/s for the slow AGC voltage and 4 dB/ms for the fast AGC voltage. This allows tracking of fading signals. The fast AGC voltage is offset by +0.65 V from the slow AGC voltage by D2 through D4, so that audio peaks must be 6.5 dB higher than the average level to affect audio gain. This eliminates excess pumping of the AGC by audio peaks, but allows fast response to transients at the beginning of a transmission. D5 clamps the no-signal voltage to +0.4 V. Attack times are set by R4 and R5 to 10 ms for the slow AGC voltage and 50 µs for the fast AGC voltage. The attack and release times are somewhat critical for good SSB reception. I spent two days tuning these time constants for rejection of impulse noise and for minimum audio distortion.

U5A is a voltage follower to isolate the holding capacitor. U5B inverts the AGC voltage for application to the IF amplifier. U6, D6 and D7 comprise a gate to select either the fast or slow AGC voltage for application to U2, which provides an adjustable gain of –10 to +30 dB. Note that R6 and C3 provide 20 dB of attenuation and transform the 100-Ω input impedance of U2 to 1000 Ω. R7 and R8 convert the 0-4 V AGC signal to 0-0.97 V to control audio gain. A 40-dB increase in signal at the AGC detector results in a 37-dB reduction in gain. The 3-dB increase is left to compensate for variations in gain slope and logarithmic-amplifier accuracy to ensure that an AGC-detector signal increase never results in a decrease in audio level.

U7 provides the "hang" AGC function that causes rapid gain increase if a signal is lost completely for more than the "hold" time. U7A discharges C4 through D7 whenever the audio output is greater than 100 mV. This causes the output of U7B to go negative. C4 is charged through R9 so that after 500 ms, U7B's output will go positive. This causes C1 to be discharged through D8 and R10, increasing the gain at a rate of 400 dB/s. This allows full gain to be achieved within a short time after the disappearance of very strong signals, rather than having to wait up to six seconds at the normal 20 dB/s rate. It is not really needed on signals below S9, but it helps when strong local signals are present.

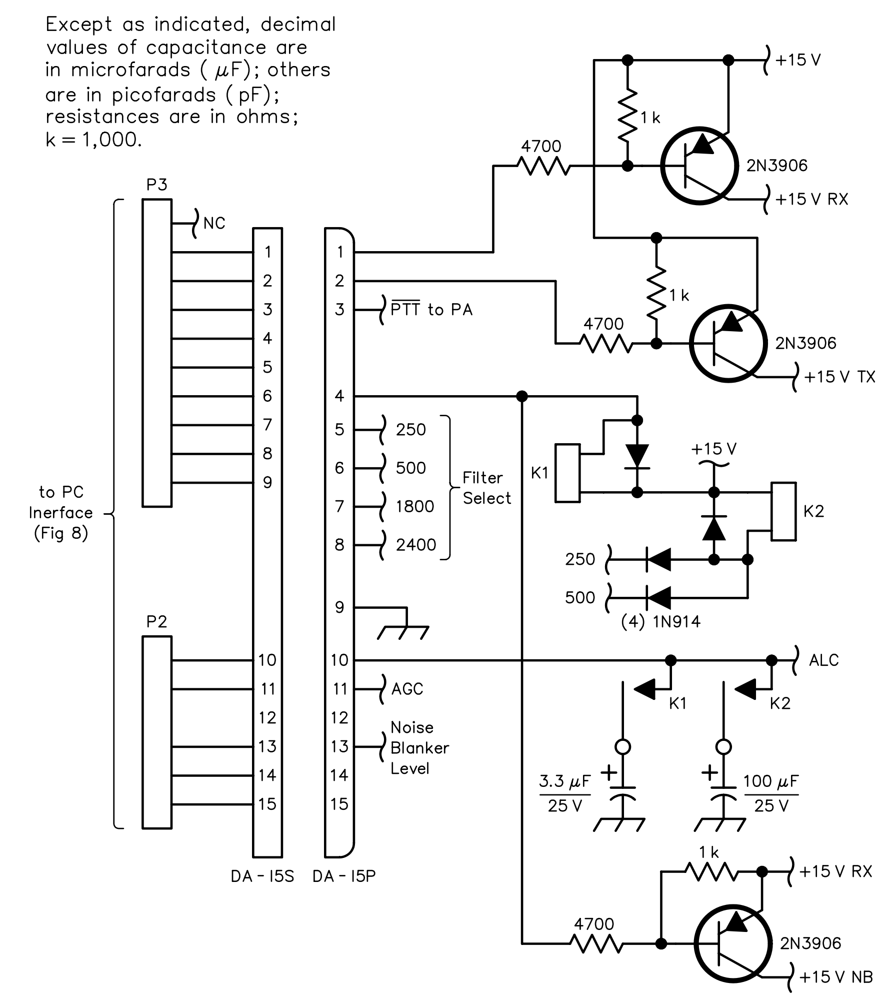

Fig 9—Transceiver control circuits. Unless otherwise specified, use 1/4 W, 5%-tolerance carbon composition or film resistors.

K1, K2—Reed relay, SPST, 12 V dc coil.

P2, P3—Molex plug, 0.1-inch spacing in line.

PC Interface

The entire radio is controlled from a personal computer. The method of controlling the DDS was described in Part 1, but there are several functions still left: filter switching, transmit RF compressor control, IF gain control and TR switching. These are controlled by a second microprocessor (MCU) as shown in Fig 8.

The MCU, U1, is another PIC16F84 with the same UART software as described in Part 1. Q1, D1 and associated resistors form the EIA-232 receiver, whose input is wired in parallel with the receiver in the DDS circuit. Both MCUs receive the same commands but only one executes each command. U1 recognizes only the commands in Fig 9.

Unlike the DDS-control MCU, this MCU can also send responses to the PC. Q2, Q3, D2 and associated resistors form the EIA-232 driver. This driver is designed to have its output wired in parallel with other similar units to allow sharing of one PC serial port among multiple radios. The driver sources 20 mA when sending a zero and is completely inert when sending a one. To pull the line to a negative voltage (one) when no MCU is sending data, the output is terminated near the PC with a 1500-Ω pull-down resistor to a –12 V supply. The diode, D2, in combination with the base-collector junction of Q3, ensures that the driver will not source or sink current when power is removed. This allows one or more radios to be turned off while controlling others from the PC.

Bits 1, 2 and 3 of MCU port A are used to select the peripheral chips being read or written to by the MCU. Data are written to the selected chip by shifting the data using bit 3 of MCU port B as the clock, and bit 2 as data-output pin. Data are read by shifting them into the MCU using bit 3 as the clock and bit 1 as the data-input pin.

U2 is an 8-bit analog-to-digital converter (ADC) that is used to sample the AGC input to the IF amplifier. R2 sets the reference voltage so that the conversion slope is 1 bit/0.5 dB of receiver gain. U3 contains four 6-bit digital-to-analog converters (DACs) that are used to control IF gain, RF clipping level and noise-blanker gain. One DAC is unused. J2 connects the DACs and ADC to the rest of the transceiver.

U4 is a CMOS shift register and latch used as a parallel output port. Eight Darlington transistors, contained in U5, buffer the output of U4. The outputs are open-collector and are connected via J3 to the circuit shown in Fig 9 to control power to the noise blanker, transmit and receive sections of the transceiver and the filter-selection relays.

The commands used to control the receiver are shown in Fig 10. They have the structure defined in Part 1. In the case of commands involving the DACs, the command contains a data byte with a six-bit value that is output to the appropriate device. The filter-selection command uses four bits to control the filter-selection relays. Other commands have no data field. The response to an AGC Request command contains the eight-bit digitized value of the IF AGC line.

Note that the transmit/receive timing is controlled by the MCU. When a transmit command is received, the MCU mutes the receiver, switches out the receive audio stages and the receive IF amplifiers and enables the TR relay. After a time delay for the TR relay to settle, it switches in the transmit IF amplifier and compressor, waits for transients die out, then ramps the IF amplifier gain up to the desired clipping level. The reverse sequence is executed on receipt of the command to go to the receive mode. Table 2 lists other internal transceiver control lines.

Test Results: AGC System

Several performance parameters of the transceiver were tested on the bench as described below. Dynamic AGC response was tested using a pulsed signal at various levels from –60 to +10 dBm with a 10-s period. There was no overshoot on the AGC voltage applied to the IF amplifier. Overshoot of the audio output never exceeded 7 dB of the final value and undershoot was about 3 dB maximum. Stabilization of the output level occurred within 30 ms.

The AGC system was also tested for linearity. Table 3 shows the measured response of the receiver to a CW carrier with the IF preamplifier out of circuit. The signal levels decrease by 11 dB when it is switched in. However, the software displaying the signal strength can easily compensate for this.

The AGC detector slope and intercept were adjusted using 1-µV and 1-V signals from a HP 8640B signal generator. The generator's output is accurate to within ±1.5 dB and the voltmeter is

Table 3—IF Amplifier AGC Response

Signal (µV RMS)	Signal (dBm)	AF AGC (V dc)	IF AGC (V dc)	AF AGC (dB)	IF AGC (dB)	AF–IF AGC (dB)
1,000,000	+13	3.99	1.92	–78.8	–76.8	2.0
316,000	+3	3.62	1.68	–72.4	–67.2	5.2
100,000	–7	3.28	1.44	–65.6	–57.6	8.0
31,600	–17	2.96	1.22	–59.2	–48.8	10.4
10,000	–27	2.63	0.98	–52.6	–39.2	13.4
3,160	–37	2.29	0.75	–45.8	–30.0	15.8
1,000	–47	1.99	0.52	–39.8	–20.8	19.0
316	–57	1.64	0.31	–32.8	–12.4	20.4
100	–67	1.31	0.10	–26.2	–4.0	22.2
32	–77	0.98	0.01	–19.6	–0.4	19.2
10	–87	0.65	0.00	–13.0	0.0	13.0
3	–97	0.34	0.00	–6.8	0.0	6.8
1	–107	0.00	0.00	0.0	0.0	0.0

Table 2—Transceiver Control Lines

Pin	Digital	Pin	Analog
1	Qa RX	9	Ground
2	Qb TX	10	Q4 Compressor
3	Qc TR Relay	11	Q3 AGC (I/O)
4	Qd ALC Select	12	(No Connection)
5	Qe 250	13	Q2 Blanker
6	Qf 500	14	Q1
7	Qg 1800	15	Ground
8	Qh 2400		

Table 4—RF Compressor Characteristics

Input Level (dBm)	ALC (V)	Output Level (dBm)
–10	4.00	+2.5
–20	3.21	+0.5
–30	2.39	–1.0
–40	1.55	–2.5
–50	0.72	–4.0
–58	0.00	–6.0

Table 5—RF Compressor Characteristics

ALC Filter Capacitor (µF)	Time Constant (dB/ms)	IMD (dBc)
47	0.1	<–40
6.8	0.7	–35
3.3	1.5	–30
1.0	5	–21
none	1000	–12

accurate to within 0.5% or ±0.6 dB. The transceiver was then operated for three days and the response measured. The maximum deviation of the AGC voltage from the ideal response of 33 mV/dB was +0.01/–0.05 V or +0.3/–1.5 dB. This is within the error range of the measurement equipment.

When the AGC value was read from the PC, the displayed value was accurate within ±1 dB for all but the extreme upper end of the range, above 0.5 V of input signal. The maximum excursion was 2 dB at 1 V of RF input.

RF Compression

The RF compression range was first tested by injecting a 9-MHz CW signal into the IF amplifier module and measuring the output level on a HP 8555A/8552B spectrum analyzer. The results are shown in Table 4. They met expectations.

Distortion of the transmitted signal was also measured with various time constants for the ALC. A two-tone audio signal generator (700 and 1700 Hz tones at 0 dBm/600 Ω per tone) drove the balanced modulator and the output was checked with a spectrum analyzer. The results are shown in Table 5.

Only one IMD product (2700 Hz) passes through the final crystal filter, so the IMD levels are measured by referencing that tone to the 1700 Hz tone. No other IMD products could be found above –60 dBc, which was the limit of measurement.

LO Phase Noise

LO phase noise was measured by connecting a low-noise crystal oscillator (described in Part 1) at the antenna terminals and measuring the amplitude of noise sidebands surrounding it on the digital S-meter in the transceiver control program. Measurements were made with 2400-Hz and 250-Hz bandwidths on both sides of the test signal and the results are shown in Table 6. The possible measurement error in the test setup is ±3 dB.

No spurs were noted at ±36 kHz from the signal, so the reference frequency component of the PLL error voltage is adequately suppressed. The spurious components at ±10 kHz and ±20 kHz are less than 50 Hz in width and are probably generated by other equipment in close proximity rather than the transceiver under test. The phase noise is within predicted limits except for the area below 1500 Hz, where it is at least 2-3 dB higher than anticipated, but certainly acceptable for normal use.

Receiver Dynamic Range

Receiver dynamic range was evaluated by measuring the minimum discernable signal (MDS) and the third-order intercept (IP3). An HP 8640 signal generator was used to generate a signal for measuring the MDS and the level required for a 3-dB increase of audio output in a 2.4 kHz bandwidth was measured. In addition, 9 MHz and 32.2 MHz signals were generated to measure IF and image rejection.

Two of the low-noise crystal oscillators described in Part 1 were used with a hybrid combiner for IMD testing. The output from the combiner was 2.5 dBm/tone and a 25-kHz spacing was used. The amplitude of spurious responses was read from the digital S-meter in the transceiver control program. Readings taken from both sides of the tones were averaged.

The dynamic range looks slightly greater than expected because the noise figure of the IF preamplifier is lower than expected in one case, the IP3 higher than expected in another case. However, these measurements are only accurate to ±2 dB. To compare the third-order dynamic range with measurements made by the ARRL standard method, a small correction[5] must be applied. IF and image rejection are more than adequate and LO leakage to the antenna is essentially nonexistent. A measurement summary is presented in Table 7.

Conclusions

Almost all low-level stages of the transceiver worked as anticipated when completed. Two areas, however, required changes during testing. The original design for this transceiver used RF clipping, but on-the-air tests yielded reports of excessive audio distortion when clipping exceeded 5 dB. Consequently, clipping was abandoned as a method for RF compression, which resulted in much cleaner audio. From reports by other stations, two types of

Byte 1	*Byte 2*	*Bytes 2*	*Byte 3*	*Byte 4*	*Command*
STX	B	Bits 0-3	ETX	LRC	Select IF filter
STX	G	0-63	ETX	LRC	Set IF Gain
STX	C	0-63	ETX	LRC	Set RF clipping level
STX	Z	0-63	ETX	LRC	Set noise receiver gain (0=off)
STX	S	ETX	LRC		Request AGC voltage
	s	0-255			AGC voltage (response)
STX	X	ETX	LRC		Go to transmit mode
STX	N	ETX	LRC		Go to receive mode

Fig 10—Transceiver control command strings.

Table 6—Measured LO Phase Noise

Offset (Hz)	*Phase Noise Expected (dBc/Hz)*	*Phase Noise Measured (dBc/Hz)*
0.5 k	–104	–99
1 k	–113	–109
1.5 k	–117	–116
2 k	–122	–119
3 k	–126	–128
4 k	–131	–137
5 k	–133	–140
7 k	–137	<–140
10 k	–141	–140*
15 k	–145	<–140
20 k	–150	–147*
25 k	–152	<–153

*Narrow-band spur

Table 7—Measured Receiver Characteristics with 2.4 kHz IF bandwidth

Measurement	*IF Preamp. On (0 dB Attn)*	*IF Preamp. On (3 dB Attn)*	*IF Preamp. Off (3 dB Attn)*
Third Order Intercept (IP3)	32.8 dBm	35.0 dBm	37.0 dBm
Minimum Discernable Signal (MDS)	–128 dBm	–125.5 dBm	–122.0 dBm
Noise Figure	12.0 dB	14.5 dB	18.0 dB
Spurious Free Dynamic Range	107.2 dB	107.0 dB	106.0 dB
LO Leakage	< –85.0 dBm	–	< –85.0 dBm
Image Rejection	–104.0 dB	–	–108.0 dB
IF Rejection	–92.0 dB	–	–92.0 dB

compression seem to be desirable. A medium ALC time constant (1.5 dB/ms) for syllabic compression results in low distortion on good paths and better readability than long time constants. Under marginal conditions, the fastest possible ALC time makes signals readable where syllabic compression is ineffective.

The other problem area was the mixer. Although most literature indicates that the IF port must see a broadband 50-Ω load for low IMD, it was found that the RF port is actually more sensitive to termination in a high-level DBM. The RF band-pass filter described in Part 1 and the IF diplexer described here were necessary to cure an initial 15-dB deficit in IP3.

The low noise figure and high dynamic range (with the 3-dB IF attenuator removed) are useful on the 10-meter band where any RF amplifier would degrade the dynamic range. Atmospheric noise on this band still exceeds the noise figure by 6 dB or more.

The next part of this series will cover the linear amplifier, noise blanker and power supply.

Notes

[1]John Stephensen, KD6OZH, "The ATR-2000: A Homemade, High-Performance HF Transceiver, Pt 1" *QEX*, Mar/Apr 2000, pp 3-15.

[2]Ulrich L. Rohde and T. T. N. Bucher, *Communications Receivers—Principles and Design*, McGraw Hill, 1988.

[3]KVG filters are no longer distributed in this country. Similar filters are available from International Radio, 13620 Tyee Rd, Umpqua, OR 97486; tel 541-459-5623 (9 AM-1 PM PDT, Tues-Sat), fax 541-459-5632; e-mail **inrad@rosenet.net**; **http://www.qth.com/inrad/**. Suitable substitutes are part numbers 2301 (250 Hz), 2302 (500 Hz) and 2310 (2400 Hz). In all cases, the extra termination capacitors (30 or 24 pF) must be removed from the circuit.

[4]These were obtained from surplus telephone loading coils. An alternative is to wind an inductor on a ferrite pot core. 155 turns of #28 AWG enameled wire on an Amidon PC-2213-77 core provides 88 mH.

[5]The dynamic range should be about 4.7 dB greater with a 500 Hz bandwidth.

John Stephensen, KD6OZH, has been interested in radio communications since building a crystal radio kit at age 11. He went on to study Electronic Engineering at the University of California and has worked in the computer industry for 26 years. He was a cofounder of Polymorphic Systems, a PC manufacturer, in 1975 and a cofounder of Retix, a communications-software and hardware manufacturer, in 1986. Most recently, he was Vice President of Technology at ISOCOR, which develops messaging and directory software for commercial users and ISPs. John received his Amateur Radio license in 1993 and has been active on the amateur bands from 28 MHz through 24 GHz. His interests include designing and building Amateur Radio gear, digital and analog amateur satellites, VHF and microwave contesting and 10-meter DX. His home station is almost entirely homebuilt and supports operation on SSB, PSK31, RTTY and analog and digital satellites in the 28, 50, 144, 222, 420, 1240, 2300, 5650 and 10,000 MHz bands from Grid Square DM04 in Los Angeles. The mobile station includes 10-meter SSB, 144/440-MHz FM and 24-GHz SSB.

Next Issue in QEX/Communications Quarterly

L. B. Cebik continues his series on LPDAs with a look at some slightly larger arrays (164-foot booms). L. B. explores tweaking and optimization of design parameters with as many as 42 elements. Segmentation limi-tations imposed by software and computing power are addressed. This is serious stuff for those of you interested in HF gain that spans more than an octave of frequency. Do you have a few acres lying fallow?

Paul Hewitt, WD7S, gives you something to drive your six- and two-meter arrays: A no-bandswitch, dual-band, legal-limit linear amplifier. This project neatly exploits transmission-line theory to achieve its dual-band aspect. Come take a spin around the impedance chart with us and boost your signals.

Add synthesis and computer control to your HW-101 or other older rig! Rick Peterson, WA6NUT, brings us a PLL "spur eliminator." It's a PLL you can drive with your PC-controlled DDS to reduce or eliminate spurs outside the loop bandwidth. The PLL's VCO output is used to drive a transceiver's BFO or LO input. Remote control also creates some interesting possibilities for the experimenter. In the first part of a series, Sam Ulbing, N4UAU, presents some work he has done to control his rigs over UHF links. He uses off-the-shelf UHF transceivers and explains the difference between Part-97 auxiliary operation and Part-15 operation.

RF

By Zack Lau, W1VT

A No-Tune 10 GHz Filter

Over the past decade, it has been a tough engineering challenge to design a no-tune 10 GHz filter with a band-width narrow enough for a high-performance, single-conversion 144 MHz IF transverter. A no-tune design would make home construction much easier for those without expensive test equipment. It would also enhance reliability, as there would be no adjustments to be jarred out of alignment. This is quite important for mast-mounted transverters—the top of a tower on a windy day is a poor environment for delicate circuitry.

The first step to the solution is establishing the required bandwidth.

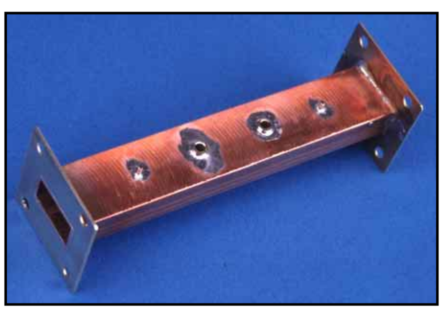

No-Tune WR-75 10 GHz bandpass filter

The image is separated from the passband by twice the IF, 288 MHz away. It is important to filter out the image for receiving—failing to remove it can degrade receiver sensitivity by as much as 3 dB. Similarly, transmitting the image degrades your effective transmit power. The reduction on transmit could be as much as 6 dB, if your system is limited by PEP, rather than average, power. The two mixing products will add coherently, resulting in a 6-dB, instead of 3-dB increase in peak power. The situation is even worse if there is significant LO feedthrough. This can be a problem with harmonic antiparallel mixers, as well as balanced mixers used outside their optimum frequency range. I'd recommend at least 20 dB of image rejection on receive and 40 dB for transmit.

Here's a rough rule of thumb for calculating the bandwidth: First, realize that for each resonator, the attenuation increases by 6 dB for each octave or 20 dB for each decade from the cutoff frequency. For a band-pass filter, the cutoff frequency is half the bandwidth. Suppose you need a LO

225 Main St
Newington, CT 06111-1494
zlau@arrl.org

attenuation of 20 dB. You could use a single resonator at one-tenth the bandwidth or three resonators, each with a little less than half the bandwidth. For instance, most people prefer a LO 144 MHz lower than the operating frequency. For a single tuned resonator, such as a pipe cap, the bandwidth ought to be 29 MHz. For a three resonator filter, a bandwidth of 144 MHz would have 18 dB of LO attenuation.

Alternately, this can be written as

$$20 \times n \times \log\left(\frac{2\times\Delta f}{BW}\right) \qquad \text{(Eq 1)}$$

where n is the number of filter resonators, Δf is the difference between the center frequency and frequency of interest, and BW is the filter bandwidth. Thus, 140 MHz away from the center of a 90-MHz-wide three-resonator filter, one calculates an attenuation of 30 dB. This corresponds well to a measured value of 33 dB. A second set of measurements on the same filter—with isolators at both ends—resulted in measured bandwidth of 95 MHz and 28 dB of attenuation at 137 MHz offset, the same as the calculated value.

It may be more convenient, however, to know the required bandwidth, given the desired frequency offset and number of resonators.

$$BW = \frac{2\times\Delta f}{10^{\frac{attn}{20\times n}}} \qquad \text{(Eq 2)}$$

Thus, for 30 dB of attenuation at an offset of 144 MHz with a three-pole filter, the bandwidth is 91 MHz. A narrower filter would result in even more attenuation, at the expense of higher loss and tighter construction tolerances. Scaling all dimensions by just 0.43% would move the filter 45 MHz, increasing the loss at 10368 MHz by 3 dB. Theoretically, the desired frequency would move from the center of the passband to the –3-dB cutoff point.

I wouldn't use this approximation for calculating filter attenuation close to the passband; the type of filter response becomes important. A Chebyshev filter with lots of ripple will have a steeper response than Butterworth or Bessel filters. It won't work far from the passband either—the stray coupling around the filter becomes more of a factor. For instance with no-tune filters on printed circuit boards, the maximum attenuation might be as low as 50 dB. The filter elements radiate, and thus couple the input and output circuits through the air. Thus, a calculation of 70 dB is meaningless, although the filter has five perfectly tuned resonators.

Microstrip filters are commonly used at lower frequencies, but there is just too much loss and too little etching tolerance for a 90-MHz-wide filter to be practical at 10 GHz. Thus, 10 GHz microstrip transverters typically have a first IF at 1.2 or 1.3 GHz. Amateurs in the US, however, typically prefer 144 MHz for the IF, necessitating another frequency conversion. Nonetheless, most amateurs prefer the simplicity of single conversion. In addition, some mixers, such as "rat-race" balanced mixers using sections of 1/4 λ transmission lines, operate optimally when the RF and LO frequencies are close together.

My choice for this difficult task is waveguide, which has very little loss. More importantly, surplus waveguide is sometimes available at reasonable cost. Surplus waveguide is often made to very close tolerances, allowing simple filters to be made with relatively simple machining operations. A post-type waveguide filter can be

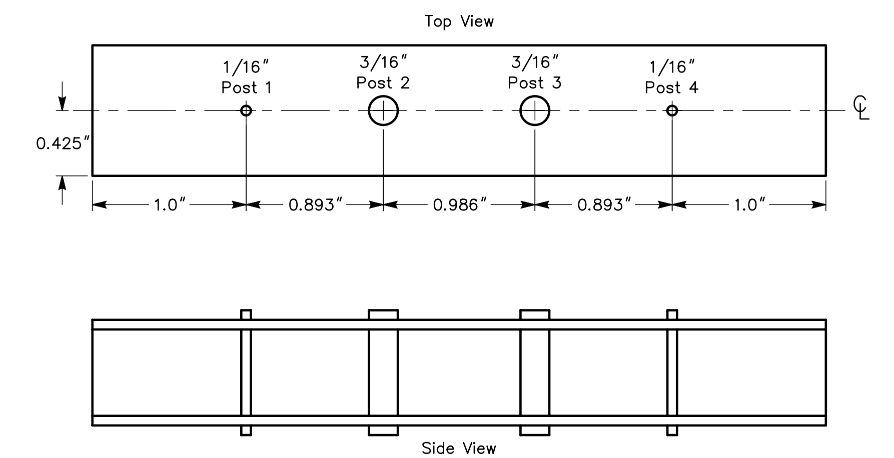

Fig 1—Construction details of the WR-75 filter. Posts 1 and 4 are 1/16-inch brass rod. Posts 2 and 3 are 3/16-inch brass tubing; the wall thickness isn't important. The waveguide is 4.8 inches of WR-75.

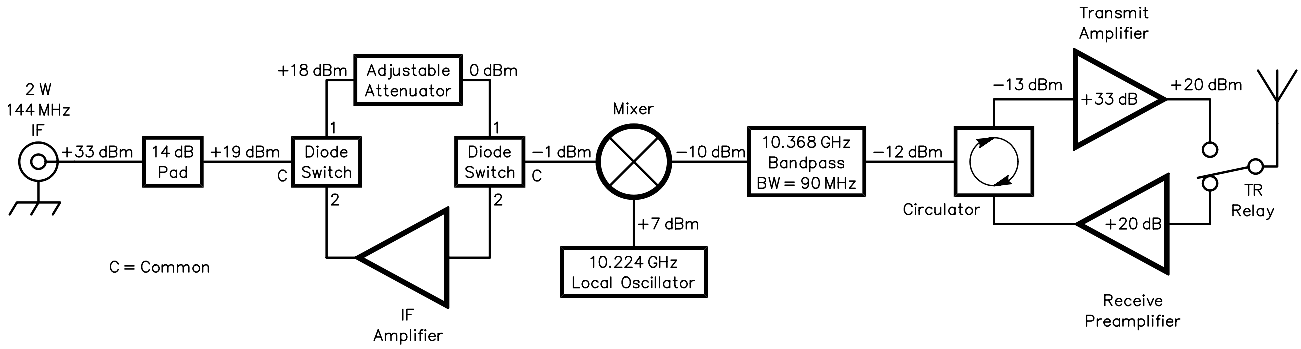

Fig 2—Block diagram of a 10 GHz transverter using a circulator and surplus parts. The power levels in dBm are typical transmit levels.

made by accurately drilling holes and soldering in standard size brass tubing sections to separate the waveguide into tuned resonators. The post spacing determines the resonant frequency of the sections, and the tubing size determines the coupling between the sections. Brass rod is also useable, although thick brass rod may be more difficult to solder.

It is important that as a waveguide approaches cutoff, the guide wavelength increases. Thus, as we more closely approach cutoff, guide sections must be longer to form resonant cavities at the desired frequency. This is quite useful for reducing the required accuracy in machining the filter. Thus, I discovered that making a filter out of WR-75 is much easier than making one out of WR-90, due to the relaxed tolerances.

Table 1 shows the dimensions of similar filters for WR-90 and WR-75 for different center frequencies. Both filters use four posts to divide the waveguide into three resonators. With WR-90, reducing the spacing by 6 mils increases the frequency 50 MHz, while a 10 mil (0.01 inch) reduction is required to similarly move a WR-75 filter. Still, this does require rather precise drilling. I used a Sherline milling machine to make the accurately spaced holes.[1] I rely on the accuracy of the lead screw to measure the distance between holes.

The dimensions were obtained using *WGFIL.COM*, a DOS waveguide-filter synthesis program developed by Dennis Sweeney, WA4LPR. It is available for non-commercial use at **http://www.cwt.vt.edu:3204/**. It was originally described in the Proceedings of the '89 Microwave Update and allows the user to design a post or aperture-coupled waveguide filter with Butterworth, Chebyshev or Equal Element responses.[2] It allows some modification of the post size, so with care one can use standard sizes. Using standard size tubing and drill sizes will greatly simplify construction.

[1]Notes appear on page 55.

Construction

A drawing of the precise hole locations in WR-75 waveguide is shown in Fig 1. The goal is to space the holes along a centerline as accurately as possible, preferably with a tolerance of a few mils (thousandths of an inch). Fortunately, this isn't too difficult, if one is reasonably skilled in using machine-shop equipment. If such equipment isn't available, it may make more sense to build a tuned filter that allows for greater errors in fabrication. Typically, the spacings are reduced slightly to increase the resonant frequencies. Tuning screws adjust the frequencies downward.

As pointed out by Glen Elmore, N6GN, it is very important to center the posts in the waveguide.[3] I find this easy to do by scribing a line using either side of the waveguide as a reference, and then splitting the difference between the two lines. By using the exact same scribing technique with both lines, the errors tend to cancel, resulting in a very

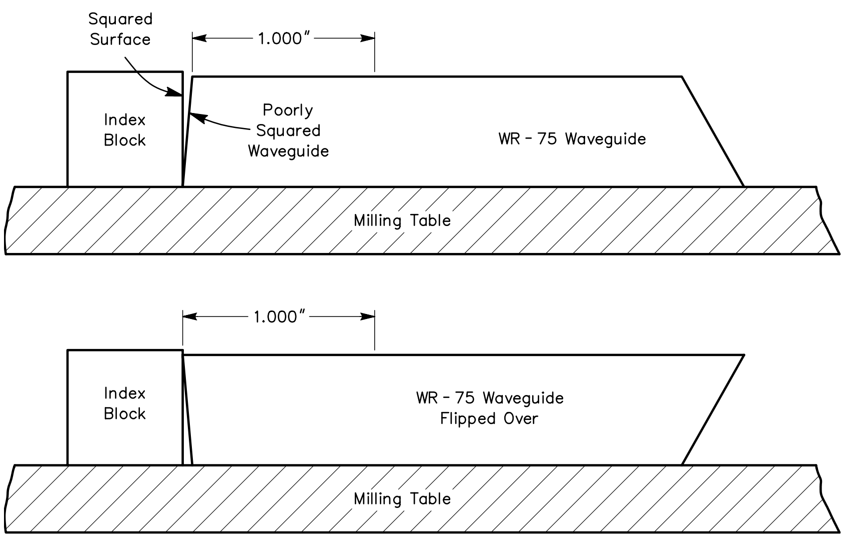

Fig 3—The use of an index block with a squared surface preserves milling-machine accuracy despite the imperfect waveguide end when the waveguide is flipped over to drill matching holes on the opposite side.

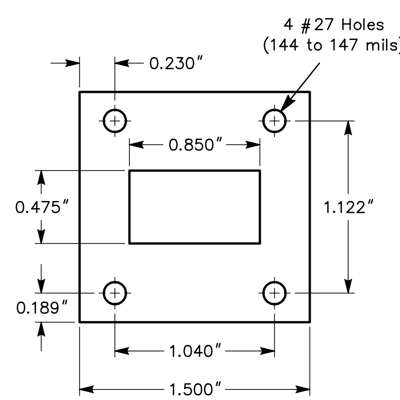

Fig 4—Homebrew WR-75 flanges made from 0.032-inch-thick brass sheet.

Table 1—Calculated Waveguide Filter Dimensions (inches)

Waveguide	*90 MHz BW WR-75 Butterworth BPF*			*90 MHz BW WR-90 Butterworth BPF*		
Center Frequency (MHz)	10318	10368	10418	10318	10368	10418
waveguide dimension h	0.75	0.75	0.75	0.90	0.90	0.90
waveguide dimension e	0.375	0.375	0.375	0.40	0.40	0.40
post 1 diameter	0.0625	0.0625	0.0625	0.125	0.125	0.125
1st to 2nd post spacing	0.893	0.883	0.873	0.822	0.816	0.810
post 2 diameter	0.188	0.188	0.188	0.281	0.281	0.281
2nd to 3rd post spacing	0.986	0.976	0.966	0.926	0.919	0.913
post 3 diameter	0.188	0.188	0.188	0.281	0.281	0.281
3rd to 4th post spacing	0.893	0.883	0.873	0.822	0.816	0.810
post 4 diameter	0.0625	0.0625	0.0625	0.125	0.125	0.125

accurate indication of the centerline.

To insure accurate holes, I used a center drill exclusively to start the holes. A #1 center bit has a 3/64-inch drill and a 1/8-inch body. Naturally, drilling the 1/16 holes on the bottom of the waveguide was a little bit of a challenge, since the center drill is too large to go through the waveguide. I chose to use the center drill to mark the two 3/16-inch bottom holes. The 1/8-inch drill body easily fit through the 3/16-inch top holes. These 3/64-inch center-drill holes were used to index the other two holes. I then removed the waveguide from the milling vise and scribed lines to mark the locations of all four holes. I don't recommend pushing a 1/16-inch drill bit through the waveguide to drill both the top and bottom holes. Ordinary drill bits wander around when starting holes—this is no way to drill precision holes.

This procedure is a bit of a tradeoff. There is at least a few thousandths of an inch inaccuracy in using the relatively large 3/64-inch holes as indexes. Fortunately, I found this good enough for my filter. Better accuracy might be obtained by using the high accuracy feed screw of a milling machine to set the distance between posts. Obviously, a digital readout makes this a snap, but it isn't too difficult with the 0.050-inch/turn hand screws of a Sherline Mill, if you pay attention and can work without interruption. Flipping the waveguide over to drill the second set of holes is still tricky. A Starret 827A edge finder only works if the waveguide end is truly square—perhaps a bad assumption for a beginning machinist. A better idea may be to index the waveguide with a known-square reference at least as high as the waveguide, as shown in Fig 3. This eliminates the need for the waveguide to be perfectly square. The hole makes it a bit of a challenge to square the waveguide ends. It is much easier to square a solid piece of metal.[4]

I used 1/16-inch brass rod and 3/16-inch brass tubing for the posts. I considered using 1.5-inch lengths of 3/16-inch brass rod—I think that if they were silver soldered there would be enough mechanical strength to use them as mounting hardware. The posts could be tapped and secured to an equipment chassis with screws. A post length of 1.5 inches is a good match for square WR-75 flanges.

I attached the homebrew waveguide flanges after soldering in the posts. The flanges are made out of 0.032-inch brass sheet, as shown in Fig 4. I recommend using a commercial flange as a guide. It is too easy to swap the orientations of the holes, resulting in a flange that is cross-polarized with normal transitions. In the past, I've made the large rectangular hole by drilling a pair of 3/8-inch holes and carefully enlarging them to match WR-75 with a nibbling tool and files. Not surprisingly, the miniature mill does a much quicker job. Thanks to Mark, NK8Q/3, for looking up the flange hole spacing and dimensions in the Continental Microwave and Tool catalog.[5]

Table 2—Frequency Response of the 10 GHz Waveguide Bandpass Filter

f (MHz)	*Insertion loss (dB)*
10031	51
10130	43
10150	41
10166	39
10190	36
10210	33
10220	31
10228	30
10238	28
10258	24
10278	19
10298	12.4
10318	4.6
10323	2.9
10328	1.6
10333	1.0
10338	1.0
10343	1.1
10348	1.6
10353	1.8
10358	1.8
10363	2.1
10368	2.1
10373	2.2
10378	2.3
10383	2.2
10388	2.5
10393	2.6
10398	2.8
10403	3.1
10408	3.5
10413	4.0
10418	4.6
10438	8.0
10458	12
10478	17
10498	21
10530	27
10547	30
10600	36
10620	38
10638	40
10739	46
10774	48

Using the Filter

If you use surplus parts, the conversion technique in Fig 2 works well. A surplus LO brick and mixer are attached to the filter, and the filter is attached to transmit and receive amplifiers via a circulator. The circulator avoids a 3 dB of loss that would result if a hybrid or splitter were used. This may not be a problem—low-level gain is relatively easy to get these days. This was much more of a concern 10 years ago, when each 9 dB of gain required an expensive FET transistor. Not only are FETs much cheaper now, but there are also useable MMICs. There is quite a demand for LO bricks, but they do show up at flea markets occasionally. Get there early, 10 GHz LO bricks are popular with dealers for resale.

Here's an easy way to obtain a circulator with a WR-75 flange and two SMA connectors: Modify an isolator. WR-75 isolators seem a lot more common than transitions or circulators. While some people have converted isolators into coaxial-to-waveguide transitions, I chose to replace the coaxial 50 Ω termination with a coax connector, creating a circulator. I've used a female SMA connector with a replaceable center contact. I removed the center contact, soldered it in place and then slid the Teflon dielectric and connector flange back over the pin.

The filter loss at 10368 MHz is 2.1 dB, with a minimum loss of 1.0 dB at 10338 MHz. The return loss of the filter is rather poor, approximately 6 dB. This should not be a problem if stable low-level amplifiers are used. It does make it difficult to measure the exact bandwidth and center frequency. My first attempt yielded numbers of 90 and 10359 MHz—a later attempt using isolators at both ports gave numbers of 95 and 10375 MHz. In either case, the filter is quite suitable for removing the unwanted image that results from the mixing process. Table 2 shows the filter response I measured with the isolators.

Notes

[1]Sherline Products, Inc, 2350 Oak Ridge Way, Vista, CA 92083; tel 800-541-0735, fax 760-727-7857; **sherline@sherline.com**; **www.sherline.com**.

[2]D. G. Sweeney, WA4LPR, "Design and Construction of Waveguide Bandpass Filters," *Proceedings of the Microwave Update '89*, pp 124-132.

[3]G. Elmore, N6GN, "A Simple and Effective Filter for the 10-GHz Band," *QEX*, July 1997, pp 3-5 and 15.

[4]If you need a good introductory book about working with small milling machines, I recommend *Tabletop Machining*, by Joe Martin. Of course, it is heavily biased toward the use of his Sherline products. See Note 1 for contact information.

[5]Continental Microwave & Tool Company, Inc, 11 Continental Dr, Exeter, NH 03833; tel 603-775-5200, fax 603-775-5201; **cmt@contmicro.com**; **http://www.contmicro.com/**.

Letters to the Editor

On Impedance Matching of Power Amplifiers and Loads

Dear Editor,

Desmond Thackeray, in his letter to the editor (*Communications Quarterly*, Summer 1999, p 4) commenting on my letter (Winter 1999, pp 5-7) has rightly questioned the value of "resurrecting" a definition (my excerpt "2") from the IEEE dictionary: The output impedance of an active device is the ratio of the sinusoidal component of output voltage and the corresponding component of current when it is operating normally. Clearly, this statement is only correct in the case of an RF power amplifier when by "operating normally" we mean that the amplifier has been tuned for maximum power output, and hence, it is conjugately matched to its load. Since this is what we want to establish, I see in retrospect that this definition is not helpful and could be misinterpreted: It is a point well taken.

Thackeray continues, though, quoting from Terman (1943), who wrote that the output impedance of a vacuum tube is defined as the impedance that the plate circuit of the tube offers to an externally applied voltage. Terman continues by stating that for a triode, this output impedance approximates the plate resistance of the tube (R_p). This definition applies only to class-A small-signal amplifiers, which—if conjugately matched—have efficiency of 50%. This line of thought has no relevance here.

To begin anew, we need to understand that there are two definitions of resistance:

A) Resistance is the factor by which the mean-squared conduction current is multiplied to give the corresponding power loss.

B) Resistance is the real part of impedance, which can be lossless.

That the source impedance of an RF power amplifier is "dissipationless" is fundamental to an understanding of why we measure what we measure. Power is not dissipated in Z_{out}, power is generated at this impedance for transfer to the load. To measure Z_{out}, Z_{load} has to have a finite and non-zero real component. When conjugately matched, Z_{out} and Z_{load} are complex conjugates, so $R_{out} = R_{load}$. Understanding this is important, because the ability of HF tuned power amplifiers to be conjugately matched has been unjustly disputed, largely by the argument that conjugate matching establishes an upper limit of 50% efficiency.

In the case of an RF power amplifier delivering power to an antenna system, no significant part of the available power should be dissipated anywhere in the matching network or antenna system. An antenna's radiation resistance is virtually dissipationless, for example. The following portrayal is paraphrased from a series of correspondence with John Fakan, KB8MU, in 1998. I hope it helps clarify my point.

Consider an alternator driven by an overshot water wheel. This is an easy-to-visualize example of a source that exhibits an obvious source impedance and lack of dissipation. At some flow level, the water wheel delivers a maximum of available energy; it transfers that energy to the alternator, which can be loaded to the point where it delivers the maximum available power to its load. The wheel would slow in response to an increasing load, allowing each bucket to fill more completely and thereby increasing the rate at which the wheel can supply energy to it load. At the point when the buckets were always full, any further decrease in rpm would result in lower power levels, because the torque could no longer increase.

Forgetting about the mechanism for a moment, just remember that energy transfer from the water wheel to the alternator shaft reaches a maximum at one specific speed. To mechanical engineers, that concept defines the mechanical impedance of the source. The output of the alternator is sinusoidal and exhibits a certain RMS voltage when no current is flowing in its load. When the load impedance is reduced, current will flow and the voltage will decrease but the electrical energy will flow at some power level to the load. The load impedance may be complex or not: It does not matter as long as the real part of the impedance is not infinite.

If we continue to decrease the load impedance, the energy transfer would increase up to the point where the alternator was no longer able to supply current at a greater rate. We know this would happen because we know something about the rate at which energy could be made available to the alternator. The alternator delivers only some fraction of the energy it is receiving from its source.

Further decreases in the load impedance result in still lower power levels into the load. We can find a value of load impedance for which electric energy transfer is a maximum. By definition, we also know the source impedance of the alternator without ambiguity. We do not have to know anything else other than the load impedance and that we are at the maximum power point. The source impedance of the alternator (Z_s, which is an IEEE-definition-B impedance) is exactly the complex conjugate of the load impedance (Z_{load}), by definition. To make further progress, readers must be comfortable with this point.

Were the load-current level increased by decreasing load resistance, the alternator's output voltage level would decrease. Why would it do this? Is it because of an IR drop across an IEEE-definition-A resistance within the alternator's circuitry? Or is it because the water wheel is now delivering less energy to the alternator's shaft? Is it a combination of these two? As far as analyzing the energy-delivering capabilities of the alternator to its load, it simply doesn't matter what mechanisms determine the alternator's characteristics as a source. It is completely sufficient to specify its characteristics in terms of the variables of interest: in this case, voltage and current.

The appropriate product of the voltage and current tells us the power level; the ratio of the variables defines the impedance. Until we actually know why the voltage decreases with increasing current, we can know nothing about the electrical efficiency. This water-wheel-driven alternator example is, in my view, a direct analogy to an RF power amplifier: The available energy is the stored energy in the tank circuit, the energy input to the tank circuit is provided by the pulses of current flowing in the anode circuit of the vacuum tube, and the power output (at the output of the π-tank circuit) is the power transferred to the load.

When we measure the output impedance (at the output of the π-tank circuit) of an amplifier tuned for maximum output power, we see $Z_{out} = Z_{load} = R_{load}$ for the simple case where the load impedance is a pure resistance. It matters naught why an increase in output current results in a decrease in output voltage when analyzing the energy-delivery capabilities of an RF power amplifier to its load; we need not worry about the "pulsey" nature of the current flowing in the anode circuit. Our measurements are taken at the output terminals of the π-network tank circuit. Here, smooth sinusoidal

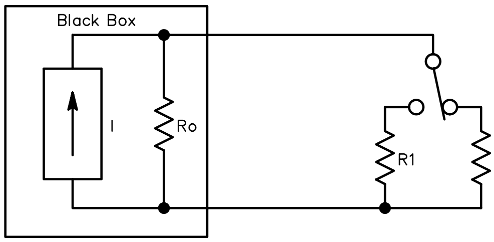

Fig 1—Load-pull method to find value of Ro.

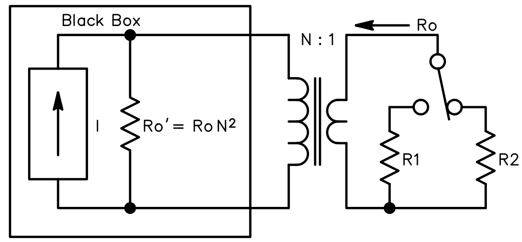

Fig 2—Finding Ro¢ when a transformer is in the circuit.

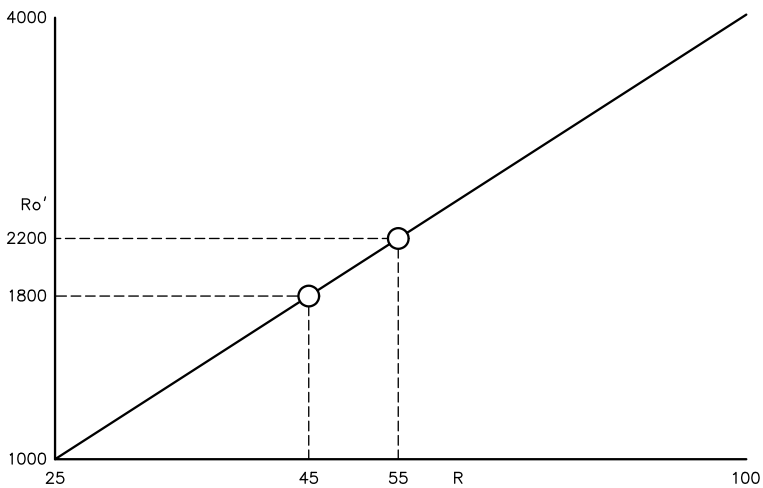

Fig 3—Variation of Ro¢ versus R for a conventional transformer.

energy is passed to the load. All we need understand is that we can we can find a maximum in available power, because the input power is finite.

The variables of interest are measured at the output terminals of the power amplifier, where they are sinusoidal and directly proportional to input power in the case of linear amplifiers. This, in accordance with the above example, is the message of Norton and Thevenin. Ponder this water-wheel-and-alternator example. It is perhaps difficult to think of a better analogy.—*John S. (Jack) Belrose, VE2CV, 17 Rue de Tadoussac, Aylmer, QC, J9J 1G1, Canada;* **john.belrose@crc.ca**

Doug,

A subject of interest to radio amateurs is that of *measuring* the output impedance of an RF amplifier while it is delivering some adjustable level of output power to a load resistance. A resonant network: (1) transforms impedance from some high value (the plate load of a vacuum tube) to 50 Ω, and (2) filters out harmonics.

One such network is the π (Fig 4), as used in nearly all amateur, vacuum-tube PAs. This letter discusses a newly discovered problem with one measurement method known as "load-pull." The following analysis has been reduced to its simplest *linear* form to emphasize the basic ideas and the problem. This problem exists in class A, AB, B and C amplifiers.

Fig 1 shows a "black box" containing a hidden current source and resistance. The generator current and resistance values are constant. A known resistor value, *R*, is connected across the output. We seek the value of the unknown resistance, *Ro*. This can be done by changing the known resistor from *R1* to *R2*, measuring *V1* and *V2* with a voltmeter and then solving for *Ro* as follows (see Reference). The value of current *I* (>0) does not matter.

$$V1 = I \bullet \left(\frac{R1Ro}{R1+Ro}\right) \quad V2 = I \bullet \left(\frac{R2Ro}{R2+Ro}\right)$$

$$\frac{V1}{V2} = \frac{R1R2 + R1Ro}{R1R2 + R2Ro}$$

$$Ro = \frac{V2 - V1}{\dfrac{V1}{R1} - \dfrac{V2}{R2}} \qquad \text{(Eq 1)}$$

Voltage *measurements* are required because *V1* and *V2* cannot be *calculated* without a knowledge of *Ro*, which is unknown. Note also that if *R1* and *R2* are close in value, the voltage and resistance measurements must be very accurate because the numerator and denominator involve the differences of two nearly equal numbers.

Of special interest is the more practical circuit of Fig 2, which has a step-down transformer with turns ratio *N*, or impedance ratio N^2. In this case, the calculated value of *Ro* is multiplied by N^2 to find the resistor *Ro′* inside the box.

$$Ro' = Ro \bullet N^2 \qquad \text{(Eq 2)}$$

Fig 3 shows how Ro', calculated using Eq 1, varies as the average value of $R_{avg} = (R1 + R2) / 2$ goes from 25 to 100 Ω. It is a straight line. In these first two examples, *R1* and *R2* do not have to be close in value to get good accuracy for *Ro*.

Fig 2 is of special interest because it resembles, superficially, the circuit of Fig 4, an RF power amplifier whose plate load resistance is transformed from the desired value of say, 2 kΩ, to a 50-Ω load by a π network. The π network at 3.75 MHz has an impedance of 2 kΩ and an operating Q of 12. The LC values are found in the tables in Chapter 13 of *The ARRL Handbook*. Here the impedance ratio is 2000 / 50 = 40 and the corresponding conventional-transformer turns ratio in Fig 2 would be $40^{1/2} \approx 6.325$. We would like to multiply the value of *Ro* found in Eq 1 by 40 to find the value of the tube's output resistance, which is its dynamic, loss-less plate resistance rp (see Reference).

The problem is that a π network does not behave as a conventional transformer as described in Figs 2 and 3. Instead, its input impedance (real part and phase) varies with output *R* as shown in the polar plot of Fig 5. The value of this input impedance is found very rapidly by *Mathcad* from the continued fraction of Eq 3.

$$Z_{in} = \cfrac{1}{\cfrac{1}{\cfrac{1}{\cfrac{1}{R} + j\omega C2} + j\omega L} + j\omega C1} \qquad \text{(Eq 3)}$$

In Fig 5, this resistance varies quite slowly from $45 \le R \le 55\ \Omega$ and the phase angle varies as shown. The problem is not so much the change in phase, which *slightly* detunes the network over that range (confirmed by *ARRL Radio Designer*), but rather the almost constant resistance. The phase change requires *R1* and *R2* to be close in value. A basic fact of the π network, as used in this application, is that the magnitude of the impedance changes *very slowly* with *R*, not at all like a conventional transformer. This means that if we change load *R* from 45 to 55 Ω, measure voltage and use Eq 1 to calculate the dynamic output resistance of the tube, we do not get the correct answer, because the method *requires* the kind of transformation that Figs 2 and 3 imply.

In addition, we cannot say that the output impedance of the amplifier at the coax connector is what the load-pull test suggests. The true output impedance is rp/40, which is not the same as the load pull-value.

The unfortunate conclusion is that the load-pull method is not applicable to a π-network PA. As the author of the referenced article, I must admit that I did not appreciate this problem until recently, when I looked at it more closely using simulation with *Radio Designer* and mathematical analysis using *Mathcad*. I "assumed" that a π network behaves as a conventional transformer. It transforms, but it is not a true "transformer," so it was a poor assumption. The article of the Reference considers only the simple situation of Fig 1 in this article and does not mention the π network. The problem of that network should have been anticipated.

The load-pull method will work much better with a wide-band transistor amplifier that uses conventional or transmission-line transformers whose windings are much shorter than λ/4. A low-pass filter should not be used because of the uncertain relationship between its output load and its input impedance, but a resistive-attenuator load followed by a spectrum analyzer will exclude harmonics from the measurements. This method measures the magnitude of the complex output impedance.—*73, William E. Sabin, W0IYH, 1400 Harold Dr SE, Cedar Rapids, IA 52403;* **sabinw@mwci.net**

Reference: Sabin, W. E., W0IYH, "Dynamic Resistance in RF Design," *QEX*, Sep 1995, p 13; feedback Dec 1995, p 29.

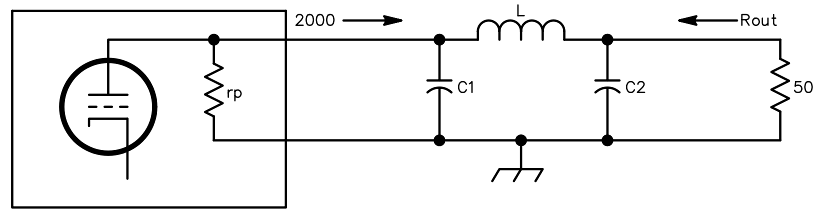

Fig 4—PI network from tube to 50 Ω load.

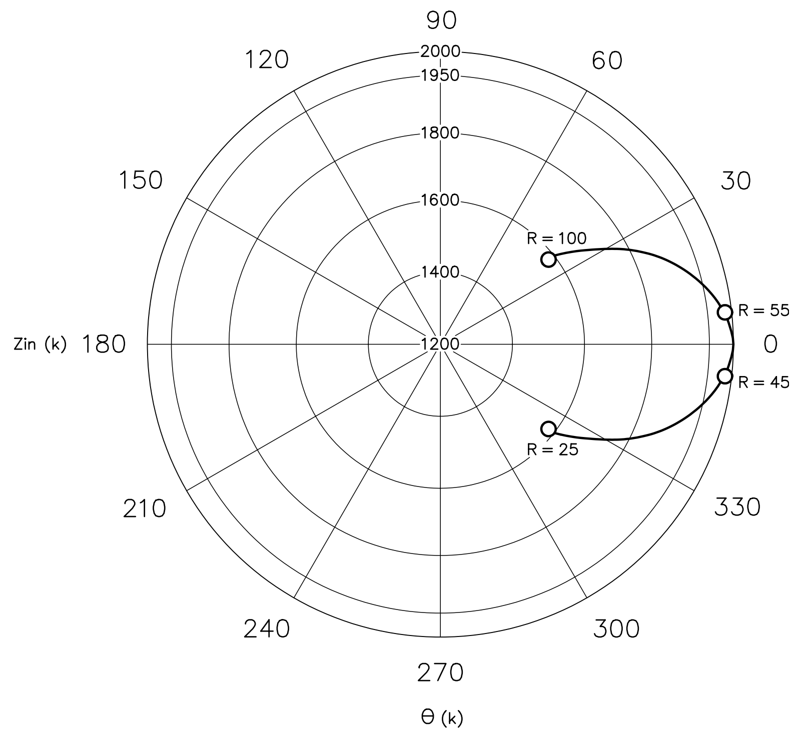

Fig 5—Input impedance and phase of the Pi network as a function of output load resistor R.

Dear Doug,

Both the "loading" and "conjugate-match" concepts are valid models under certain conditions. However, they are just models of behavior and not "timeless truths." There is nothing inside an RF-power transistor that looks like either a voltage source or a source impedance.

The "loading" model is valid when the RF transistor is operated below its maximum frequency. In this case, an amplifier works like a wall outlet: As you lower the load impedance, you draw more power. You would not want to conjugately match a wall outlet! Neither do you want to conjugately match the amplifier under these conditions, as it would become inefficient and exceed its ratings. Rather, you load it to get the power desired.

The "conjugate-match" model is valid when an RF transistor is operated near its maximum operating frequency. Here the drain capacitance and lead inductance, in combination with on-state resistance and finite current capability, create the effect of a conjugate match. A certain load impedance produces maximum output power and power decreases as you move away in any direction; however, it is not truly a conjugate match. The contours on a Smith chart are elliptical rather than circular, and maximum efficiency generally occurs at an impedance significantly different from that for maximum power.

For more details, see: (1) H. L. Krauss, C. W. Bostian, and F. H. Raab, *Solid State Radio Engineering*, Wiley and Sons, New York, 1980; (2) S. C. Cripps, *RF Power Amplifiers for Wireless Communication*, Artech, Norwood, Massachusetts, 1999. With best regards—*Frederick H. (Fritz) Raab, PhD, Green Mountain Radio Research Company, 50 Vermont Ave, Fort Ethan Allen, Colchester, VT 05446;* **fhraab@poweruser.com**

Dear Doug,

I was pleased to learn that the ARRL had purchased *Communications Quarterly*. I have read it and I believe it to be a good magazine that treats its technical material in a near-professional manner.

Regarding the amplifier-match debate: I have studied the article, editorial and letters that appeared in the Spring 1998 issue of *Communications Quarterly*. I support the analysis and conclusions of Warren Bruene, W5OLY. First-hand professional experience provides my support.

During the last five years of my career at Bell Labs (1985-1990), I supervised a group that designed 880-MHz linear power amplifiers for cellular-telephone base stations. Theory and numerous tests confirmed that the conjugate match was neither achieved nor needed. The RF PA designer experimentally finds the best load impedance by trading off linearity, dc-RF conversion efficiency, maximum power output and transistor dc power dissipation. The design is started by transforming the external 50-Ω load to the complex-impedance transistor load recommended by the transistor manufacturer. The transformer circuit is then adjusted until the "best" tradeoffs are realized. At no stage in the design process is any effort made to measure amplifier output impedance (R_{out})—that is, the impedance seen looking back into the amplifier output port.

The conjugate match was derived over 150 years ago as the condition for extracting the maximum output power from a battery; that is, $R_{load} = R_{out}$. Unfortunately, the match damages the battery and so is not used in practical systems. The conjugate match should only be attempted when the power source is "free" and cannot be damaged by the match; for example, a receiving antenna or solar cell. For these sources, it is the designer's goal to "suck out" as much power as possible and conversion efficiency be damned!

There are some conditions where power amplifiers do show conjugate matches:

1. In audio PAs, the output impedance can easily be made to equal the speaker resistance by proper adjustment of negative feedback. Upscale audio PAs have a "damping-factor" knob that is used to vary R_{out}.
2. Mr. Bruene, in the Spring 1998 *Communications Quarterly*, provides a graphical method to calculate RF PA R_{out} using the tube's E_p/I_p curves. He shows that a conjugate match can be reached (if the 4PR65 tube is driven hard) because of severe lowering of plate resistance (R_p) at those moments when the plate voltage swings low.
3. Messrs Maxwell and Belrose (same issue) report on output-impedance measurements made on a parallel-6146 RF PA. They claim R_{out} = 53 Ω (conjugate match) at 120 W, and 37 Ω at 25 W.

To verify these last results, I used Bruene's method to estimate R_{out} of a 6146 class-AB1 PA. The design parameters were: $B+ = 750$ V, $P_{out} = 60$ W, $R_{load} = 4$ kΩ. For these conditions, the peak plate voltage swing is $V_p = (P_{out} \times 2R_{load})^{1/2} = 693$ V. Thus, the max-imum instantaneous plate voltage is $E_{p(max)} = 750 + 693 = 1443$ V and the minimum voltage is $E_{p(min)} = 750 - 693 = 57$ V. Consulting the RCA tube man-ual, I derived these values for R_p, the small-signal (slope) plate resistance: $R_p = 1$ kΩ at $E_{p(min)} = 57$ V, $I_p = 350$ mA and $V_g = 0$ V. $R_p = 20$ kΩ at $E_pB+ = 750$ V, $I_p = 25$ mA, and $V_g = -50$ V; I_p is the instantaneous plate current and V_g is the grid voltage. Using Bruene's formula, I found the source resistance $R_s = 4.2$ kΩ as seen looking at the tube plate in parallel with the LC tank. Thus, conjugate match at 60 W is achieved. At 1/4 output power (15 W), the plate voltage swing is halved: $V_p = 693/2 = 347$ V and $E_{p(min)} = 404$ V. For this condition, R_s is near 15 kΩ and conjugate match is not reached.

The theory and experiments described above show that a conjugate match may be achieved at only one value of output power and this is not necessarily maximum output power. What is "maximum output power" of a linear PA? It should be the highest power at which a two-tone IMD test meets some specified requirement (such as third-order products at –30 dB). This is always well below the maximum power capability of the tube.

I believe that PA conjugate matching is of academic interest but has little practical value. Since a conjugate match does not necessarily improve the performance of an RF power amplifier, why continue this academic discussion? Whom should the reader believe? In engineering, there is no Supreme Court to dictate the correct answer. Here is an opportunity for the new management to put the matter to rest and concentrate on subjects that are more practical.—*73, Reed Fisher, W2CQH, ARRL TA, 2514 E Maddox Rd, Buford, GA 30518;* **w2cqh@arrl.org**.

Doug,

We agree that when determining the optimum load impedance, we are computing or measuring the impedance that we match to—and when we do, the amplifier delivers design power. However, when we connect the design load impedance across the output terminals of the amplifier, the amplifier behaves as if it had an output impedance equal to that of the load. We can prove this by measurement.

We feel the battery and audio-PA analogies are not relevant to the present discussion. The calculations for a 6146 tube contribute nothing new to the debate, since this exercise only repeats, for a tube more commonly used, calculations which Bruene has previously done. We discuss dynamic plate resistance R_p briefly in our Fall, 1997 *Communications Quarterly* article.

We have no need to know the magnitude of R_p. It is not a parameter that can be put in a circuit, since it changes with time. It is not used in design, nor can we measure it (except for class-A amplifiers). The value of R_p (V/I) is low (a few hundred ohms) during the interval of time that power is delivered to the input terminals of the tank circuit. The value of R_p is very large (tens of kilohms) when no power is delivered to the tank circuit (for half or more than half of the RF cycle); while the load impedance, R_L, is a few thousands of ohms.

The RF engineer does not have to

think about conjugate matches if he does not wish to. Yet this does not corroborate that HF tuned power amplifiers, when tuned to provide design power, are not conjugately matched. They are, and this is a very useful concept (my physics background). In summary, Mr. Fisher is writing about a resistance, R_s, that has nothing to do with the output impedance of an HF tuned power amplifier, is not used for design and cannot be measured. Discussing it only confuses the issue. What is the sense of further discussion when two sides are addressing a different parameter using words that do not mean the same thing?—*73, Jack Belrose, VE2CV*

Notes on "Ideal" Commutating Mixers (Nov/Dec '99)

Hi Doug,

I enjoyed your article on mixers. I'm glad you're trying to clear the air about them. Much misinformation and many oversimplifications have only confused the situation. I've had the opportunity to learn this in the "school of hard knocks" while designing a commercial HF spectrum analyzer.

As you pointed out, commutating mixers are linear. I don't think this simple fact can be overstressed. While microwave mixers generally exploit nonlinear behavior to generate the product of two signals, HF-mixer designers do their best to design the most-linear circuit possible. Otherwise, IMD would make the rig nearly useless on our crowded bands.

One of my first "brain-locks" on mixers was this linear/nonlinear conflict. We know that linear, *time-invariant* circuits do not produce distortion or mixing products. When we predict the output of a circuit using convolution (or Fourier analysis), we may be using simplified formulas that assume the circuit is time-invariant. So, the key to understanding the ideal commutating mixer is to realize it is a linear, *time-varying* circuit. The best HF front-end mixers are linear switches that route the RF input based on the phase of the LO. These switches can be diodes or transistors, but the principle remains the same. I have found that in a well-designed commutating mixer, the nonlinear distortion products are generally much lower than the distortion caused by switching.

Using an off-the-shelf diode-ring mixer, I ran the LO into the IF port and a two-tone signal into the RF port; for an IF, I used a spectrum analyzer on the LO port. Then I reduced the LO frequency to 0 Hz by substituting a dc current into the IF port. Even with very low dc current levels, the two-tone, third-order IMD (IMD_3) was greatly reduced, compared with a sine-wave LO. When I substituted a square-wave LO (with the same current into the mixer), I got an intermediate result for IMD_3: much better than with the sine wave, but not nearly as good as in the dc case. What was going on? The results should have been independent of LO frequency, since the diode-ring mixer is designed to have no energy storage (although there is some in the diode capacitance and transformers.) So the dc and square-wave LO cases should have given roughly the same distortion levels if we were seeing nonlinear distortion with the diodes biased fully on by the LO, but this assumes that the LO square wave has zero transition time.

The finite transition time of real waveforms causes two problems. First, the nonideal switching element (the diode) is in its nonlinear region for a significant period of time. It is starved of LO current for a fraction of its operating cycle and so generates severe distortion during the transitions. The second problem is that during the transition time, the exact time when the switch turns on or off is modulated by the RF signal. This is equivalent to phase modulating the LO; these sidebands appear on the IF as IMD. Reducing the transition time can reduce both of these sources of distortion. However, this requires lots of current in the LO drive circuit and makes the LO rich in harmonics. These harmonics can combine with the harmonics of other LOs in the receiver: This is the source of birdies. Engineering is always the art of compromise.

Transition distortion is why square-wave drive is better than sine-wave drive. It has been incorrectly stated that because the diodes clip the LO, sine-wave drive is as good as square-wave drive. Obviously, there is very little difference at peak drive, but there is a considerable difference in these two cases during the transition period. Generally, passive Schottky-diode mixers have very fast transitions (little charge storage) but require high LO power. This can cause EMC problems and birdies, as mentioned above. Active mixers have inherent decoupling of the signal and the LO, so are better at reducing zero-crossing distortion; however, active mixers simply can not switch as quickly as Schottky, hot-carrier devices, so transition nonlinearities are a bigger problem.

Historically, most of the circuit elements we use can be treated as time-invariant, linear devices; however, time-varying components are becoming much more important in modern electronics. We now run into switching power supplies, switched-capacitor filters, DSP sample-and-holds, various "pumped" components at microwave and many other linear, time-varying networks and components. So maybe it's time for more discussion of these interesting devices and I would suggest that *QEX* including *Communications Quarterly* is the right forum.—*73, John Gibbs, KC7YXD,17623 15 Pl W, Lynnwood, WA 98037*

A Class-B Audio Amplifier (Mar/Apr '00)

Gentlemen,

I find the March/April issue of *QEX/Communications Quarterly* contains many interesting opinions on a wide variety of subjects. It was particularly disturbing, though, to look at Figs 2 and 3 on p 46 and find positive feedback in one schematic and negative in the other. Perhaps Figure 2 should have been labeled "high-power Schmitt-trigger circuit!" Kindest regards—*Bruce Meyer, W0HZR, 9410 Blaisdell Ave S, Bloomington, MN 55420;* **blmeyer@wavetech.net**

Thanks, Bruce, for pointing out the error in Fig 2. The inverting and non-inverting inputs of the op amp are swapped—Ed.

A Synthesized Down-Converter for 1691-MHz WEFAX (Mar/Apr '00)

There are several errors in the down-converter article: The EMWIN Web site is at **iwin.nws.noaa.gov/emwin/wintip.htm**.

In Fig 2, the PLL IC (U3) is a Motorola MC12179D. The crystal should be 6.068359 MHz (International Crystal F.O. 8030953, GP-26C, catalog #004331612). The connections at C12 are wrong. Pin 2 of the VCO connects directly to pin 8 of the mixer, U2; C12 connects that track to R8. (The connection dot and the U2 pin 8 lead between C12 and R8 belong at C12's right-hand end.)

In Fig 5 the component layout, C12 (1500 pF at center, below the 250 Ω resistor) needs to be moved to the left 3/16-inch, so it connects the VCO output, pin 2 (a backward L-shaped pad) to R8 (250 Ω).—*Jim Kocsis, WA9PYH, 53180 Flicker Ln, South Bend, IN 46637;* **jimpyh@worldnet.att.net**

CLOVER-2000

High Performance HF Radio Protocol

Fast, Reliable, Economical Communications

PCI-4000/2K Internal Modem

DSP-4100/2K External Modem

CLOVER-2000 is an advanced modem waveform and protocol that is specifically designed for high rate data transmission via High Frequency (HF) radio. Available for use in HAL DSP-4100/2K or PCI-4000/2K modems, CLOVER-2000 automatically adapts to changing HF propogation conditions.

High Throughput & Adaptive ARQ:
CLOVER-2000 sends data over standard HF SSB radio channels at 3000 bps. Including error correction and ARQ overhead, CLOVER-2000 will deliver up to 2000 error-corrected bits/second over an HF radio link. The -50dB occupied bandwidth of the transmitted signal is only 2000 Hz. CLOVER-2000 may be used with *any* good-quality HF SSB transmitter and reciever.

The CLOVER demodulator measures Signal-to-Noise ratio (SNR), Phase Dispersion (PHS), and Error Corrector activity (ECC) of each data block received. This information is used to determine which of the five modulation formats should be used during the next 5.5 second transmission. In contrast, other adaptive systems use only 1 or 2 modulation formats and selection is based only upon errors as they are received and not on real time measurements of actual channel parameters.

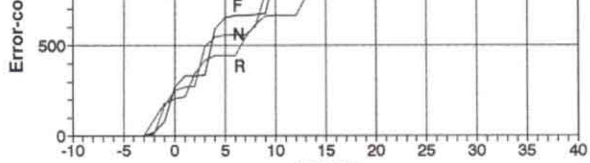

CLOVER-2000 Data Throughput

Error Correction Coding:
CLOVER uses Reed-Solomon error correction coding to combat burst-errors that occur on typical HF transmissions. Other ARQ modes may not include in-block error correction or use formats that require long interleave times to combat burst errors.

Bi-directional ARQ:
The CLOVER ARQ protocol allows real-time adaptive transmission of data *in both directions* on the ARQ link *without the need for special "over"* commands. CLOVER is also data transparent; the modem will send any 8-bit stream provided without modification and without requiring special command sequences. CLOVER-2000 is a low-cost and high throughput solution to your HF data communications problems. It is the "waveform of choice" for thousands of users throughout the world.

HAL COMMUNICATIONS CORP.
1201 W. Kenyon Road, P.O. Box 365
Urbana, Illinois 61801-0365
Phone: (217) 367-7373 FAX (217) 367-1701
www.halcomm.com

ASTRON CORPORATION 9 Autry Irvine, CA 92618
(949) 458-7277 • (949) 458-0826

UL E151765 cUL LISTED 2F29 E151765

...POWER ON WITH ASTRON

SWITCHING POWER SUPPLIES...

MODEL SS-10TK

MODEL SS-12IF

SPECIAL FEATURES:

- HIGH EFFICIENCY SWITCHING TECHNOLOGY SPECIFICALLY FILTERED FOR USE WITH COMMUNICATIONS EQUIPMENT, FOR ALL FREQUENCIES INCLUDING HF
- HEAVY DUTY DESIGN
- LOW PROFILE, LIGHT WEIGHT PACKAGE
- EMI FILTER
- MEETS FCC CLASS B

PROTECTION FEATURES:

- CURRENT LIMITING
- OVERVOLTAGE PROTECTION
- FUSE PROTECTION.
- OVER TEMPERATURE SHUTDOWN

SPECIFICATIONS:

INPUT VOLTAGE: 115 VAC 50/60HZ
OR 220 VAC 50/60HZ
SWITCH SELECTABLE

OUTPUT VOLTAGE: 13.8VDC

AVAILABLE WITH THE FOLLOWING APPROVALS: UL, CUL, CE, TUV.

MODEL SS-18

DESKTOP SWITCHING POWER SUPPLIES

MODEL	CONT. (Amps)	ICS	SIZE (inches)	Wt.(lbs.)
SS-10	7	10	1⅞ x 6 x 9	3.2
SS-12	10	12	1⅝ x 6 x 9	3.4
SS-18	15	18	1⅜ x 6 x 9	3.6
SS-25	20	25	2⅞ x 7 x 9⅝	4.2
SS-30	25	30	3¾ x 7 x 9⅝	5.0

MODEL SS-25M

DESKTOP SWITCHING POWER SUPPLIES WITH VOLT AND AMP METERS

MODEL	CONT. (Amps)	ICS	SIZE (inches)	Wt.(lbs.)
SS-25M*	20	25	2⅞ x 7 x 9⅝	4.2
SS-30M*	25	30	3¾ x 7 x 9⅝	5.0

MODEL SRM-30

RACKMOUNT SWITCHING POWER SUPPLIES

MODEL	CONT. (Amps)	ICS	SIZE (inches)	Wt.(lbs.)
SRM-25	20	25	3½ x 19 x 9⅝	6.5
SRM-30	25	30	3½ x 19 x 9⅝	7.0

WITH SEPARATE VOLT & AMP METERS

MODEL	CONT. (Amps)	ICS	SIZE (inches)	Wt.(lbs.)
SRM-25M	20	25	3½ x 19 x 9⅝	6.5
SRM-30M	25	30	3½ x 19 x 9⅝	7.0

MODEL SRM-30M-2

2 ea SWITCHING POWER SUPPLIES ON ONE RACK PANEL

MODEL	CONT. (Amps)	ICS	SIZE (inches)	Wt.(lbs.)
SRM-25-2	20	25	3½ x 19 x 9⅝	10.5
SRM-30-2	25	30	3½ x 19 x 9⅝	11.0

WITH SEPARATE VOLT & AMP METERS

MODEL	CONT. (Amps)	ICS	SIZE (inches)	Wt.(lbs.)
SRM-25M-2	20	25	3½ x 19 x 9⅝	10.5
SRM-30M-2	25	30	3½ x 19 x 9⅝	11.0

MODEL SS-12SM/GTX

MODEL SS-10EFJ-98

CUSTOM POWER SUPPLIES FOR RADIOS BELOW

EF JOHNSON AVENGER GX-MC41
EF JOHNSON AVENGER GX-MC42
EF JOHNSON GT-ML81
EF JOHNSON GT-ML83
EF JOHNSON 9800 SERIES
GE MARC SERIES
GE MONOGRAM SERIES & MAXON SM-4000 SERIES
ICOM IC-F11020 & IC-F2020
KENWOOD TK760, 762, 840, 860, 940, 941
KENWOOD TK760H, 762H
MOTOROLA LOW POWER SM50, SM120, & GTX
MOTOROLA HIGH POWER SM50, SM120, & GTX
MOTOROLA RADIUS & GM 300
MOTOROLA RADIUS & GM 300
MOTOROLA RADIUS & GM 300
UNIDEN SMH1525, SMU4525
VERTEX — FTL-1011, FT-1011, FT-2011, FT-7011

NEW SWITCHING MODELS

SS-10GX, SS-12GX
SS-18GX
SS-12EFJ
SS-18EFJ
SS-10-EFJ-98, SS-12-EFJ-98, SS-18-EFJ-98
SS-12MC
SS-10MG, SS-12MG
SS-101F, SS-121F
SS-10TK
SS-12TK OR SS-18TK
SS-10SM/GTX
SS-10SM/GTX, SS-12SM/GTX, SS-18SM/GTX
SS-10RA
SS-12RA
SS-18RA
SS-10SMU, SS-12SMU, SS-18SMU
SS-10V, SS-12V, SS-18V

*ICS – Intermittent Communication Service